TRENTON AND BLACK RIVER CARBONATES IN THE UNION FURNACE ROADCUT, STATE ROUTE 453, HUNTINGDON COUNTY, PENNSYLVANIA

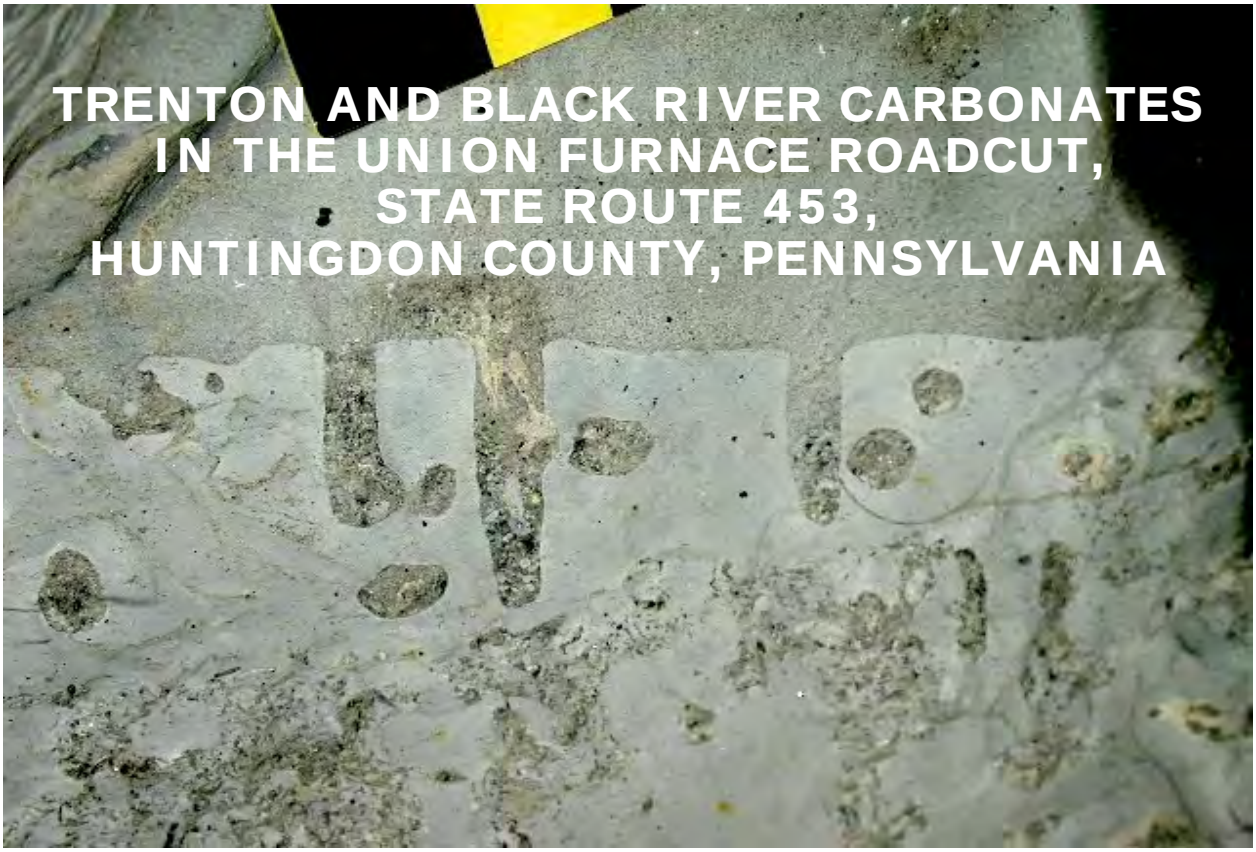

Pre-Conference Field Trip Guidebook
82nd Annual Field Conference of Pennsylvania Geologists
October 5, 2017

Pre-conference Field Trip Guidebook

82nd Annual Field Conference of Pennsylvania Geologists

October 5, 2017

TRENTON AND BLACK RIVER CARBONATES IN THE UNION FURNACE ROADCUT, STATE ROUTE 453, HUNTINGDON COUNTY, PENNSYLVANIA

Field Trip Leaders:

Christopher D. Laughrey and Jaime Kostelnik
Weatherford Labs
Golden, Colorado

With contributions by:

Arnold G. Doden, GMRE, Inc.
David P. Gold, Penn State University
John A. Harper, PA Geological Survey, Retired
Linda Morrow, Arch Spring Farm
George Pedlow

Cartoons by John A. Harper

TABLE OF CONTENTS

LIST OF ILLUSTRATIONS

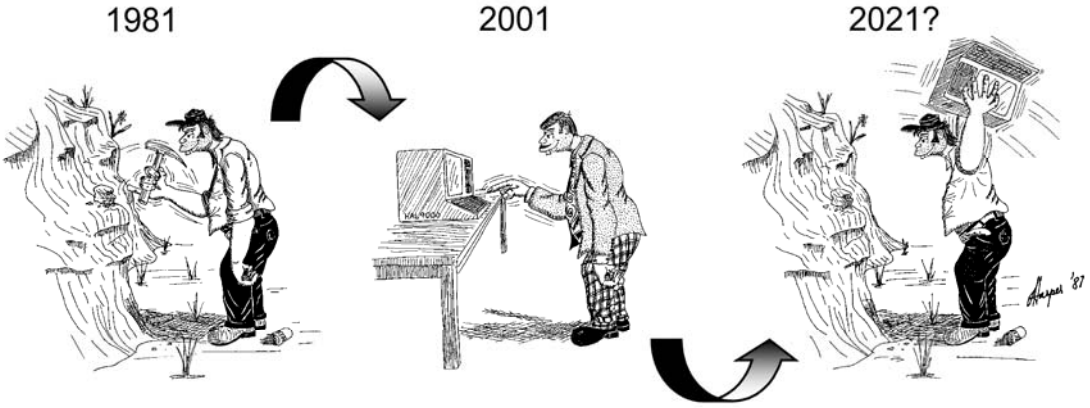

The evolution of geology in the 21st century

GRAYWACKE -An advanced form of senility, especially prevalent among sedimentary petrologists.

TRENTON AND BLACK RIVER CARBONATES IN THE UNION FURNACE ROADCUT, STATE ROUTE 453, HUNTINGDON COUNTY, PENNSYLVANIA

Introduction

Carbonate rocks of the Upper Ordovician Trenton and Black River Formations are the targets of active petroleum exploration in western and north central Pennsylvania (Figure 1), as well as the rest of the Appalachian basin. The potential reservoir targets are fractured dolostone or limestone traps in narrow grabens that are related to basement structures (Avary, 2002). Although this is a seismic play searching for structural traps, the sedimentary geology of the Trenton and Black River Formations is also critical to exploration efforts. The distribution of porous and permeable carbonate facies undoubtedly influenced the subsurface fairways traveled by dolomitizing fluids; in many instances these fluids initially entered the Trenton and Black River rocks along vertical fractures related to faulting, but then spread out laterally through permeable grainstones (Colquhoun and Trevail, 2000). In these cases understanding the sedimentary history of the carbonates means understanding their reservoir storage capacity. The spatial distribution of reservoir seals, reservoir compartmentalization, and diagenetically controlled pore geometry are partially or wholly sedimentological features. The Trenton/Black River play is basin wide in scope, and accurate stratigraphic correlations and analyses are necessary for rigorous petroleum exploration and development (Figure 2). Sequence stratigraphic analysis promises to provide such correlations and analyses (Cornell et al., 2001), but robust facies analyses must first be available before high-resolution surface and subsurface sequence stratigraphy can be accomplished (see Pope and Read, 1997). Finally, the sedimentary geology of the Trenton and Black River Formations has a direct bearing on understanding the petroleum source rocks of this play, as well as the migration and accumulation of oil and gas in these rocks (Ryder et al., 1998; Obermajer et al., 1999).

The primary purpose of this field trip is to acquaint geologists with the complex diversity of carbonate depositional facies that characterize the Trenton and Black River Formations in Pennsylvania. In addition to all of the reasons listed above, such an acquaintance can facilitate core and cutting sample interpretations in subsurface work. These rocks also have been the target of petroleum exploration in the Ridge and Valley province. We wish to share with you the exciting economic geology of these rocks in this region, and hope you find the other uses people put these carbonates to as interesting as we do. Finally, as a side benefit to our excursion today, we will casually examine some of the most spectacular karst features found in Pennsylvania, and learn a little bit of history concerning some remarkable underground explorations literally happening beneath our feet.

Setting

During Ordovician time, Pennsylvania comprised a tiny portion of the Laurentian craton, lying about 25^{o} south of the equator (Figure 3). From Late Precambrian through Middle Ordovician time, this region was part of an eastward-thickening, miogeoclinal basin that accommodated mostly carbonate platform sediments (Thompson, 1999). These carbonate rocks constitute part of the " Great American Bank" (Ginsburg, 1982) that extended more than 3,000 km (1,864 mi) along nearly the entire length of what was the southeastern seaboard of the Laurentian continental mass (Figures 3A, 4). The platform prograded eastward through Cambrian and Early Ordovician time, and its eastern terminus seaward was at a continental slope beyond which lay deep ocean basin sediments. Beginning in the Middle Ordovician, the craton margin was uplifted during the Taconic orogeny (Faill, 1999). The platform was

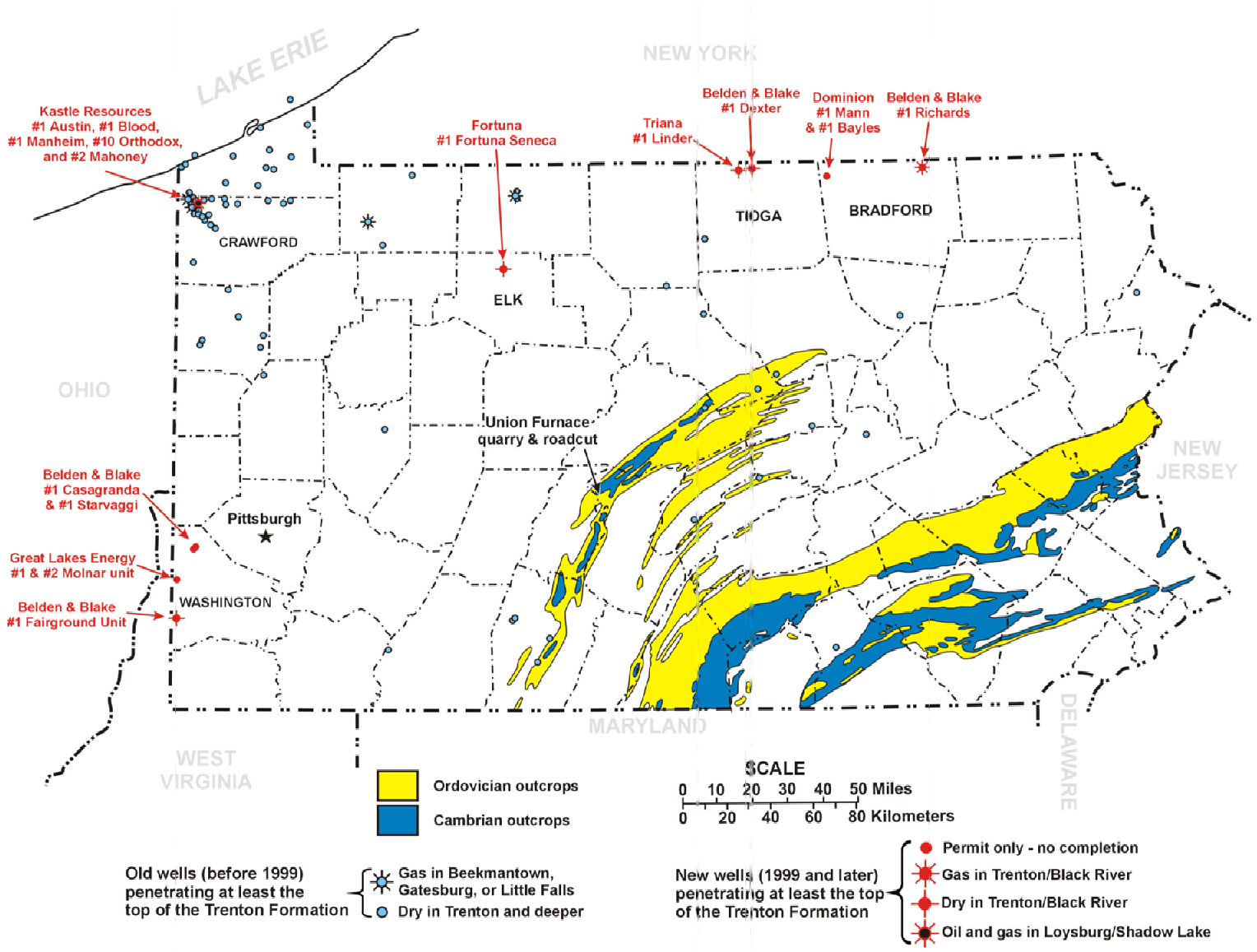

Figure 1. Location of Cambrian and Ordovician outcrops, wells that penetrate the top of the Trenton Group, and new permits for testing Trenton and Black River play in Pennsylvania. The location of the Union Furnace area is indicated.

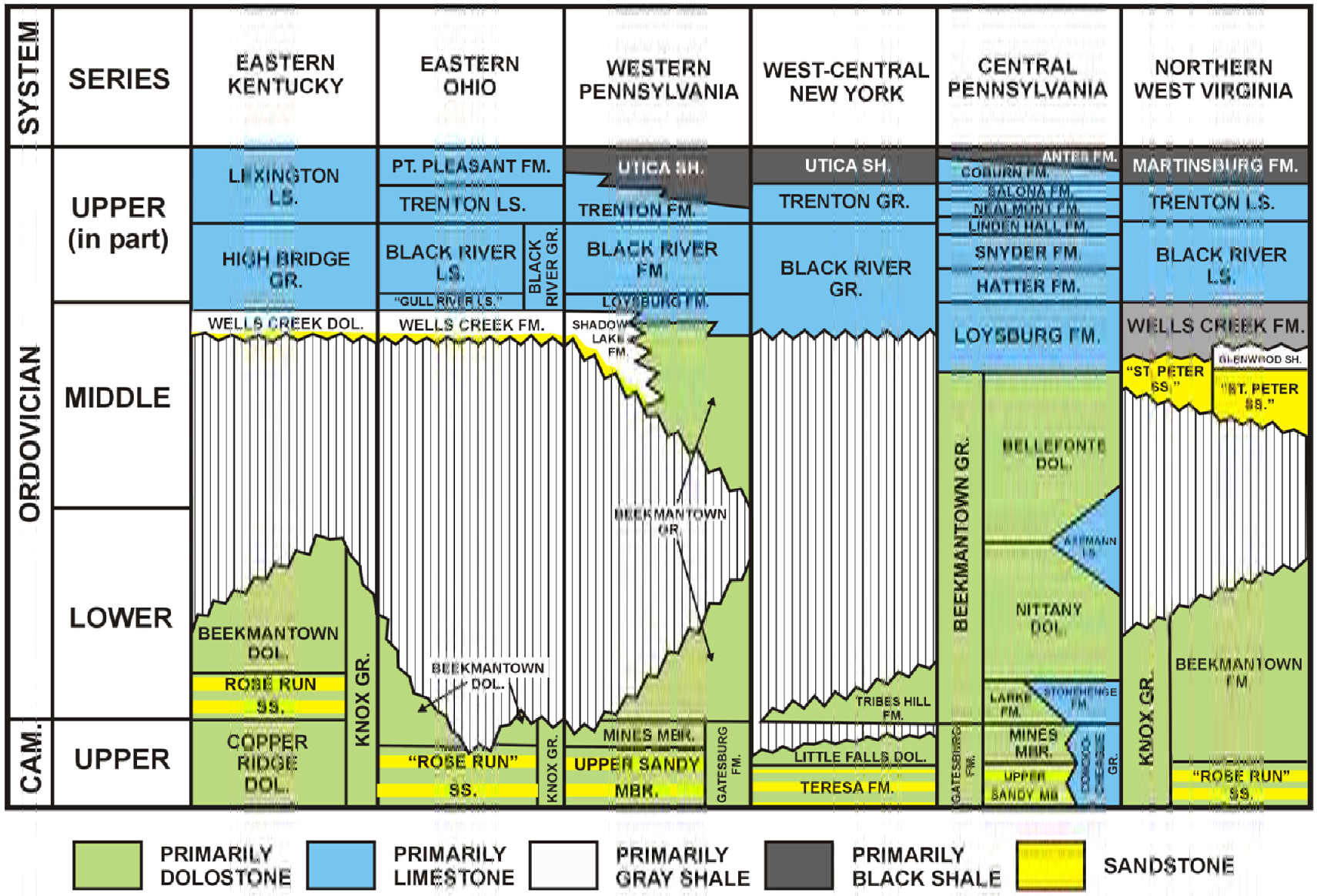

Figure 2. Regional lithostratigraphic correlation diagram for uppermost Cambrian and Ordovician rocks in the central Appalachian basin. We will examine the Loysburg through Coburn Formations of central Pennsylvania on this field trip.

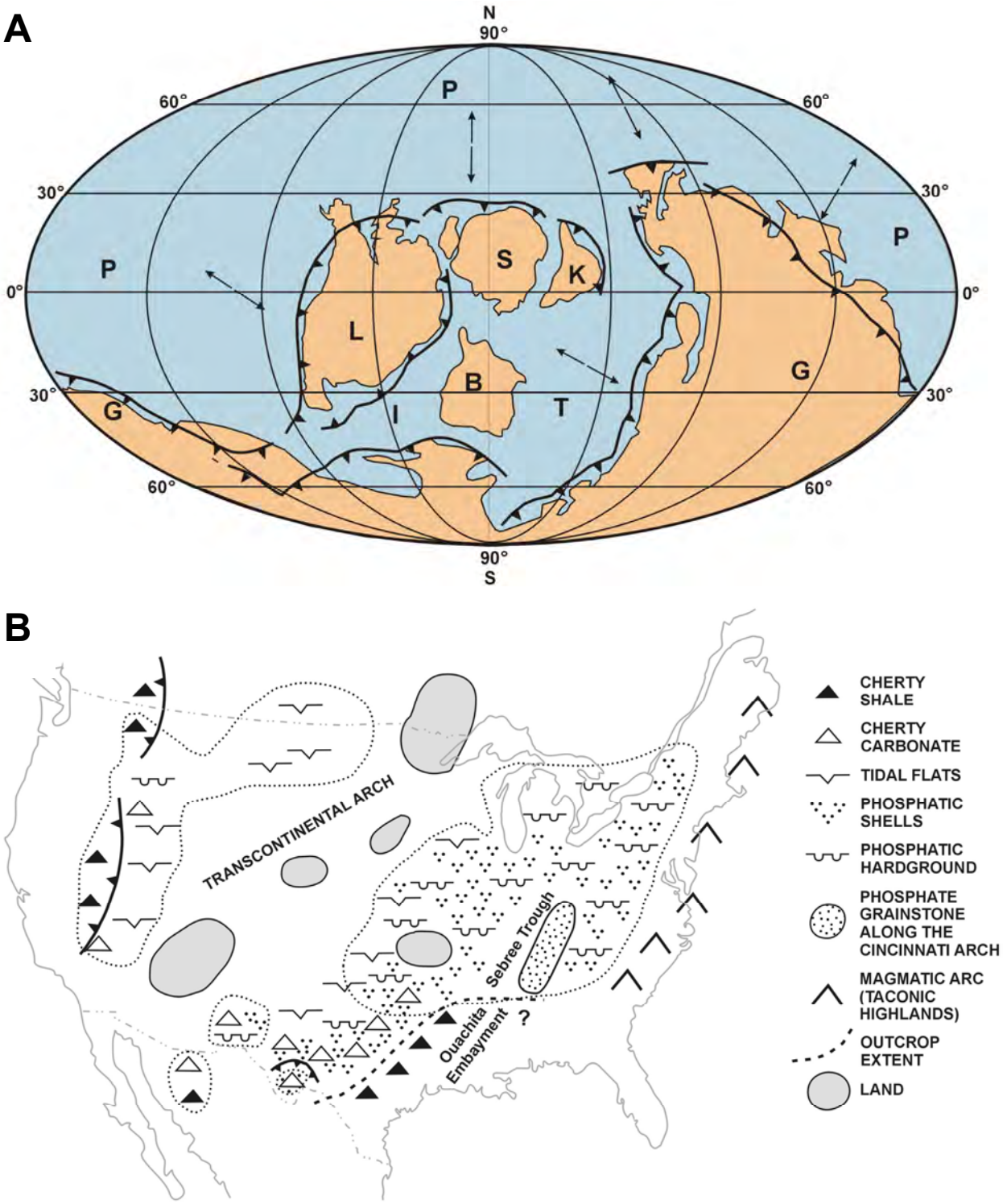

Figure 3. Late Ordovician paleogeography. A - Global reconstruction (modified from Scotese and McKerrow, 1991). B - Paleogeographic map of the United States showing the relative positions of the Taconic Highlands and the Late Ordovician carbonate platform (modified from Pope and Steffens, 2003).

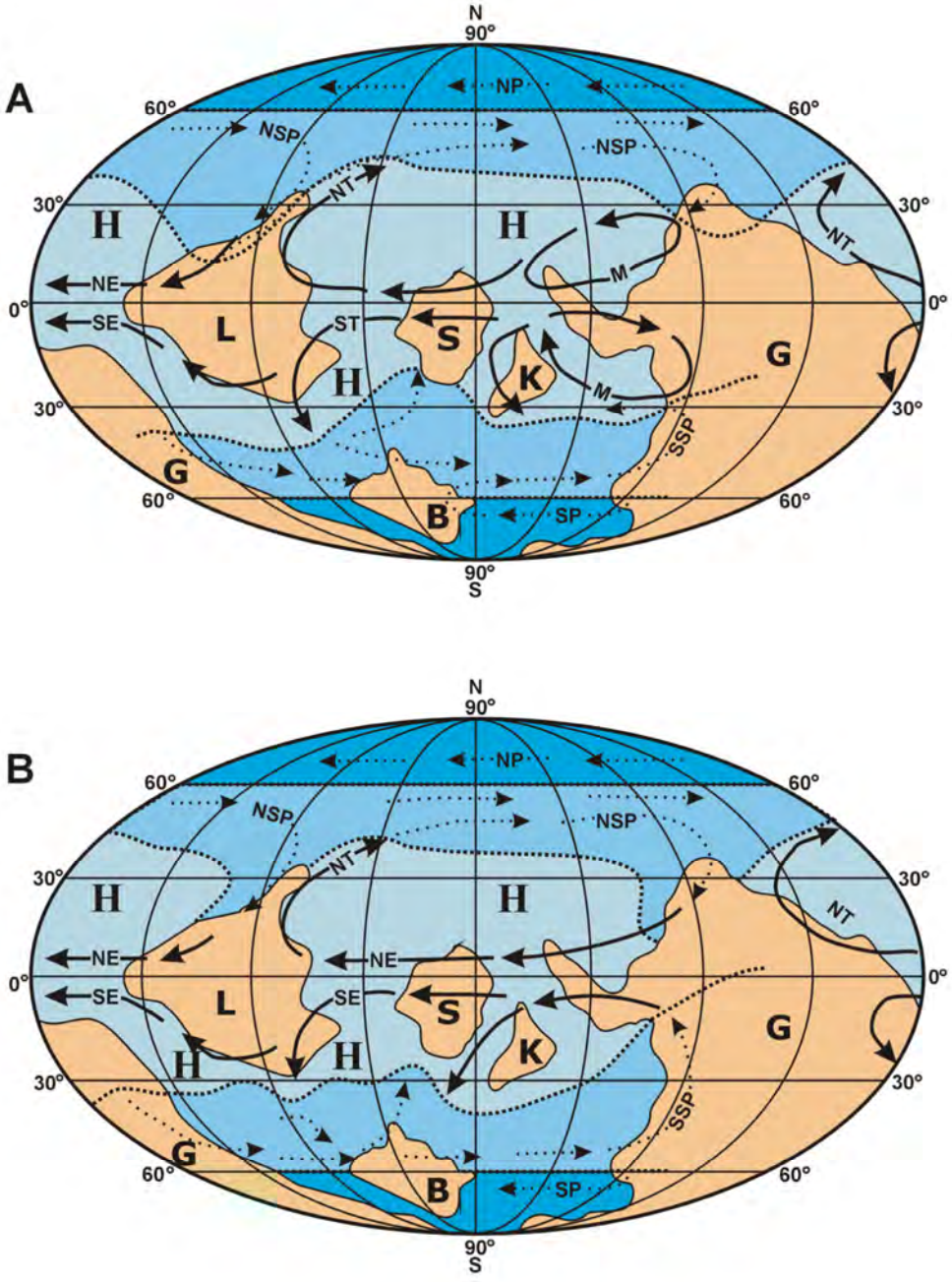

Figure 4. Paleoceanography of Earth during the Late Ordovician (modified from Wilde, 1991). A – Southern hemisphere summer and northern hemisphere winter. B – Southern hemisphere winter and northern hemisphere summer. Continents and seas are the same as those in Figure L -3. The red dot is the approximate location of the Union Furnace area. B – Balto-Scandinavia. G – Gondwana. K – Kazakhstan. L – Laurentia. S – Siberia.

progressively submerged. The Appalachian basin changed from a miogeoclinal carbonate platform to an exogeosynclinal foreland molasse basin (Thompson, 1999). This basin received large amounts of terrigenous sediment from eastern highlands, which were deposited in the foreland basin as the Taconian clastic wedge.

The distribution of landmasses and oceans suggested for the late Middle and early Late Ordovician (Figure 4) should have affected global seasonal weather patterns essentially the same as we experience today (Wilde, 1991), but with the northern and southern hemispheres reversed. Summer months feature low pressure air masses developing over large landmasses, resulting in the flow of large amounts of moist air (monsoons). Because landmasses were essentially restricted to the southern hemisphere at this time (Figures 3 and 4), monsoons would have occurred only in that hemisphere. Anti-trade monsoonal winds generated along the coast of Gondwana drove warmer water northward between Siberia and Kazakhstan, countering the flow of cooler water from northern mid-latitude high pressure systems. Because Pennsylvania lay on the southeast-facing coast of Laurentia around 25° south latitude, the dominant winds would have been trades similar to Recent trade winds, with some variation due to continental configurations. Warm maritime air from the Iapetan embayment between Laurentia and Siberia (Figure 4) would have provided abundant rainfall from the equator to about 35° or 40° south latitude.

The Ordovician stratigraphic record in Pennsylvania (Figure 5) reflects the control of tectonics and paleogeography on sedimentation. Lower and Middle Ordovician rocks tell the tale of prolonged passive margin carbonate accumulation in semi-arid conditions. Upper Ordovician clastics reveal a history of basin filling by marine and terrestrial clastics on a continental margin subjected to moist air traveling westward in lower latitude. In between are the Upper Ordovician Trenton and Black River Formations, and their equivalents, which were deposited during the transition from passive margin carbonates deposited on the Great American Bank to foreland deposition of the Taconian clastic wedge, subjected to transitional climates. These carbonate rocks developed on a northeast-trending ramp that lay northwest of the Taconic foreland basin (Read, 1980). The Trenton and Black River Groups of central Pennsylvania reflect the transition from carbonate shelf to ramp in response to flexure and increasing down warping due to the growing Taconic orogeny to the southeast. Subjacent Cambrian carbonates, the Lower to Middle Ordovician Beekmantown Group, and the Middle Ordovician Loysburg Formation were deposited on a rimmed carbonate shelf, with restricted circulation and wave action, on which vast peritidal and shallow water carbonate facies flourished (Goldhammer et al., 1987; Faill, 1999). With the reversal of plate motion that stopped the spreading of Iapetus, compressional down warping of the Laurentian continental margin occurred as the Taconic thrust belt approached from the southeast. Subsidence rates increased markedly beginning 460 ma, and marked the termination of the "Great American Carbonate Bank" (Goldhammer et al., 1987) (Figure 6). This stratigraphic sequence reveals the passive margin history of the eastern part of the Laurentian craton from Early Cambrian to Middle Ordovician time, and the shift to down warping that led to terminal drowning of the platform during Late Ordovician time.

Stratigraphic Nomenclature

Stratigraphic nomenclature for the Middle and Upper Ordovician rocks of central Pennsylvania is somewhat controversial. The stratigraphic column shown in Figure 5 represents that of the Stratigraphic Correlation Chart of Pennsylvania (Berg et al., 1983), with some modification from Faill and others (1989). These authors replaced the name Rodman Formation (Figure 5) with the name Nealmont Formation (Figure 2). The Rodman is the upper member of the Nealmont Formation in previous schemes (see Rones, 1969 and Berg

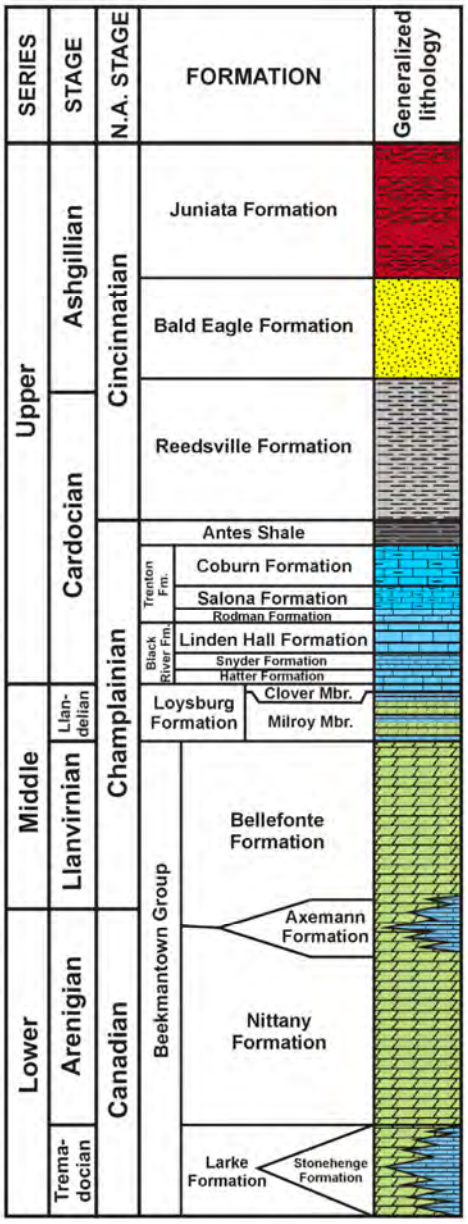

Figure 5. Stratigraphic column for the Ordovician rocks of central and western Pennsylvania. Beekmantown Group and Loysburg Formation carbonates were deposited on a stable, passive margin carbonate shelf. Clastics of the Antes Shale through Juniata Formation were deposited in response to plate convergence during the Taconic orogeny. The Black River and Trenton Groups, and equivalents, formed during progressive submergence of the earlier-formed passive margin platform.

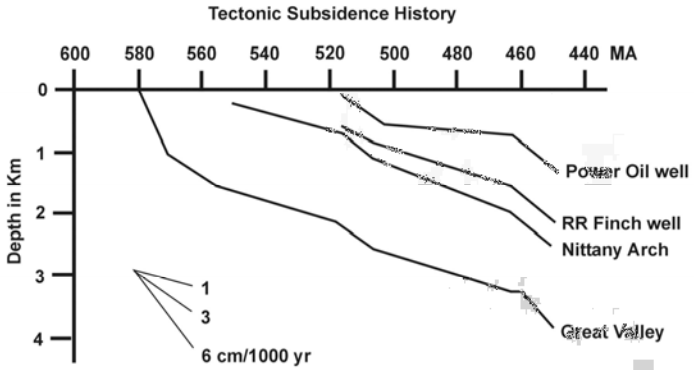

Figure 6. Ancient Appalachian tectonic subsidence history (modified from Goldhammer and others, 1987). Note the abrupt change in slope of the curves at approximately 460 ma. This time was the start of Black River sedimentation, and it marks the development of the carbonate ramp in response to the Taconic orogeny.

et al., 1983). Sudden, intricate facies changes, variations in stratigraphic thickness, and poor exposures make lithostratigraphic correlations outside of their type areas difficult. Leslie and Bergstrom (1997) showed that biostratigraphic studies based on graptolites and conodonts, and the use of K-bentonite beds and sequence boundaries as stratigraphic markers helps to lessen the confusion, but serious correlation problems within the Middle and Upper Ordovician Series still exist.

The Hatter, Snyder, and Linden Hall Formations of central Pennsylvania are equivalent to the Black River Formation of western Pennsylvania (Figure 2). Likewise, the Nealmont, Salona, and Coburn Formations in the outcrop are equivalent to the Trenton Formation of western Pennsylvania (Figure 2). Some workers have included the Hatter, Snyder, and Linden Hall Formations of central Pennsylvania in the Black River Group, and the Nealmont, Salona, and Coburn Formations in the Trenton Group (Cullen-Lollis and Huff, 1986; Leslie and Bergstrom, 1997). We use these group names in this guidebook.

K-Bentonites

Kolata et al. (1996) identified and described 29 K-bentonites from the Mohawkian rocks of central Pennsylvania. Nineteen K-bentonites are recognized and designated at the Union Furnace outcrop along PA 453. We have identified another possible K-bentonite near the top of the Hatter Formation. Cullen-Lollis and Huff (1986) and Berkheiser and Cullen-Lollis (1986) discussed the K-bentonite occurrences here at the Union Furnace exposure. Six of the K- bentonites in the Salona Formation have unique chemical signatures, and are particularly useful for regional correlations (Kolata et al., 1996). Two of these, the Deicke (Figure 7) and Millbrig K-bentonites, have been especially useful in

calibrating sequence stratigraphic correlations (Holland and Patzkowsky, 1996; Pope and Read, 1997).

There are several useful criteria for identifying the K-bentonites in the field (Kolata et al., 1996). The K-bentonites have a soapy, waxy texture when wet. They are light to dark gray, buff, orange, or tan in outcrop exposures. The variability is due to composition, variable oxidation due to ground water activity, and weathering. They appear greenish gray to bluish gray to white in cores. The K-bentonites may contain euhedral to anhedral flakes of biotite and relict glass shards. They also might contain euhedral crystals of zircon, feldspar, and apatite. The bentonites appear as fine-grained clay bands that might extrude under compactional loading by the carbonate rocks, but they weather and recess with exposure time. Chert bands in the limestones often underlie thicker bentonites. Many bentonite layers are overgrown with trees and shrubs due to the moist, nutrient-rich clay. The bentonite beds are stratigraphically persistent.

Figure 7. Photograph of the Deicke K-bentonite at the exposure along Pennsylvania Route 453 near Union Furnace, Pennsylvania.

Geochemical fingerprinting of these bentonites involves discriminant function analysis of 26 variables (elements) and four groups (beds) (see Kolata et al., 1996). The chemistry of the bentonite discerns a volcanic ash origin from a calc-alkaline destructive plate margin volcanic setting.

THE GEOLOGY OF THE UNION FURNACE AREA

Previous Studies

Kay (1944a, 1944b) developed the basic stratigraphic framework in use today, and Faill et al. (1989) provided excellent stratigraphic descriptions of the Ordovician carbonates for field mapping. Thompson (1963) examined the stratigraphy and petrography of the Salona and Coburn Formations in central Pennsylvania. Rones (1969) did the same for the Hatter, Snyder, Linden Hall, and Nealmont Formations. Both Thompson's (1963) and Rones' (1969) reports include measured sections for exposures located along the former Pennsylvania Railroad cut near Union Furnace. Wagner (1966) correlated the Middle and Upper Ordovician rocks of central Pennsylvania with those in the subsurface of western Pennsylvania, south central New York state, northern West Virginia, eastern Ohio, and southwestern Ontario. Chafetz (1969) reported on the stratigraphy and sedimentology of the Loysburg Formation in this region.

Berkheiser and Cullen-Lollis (1986) summarized the history of mining and geologic investigations of the Ordovician carbonate rocks at Union Furnace. They provided a detailed measured section of the Loysburg through Coburn Formations where they are exposed along PA 453. Berkheiser and Cullen-Lollis (1986) developed the first modern facies interpretation for these rocks, and were the first to suggest a carbonate ramp depositional environment for these sediments in central Pennsylvania (Figure 8). We found their work invaluable during our field and core studies.

Gardiner-Kuserk (1988) identified centimeter-scale cyclic sedimentation patterns in the Upper Ordovician carbonates of central Pennsylvania, and she attributed the patterns to storm events on a progressively deepening ramp. The cycles she identified are made up of repetitive successions of micrite, bioclastic or intraclastic limestone, and siliciclastic shale. The bioclastic

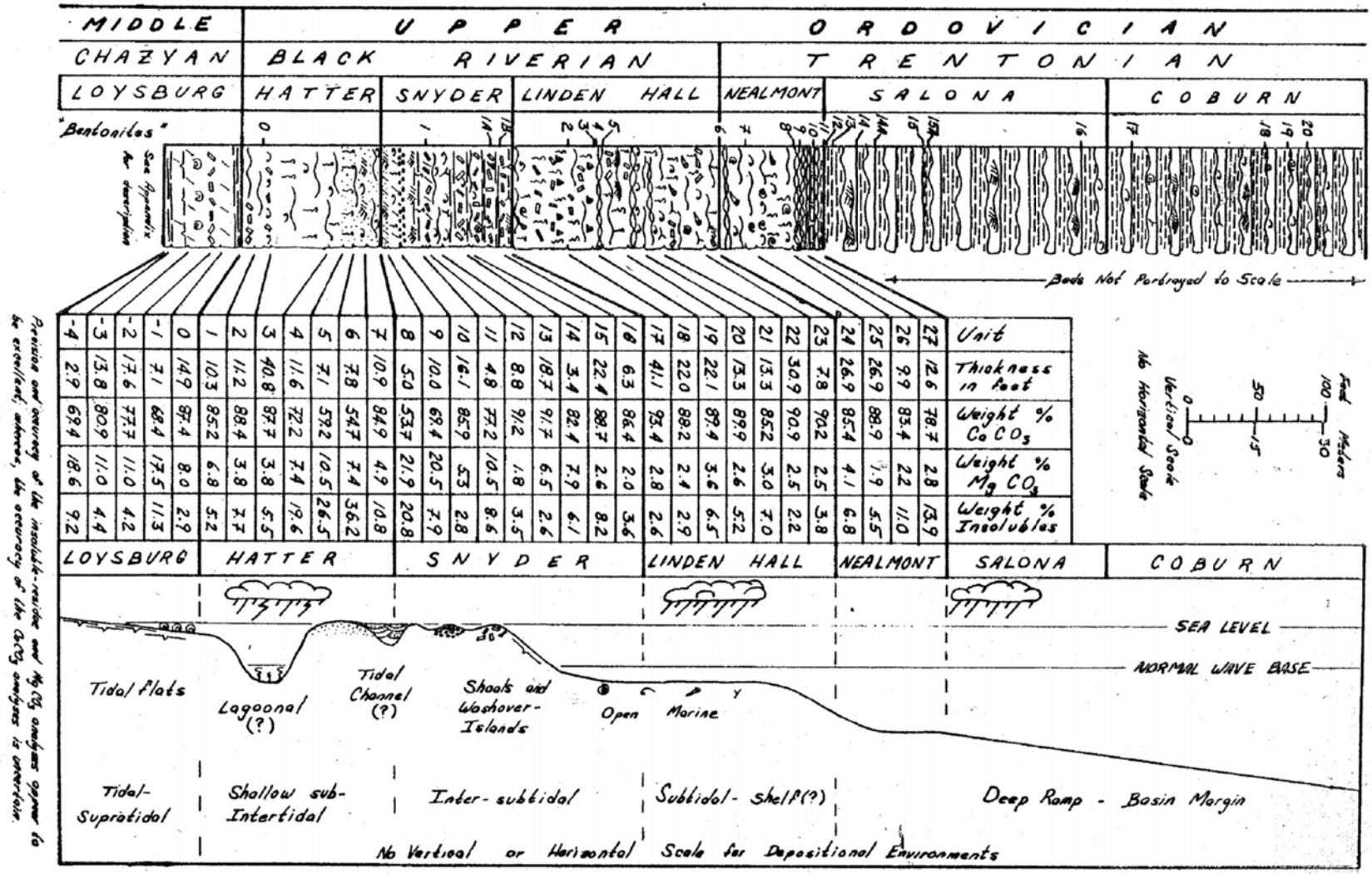

Figure 8. Berkheiser and Cullen-Lollis's (1986) interpretation of carbonate facies in the Loysburg through Coburn Formations exposed along Pennsylvania Route 453 at Union Furnace. The units numbered –4 through 27 were arbitrarily assigned for sampling and mining purposes. They are still clearly visible on the outcrop, and are useful for orientation. The units have no stratigraphic or sedimentological significance.

or intraclastic limestone occurs as a lag, and the other lithologies are arranged in fining-upward beds reflecting waning storm conditions. Gardiner-Kuserk (1988) identified five such cyclic patterns on the basis of textural attributes, carbonate allochems, sedimentary structures, and bed thickness.

Slupik (1999) investigated the sedimentology and stable isotope chemostratigraphy of the Nealmont, Salona, and Coburn Formations in central Pennsylvania. She too suggested that the rocks originated in a ramp environment. Slupik's (1999) interpretation departs from those of Berkheiser and Cullen-Lollis (1986) and Gardiner-Kuserk (1988), however, in that she interprets the Salona Formation carbonates as deposited in the deep ramp or slope environment below fair-weather wave base, but slightly above storm wave base. She interprets the overlying but above storm wave base. Thus she places the Coburn in a more proximal ramp position, implying that it is a regressive sequence. Slupik (1999) also documented a positive inorganic carbon isotope excursion of approximately 3 $^{o}/_{oo}$ (PDB) across the Nealmont and Salona Formations boundary. She correlated this isotope shift with a previously recognized δ13C positive isotope excursion observed in Upper Ordovician petroleum source rocks in eastern Iowa, and attributed it to a regional increase in organic productivity and preservation.

Carbonate Ramp Facies Models

Carbonate ramps (Figure 9) comprise a category of platform characterized by gentle slopes (typically less than one degree) on which shallow-water, wave-agitated sediments of the near shore zone pass down slope into deeper-water, low-energy deposits (Read, 1985). The transition from shallow to relatively deeper water facies occurs without a marked break in slope. Ramps differ from rimmed carbonate shelves in that continuous reef trends usually are absent, high-energy carbonate sands accumulate near the shoreline, and deeper water breccias, if present at all, lack clasts of shelf-edge lithofacies.

Carbonate ramps are subdivided on the basis of profile into homoclinal ramps and distally steepened ramps (Figure 9B and 9C). Homoclinal ramps have comparatively uniform, mild slopes (<1°) into the basin. Carbonate facies include 1) peritidal and lagoonal facies; 2) shoal-water bank complexes; 3) open-marine, deeper-ramp, muddy sediments; and 4) slope and basin lime muds and interbedded shales (Read, 1985) (Figure 9B). The Persian Gulf and Shark Bay, Australia are examples of modern homoclinal carbonate ramps (Figure 10).

Distally steepened ramps are defined by an increase in gradient in the outer, deep ramp environments (Read, 1985; Tucker and Wright, 1990) (Figure 9C). Sediment gravity flow deposits are common in this setting. Since the break in slope occurs in relatively deep water on the ramp, the resedimented deposits consist of outer ramp and upper slope carbonate sands and muds, and clasts of this material. Peritidal, lagoonal, and shoal water facies occur well back on the platform, and deep ramp carbonate mud blankets (low energy) or broad lime sand blankets (high energy) occur seaward of the shoal complexes (Read, 1985). The deep ramp lithofacies consist of argillaceous, burrowed, nodular skeletal wackestone/mudstone. The rocks contain an open marine biota, and may have slumps, breccias, and turbidities (Read, 1985). The northeastern Yucatan (Figure 11) and western Florida are modern distally steepened ramps.

The Trenton and Black River Group successions contain elements of both ramp types. The Hatter Formation to upper Linden Hall Formation at Union Furnace contains a facies succession readily interpreted as an ancient barrier-bank type homoclinal ramp (Figure 9B). These rocks exhibit an upward-deepening trend comprised of, in ascending order, peritidal, lagoonal, shoal complex, and deeper ramp facies (Figure 12). The uppermost Linden Hall and the Trenton Group, however, contains facies characteristic of an ancient distally steepened ramp (Figure 9C). The top of the Linden Hall and the Nealmont Formations exhibit an upward

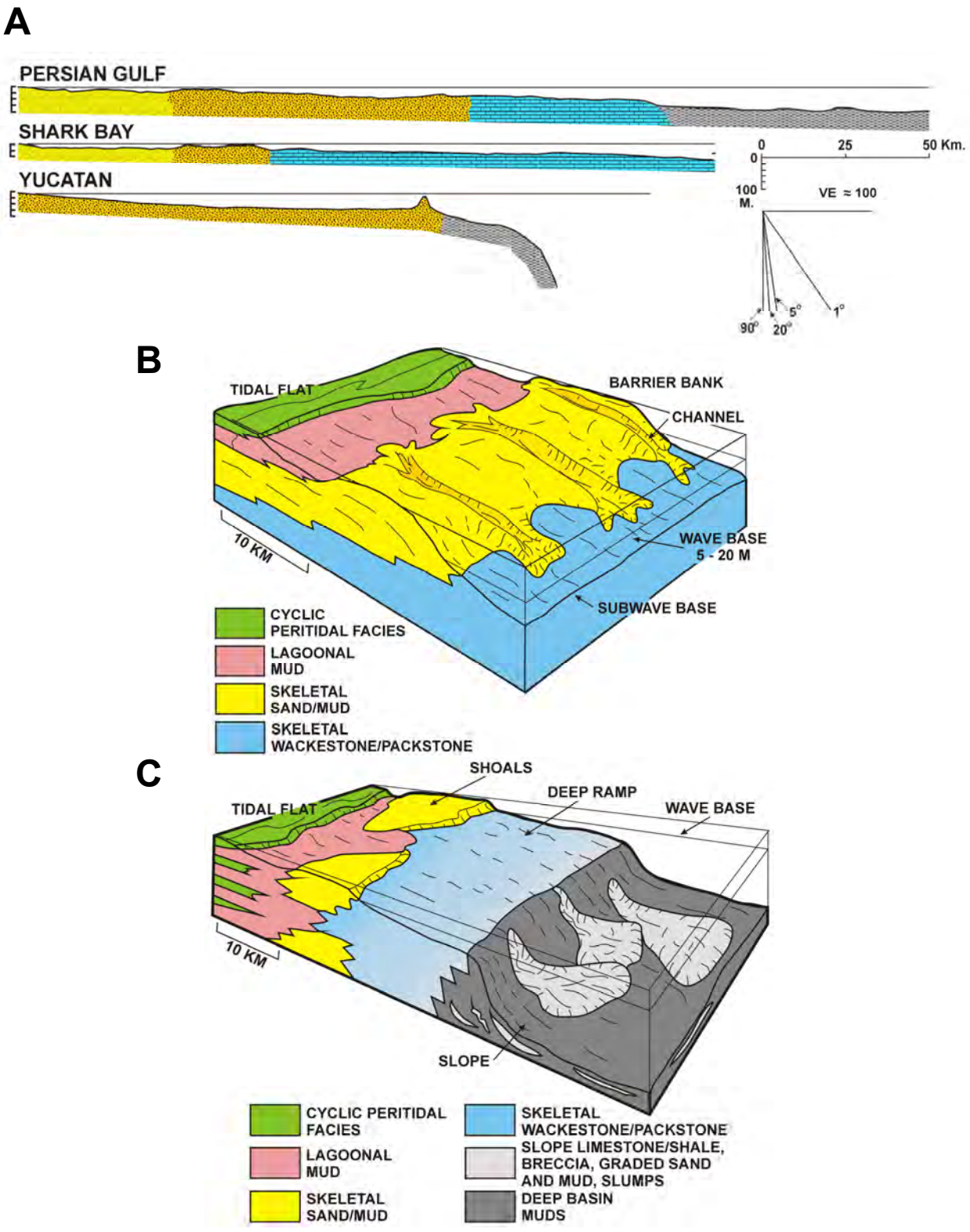

Figure 9. Carbonate ramps, modified from Read (1985). A - Modern carbonate ramps. B and C - Two of carbonate ramp model end members: the barrier-bank type ramp (B) and distally steepened ramp (C).

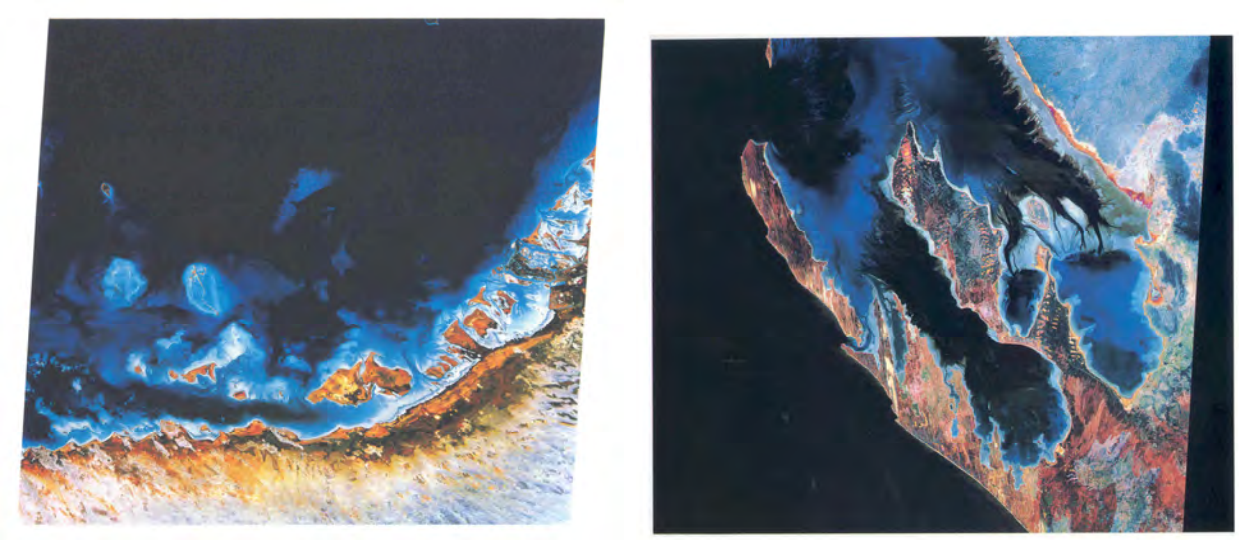

Figure 10. Modern homoclinal carbonate ramp environments. A - Landsat image of the southeastern coastline of the Arabian Gulf. The carbonate ramp slopes gently north from the coastline to the axis of the basin. Water depth at the top of the photograph is approximately 40 m (131 ft). Intertidal flats occur along the Arabian coastline and face the lagoon developed between the mainland and the offshore barrier bank complex. B - Landsat image of Shark Bay, Western Australia. Hamelin Basin, on the west side of the image, contains three principal sub environments, namely the peritidal zones that fringe the bay, a sublittoral platform that extends into the basin, and the embayment plain in the center of the basin.

deepening trend consisting of middle to deeper ramp facies. The Salona, and Coburn Formations exhibit an upward deepening, then upward-shallowing trend comprised of low-energy deep ramp facies overlain by slope and basin facies, which are, in turn, overlain by more proximal deep ramp facies (Figure 12). We present the details of our descriptions, interpretations, and arguments in the discussion of the outcrop.

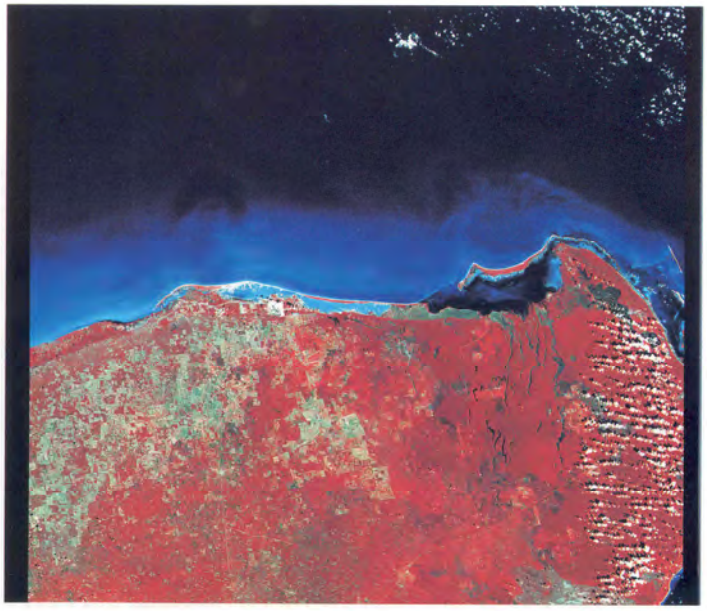

Figure 11. Landsat image of northern Yucatan, Mexico. This is a distally steepened carbonate ramp. Complex carbonate sand bodies and an adjacent lagoon are developed along the coastline updip of the platform to basin transition.

Hardgrounds

Hardgrounds are synsedimentarily lithified carbonate seafloors that become hardened *in situ* by the precipitation of carbonate cement in the primary pore space (Wilson and Palmer, 1992, p. 3). They are sedimentary horizons in marine carbonates that exhibit evidence of exposure on the sea floor as lithified rock (Figure 14). Hardgrounds form under a reasonably consistent set of physical conditions; thus geologists use hardgrounds to estimate ancient sedimentation and erosion rates, oceanic geochemistry, and both tectonic and eustatic sea level changes. Hardgrounds are often thought to mark the tops of regressive sea level changes, or at least to have

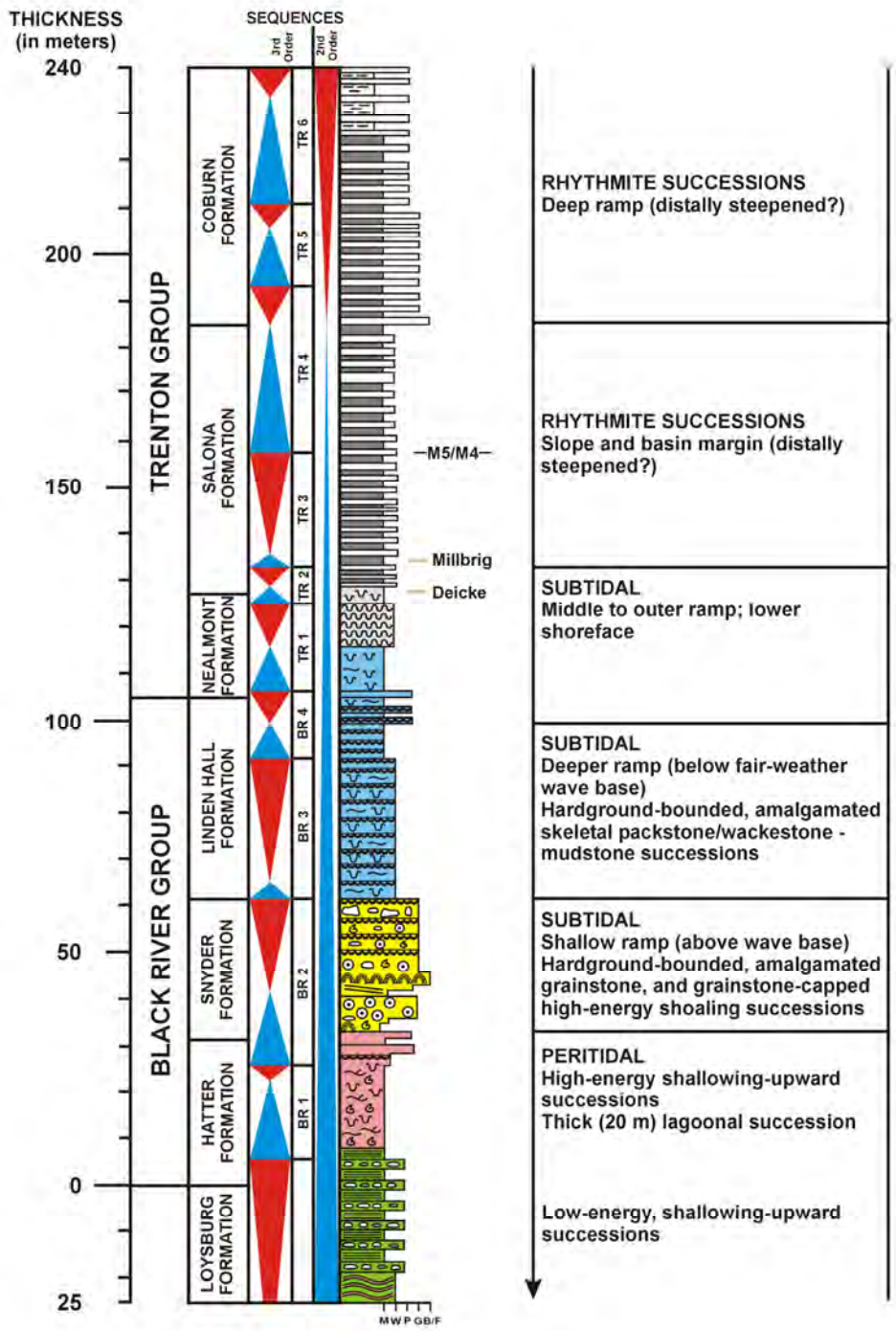

Figure 12. Our measured section (June - July, 2003) for the Trenton and Black River Groups exposed along Pennsylvania Route 453 near Union Furnace, and the vertical stacking pattern of carbonate facies there (see Figure 13 for a key to the symbols) The blue triangles indicate deepening-upward facies successions, and the red ones indicate shallowing-upward facies successions. BR 1, BR 2, etc. indicate third order stratigraphic sequences interpreted from the facies successions. M5/M4 is the positon of one particular sequence boundary from the sequence stratigraphic scheme of Holland and Patzkowsky (1996). This boundary along with the positions of the Millbrig and Deicke K-bentonites permit callibration with other Middle Ordovician stratigraphic sections in the eastern U. S. and mid-continent regions.

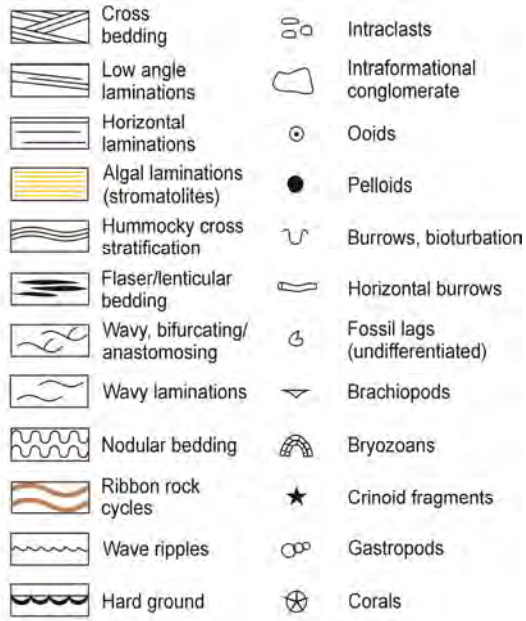

Figure 13. Legend for symbols used in the stratigraphic diagrams (Figures 12, 35, 41, 46, 49, and 54).

Figure 14. Dramatic hardgrounds exposed on the shoreface near Bimini in the Bahamas. Although often cited as evidence for the lost continent of Atlantis, Shinn (1978) demonstrated the sedimentary origin of these spectacular formations.

been followed by transgression (Fursich, 1979; James and Bone, 1991; Jones and Desrochers, 1992; Lehrmann and Goldhammer, 1999) (Figure 15). Other hardgrounds form rapidly, however, and are not associated with sea level changes (Shinn, 1969; Dravis, 1979; Brett and Brookfield, 1984; Hillgartner et al., 2001).

Paleontologists study hardgrounds to determine the different organisms that adapted to life on these hard surfaces (Brett, 1988). Well-preserved hardground biotas provide an opportunity to analyze a paleoecosystem with accuracy not possible in most fossil assemblages (Wilson and Palmer, 1992).

Hardgrounds are one of the most conspicuous and important carbonate rock features at Union Furnace. Yet they apparently have gone unrecognized here throughout decades of study at this outcrop. They have been misidentified as mud cracks by some workers (see Rones, 1969), a significant mistake because these hardgrounds signify submarine cementation, exposure, and erosion rather than subaerial exposure. Although Faill et al. (1989) did not designate hardgrounds in these rocks, they did note, “light colored, very irregular bands, 0.5 to 2 cm thick and 3 to 10 cm apart, that extend for 2 meters or more” in the Snyder Formation. They estimated that these bands (which are hardgrounds) constitute at least 15 percent of the entire Snyder Formation.

James and Choquette (1990) listed numerous criteria for recognizing ancient submarine hardgrounds, and Demicco and Hardie (1994) added to that list. Fursich, 1979 suggested a combined morphological-genetic classification of hardgrounds. Brett and Brookfield (1984) published an excellent paper on the morphology, paleontology, and origin of carbonate hardgrounds in the Trenton and Black River Groups of southern Ontario, Canada. They modified Fursich’s classification, and we find this most applicable for describing the hardgrounds exposed at Union Furnace. We recognize the following types of hardgrounds described by Brett and Brookfield (1984) (Figure 16):

- *Smooth hardgrounds*: developed on uniformly cemented beds by removal of unlithified sediment without significant erosion; lack burrow systems
- *Rolling hardgrounds*: formed by slight erosion of a nodular bed, or a bed with dwelling burrows
- *Hummocky and undercut hardgrounds*: form

through further erosion of rolling hardgrounds accompanied by differential removal of unlithified sediment from burrows and between nodules

- *Pebbly hardgrounds*: formed by erosion and collapse of hummocky and undercut hardgrounds
- *Reworked hardgrounds*: formed by removal of pebbles to other depositional sites
- *Planar hardgrounds*: formed when the sediment filling burrows lithified to the same hardness as the rest of the bed; involved significant erosional planning
- *Composite hardgrounds*: closely adjacent hardgrounds formed by renewed sedimentation and erosion, and closely spaced hardgrounds that feather into one another

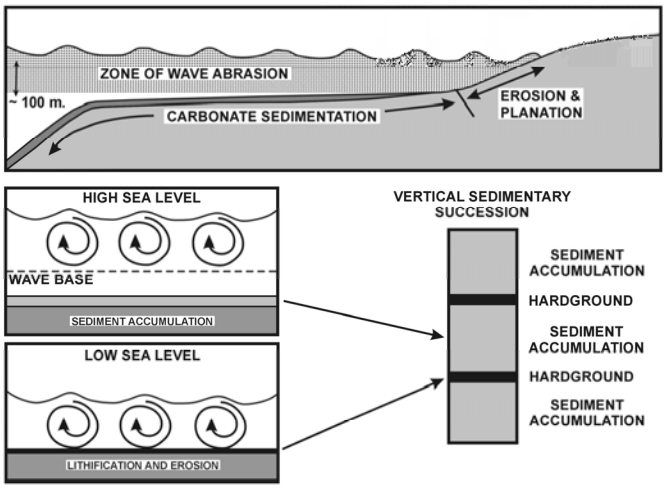

Figure 15. Diagram illustrating the effects of sea level variations on carbonate sedimentation, hardground formation, and the development of vertical sedimentary successions. Hardgrounds form when water is actively pumped through the sediments promoting submarine cementation. They also are actively eroded during low sea level stands too. Carbonate sedimentation resumes during higher sea level stands. Modified from James and Bone (1991).

These morphologies can be further modified by bioerosion to create pitted and extensively bored hardground beds. All of these hardground types are present at the Union Furnace outcrop. Hardgrounds occur in all of the formations exposed there. They are extensively developed as composite hardgrounds in the Snyder and Linden Hall Formations. Figures 17 to 19 illustrate some common hardground morphologies found at Union Furnace.

Nodular limestones often form through early diagenetic processes on the sea floor, and might be related to early hardground formation. For example, nodules of limestone produced by differential cementation of slope deposits off the Bahamas bank may be a modern analogue for nodular bedding found in ancient distal ramp carbonates (Mullins et al., 1980). When nodule growth continues in these environments, a partially continuous to continuous three-dimensional framework takes shape, which might eventually form an incipient hardground. Nodular bedding in limestones at Union Furnace might reflect initial hardground development (Figure 20). Compaction and pressure solution, however, have severely modified both the depositional and early diagenetic fabrics of nodular-bedded limestones at Union Furnace, particularly in the Nealmont Formation. It is difficult to discriminate

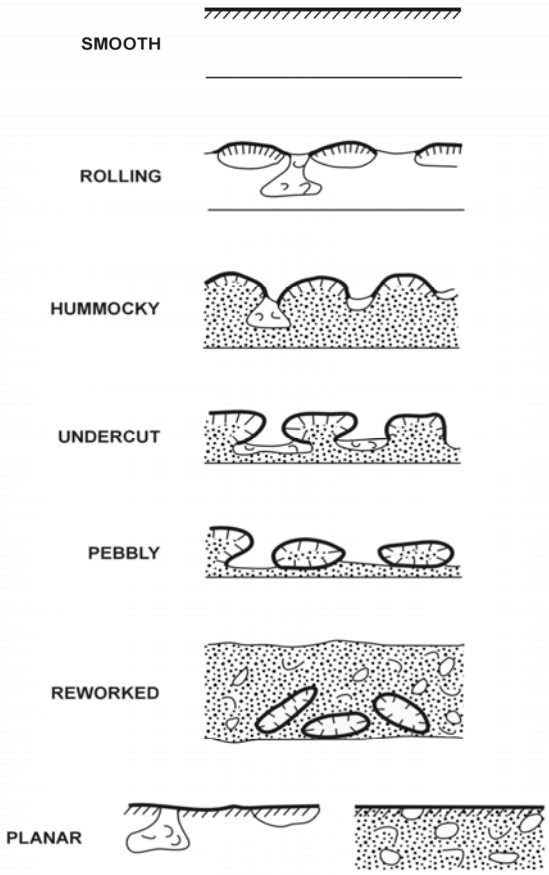

Figure 16. Brett and Brookfield's (1984) morphological classification of hardgrounds.

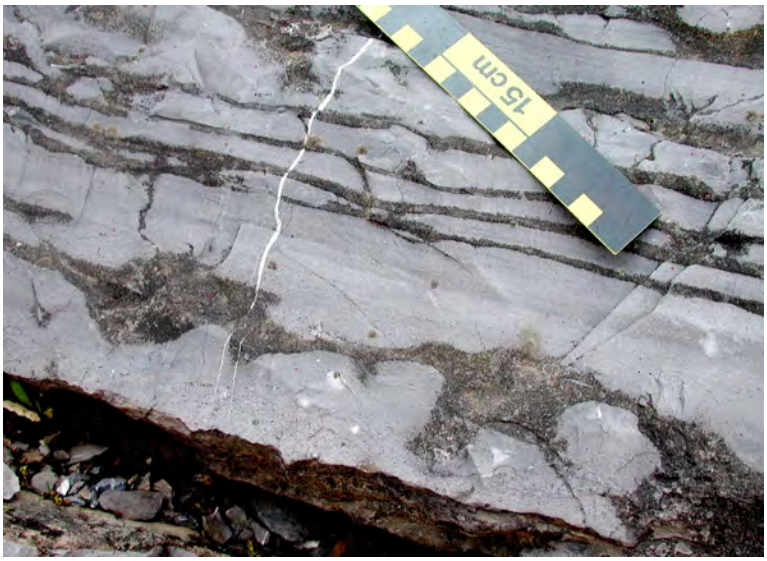

Figure 17. Hardgrounds near the top of the Hatter Formation at Union Furnace. The rocks exhibit several morphological types. Most are smooth to rolling hardgrounds, but hummocky and undercut hardgrounds developed on the lowest bed and some of the upper beds. The hardground beds are graded bioclastic grainstone. The normal grading indicates decelerating flow and resedimentation, probably from storm wave-generated suspensions. These "event depositions" were followed by periods of non-deposition long enough for hardgrounds to develop through submarine cementation. These beds are near the top of a high-energy shallowing-upward peritidal succession, and probably formed on the flank of a shallow shoal area, or in an intershoal area.

Figure 18. Undercut to pebbly hardgrounds in the Linden Hall Formation. Advanced erosion and differential removal of unlithified sediment from between lithified, eroded hardground has undercut some of the limestone. Erosion and collapse of the undercut hardground formed large intraclasts.

Figure 19. Reworked hardground in the Linden Hall Formation.

Figure 20. Nodular bedding in the Nealmont Formation. A - Isolated nodule of skeletal floatstone in organic-rich mudstone. B - Coalescing nodules of skeletal floatstone and wackestone interbedded with organic-rich mudstone in the Nealmont Formation.

between depositional, diagenetic, and compactional fabrics in many of the nodular bedded limestones.

Sequence Stratigraphy

Holland and Patzkowsky (1996) established a sequence stratigraphic framework for Middle and Upper Ordovician rocks of the southern Appalachians, the Cincinnati Arch, and the Nashville Dome. They recognized fourteen depositional sequences in the Middle and Upper Ordovician strata of these regions. Six of these sequences begin in the Mohawkian Series, and three of these (M3, M4, and M5) include the Turinian (former Black Riverian) and Chatfieldian (former Trentonian or Rocklandian-Kirkfieldian) Stages.

Cornell et al. (2001) suggested that the Black River Group of central New York state and adjacent Ontario comprises most or all of the M3 and M4 sequences. The also suggest that the Watertown, Selby, and Napanee Formations in the Trenton Group of central New York comprise M5, and that the base of the Watertown Formation should be used as the Trenton-Black River boundary.

Baird et al. (2000) interpreted four third-order sequences in the Trenton Group of central New York and southern Ontario. Smith and Nyahay (2002) identified six third-order sequences in the Trenton Group and four third-order sequences in the Black River Group in the Matejka #1 core from Chemung County, NY. We recognize what may be the same sequences proposed by Smith and Nyahay (2002) at the Union Furnace outcrop here in central Pennsylvania.

We discern four third-order sequences in the Black River Group and six third-order sequences in the Trenton Group in the strata that we measured along PA Route 453 at Union Furnace (Figure 12). The first (BR 1) begins in the lowermost Hatter Formation (Figures 12 and 35 — see p. 30). We interpret the contact between low-energy, shallowing-upward peritidal successions and distinctive lagoonal facies (about 3 m [10 ft] above bentonite B0 in Unit 2) as a combined sequence boundary/transgressive surface, as described by Holland and Patzkowsky (1996) for Ordovician carbonate sequences in the eastern United States. This boundary marks the first flooding surface beginning a set of retrogradational parasequences, i.e., an overall deepening upward trend. Lowstand facies are conspicuously absent (see Holland and Patzkowsky, 1996 and Railsback et al., 2003 for discussions of this interesting peculiarity of the Ordovician sequences). The lagoonal facies comprise the transgressive systems tract. The tidal facies of Units 4 and 5, and the high-energy shallowing-upward parasequences of Unit 5 and

lower Unit 6 in the upper Hatter Formation comprise the highstand systems tract.

The second sequence (BR 2) comprises the uppermost Hatter Formation (upper Unit 6 and Units 7 and 8) and all of the Snyder Formation (Figures 12, 35, and 41). The BR 2 sequence boundary is marked by very thin beds (centimeter scale) of coarse siltstone or very fine-grained subarkose and very silty (up to 50% quartz and plagioclase grains averaging 0.05 mm in diameter) pelloid-fossil grainstone. These beds contain ripple laminations and horizontal to wavy bedding. This interval consists of lowstand deposits that we interpret as water- or wind-borne clastics transported into a paralic carbonate environment. Above these unusual lithologies the sequence deepens rapidly through stacks of nearshore parasequences in the uppermost Hatter Formation and grainstone-capped, high-energy offshore shoaling successions in the lower half of the Snyder Formation. These facies define the transgressive systems tract. The appearance of distinctive bryozoan bioherms at the base of high-energy shoaling successions and hardground-bounded, amalgamated grainstone successions in Unit 12 marks the beginning of the highstand systems tract. The sequence shallows upward to the contact with the Linden Hall Formation.

The third sequence (BR 3) occurs within the bottom two-thirds of the Linden Hall Formation (Figures 12 and 46). We interpret the contact between the Linden Hall Formation and the underlying Snyder Formation as a combined sequence boundary/transgressive surface. This contact marks the beginning of another overall deepening-upward trend that extends a little more than 5 m (16.4 ft) up into Unit 17. We interpret the maximum flooding surface at 67.2 m (220.5 ft) in our measured section where discrete, continuous storm-generated beds replace random, lenticular storm-generated packstones that are isolated within the dominant mudstones and wackestones of the deeper carbonate ramp. Stacked, shoaling-upwards parasequences comprised of hardground-bounded, amalgamated packstone/wackestone successions that coarsen upwards into cross-bedded and hummocky cross-stratified grainstones defines the highstand systems tract.

Sequence BR 4 begins at the base of Unit 21 where yet another deepening-upward succession denotes a combined sequence boundary/transgressive surface (Figures 12 and 46). The maximum flooding surface occurs at the top of Unit 22 in the upper Linden Hall Formation. Very fossiliferous, shoaling-upwards parasequences at the top of the Linden Hall Formation represent the highstand deposits of BR 4. A subtle regional unconformity at the top of the Linden Hall Formation (Rones, 1969) marks the top of sequence BR 4.

There is a basinward shift in facies at the base of the Nealmont Formation, which we interpret as a sequence boundary at the base of TR 1, the first sequence in the Trenton Group (Figures 12 and 49). Lowstand carbonate facies occur as stacked parasequences of thick-bedded, bioturbated mudstones with discontinuous skeletal wackestone and floatstone lenses that shoal upwards to fossiliferous, wavy and cross-bedded packstones. Undulatory, argillaceous lamina and bands are common in the lower 7 m (23 ft) of the formation. An abundant and diverse normal marine fauna and high degree of bioturbation indicate relatively shallow water conditions of the lower shoreface (Arens and Cuffy, 1989; Slupik, 1999). Above these lowstand deposits, transgressive carbonate facies in the Nealmont Formation indicate deepening outer ramp environments to about the 122 m (400 ft) mark of our measured section near the base of Unit 26 (Figure 49). At this point, distinctive nodular bedding characterizes the rest of the formation up to the contact with the Salona Formation. This nodular facies, often mapped as the Rodman Member of the Nealmont Formation, is more fossiliferous and coarser grained than underlying rocks in the Nealmont Formation. Rones (1969) mapped the Rodman as an offlapping succession, and Arens and Cuffy (1989) documented wave-induced shoaling and bioherm development in this member at other locations. We interpret this facies as shallowing highstand deposits.

The second sequence in the Trenton Group, TR 2, is condensed – only about 2 m (6.6 ft) in thickness. It begins at the base of the Salona Formation with burrowed, deeper water mudstones that overlie the nodular wackestones and floatstones of the Nealmont Formation (Figures 12 and 49). We interpret these mudstones as deepening through the Deicke K-bentonite (B12) and the K-bentonite immediately above the Deicke, B13 (Figure 49). We consider these remarkably thick and well-preserved K-bentonites to have been deposited in relatively deep water on the outer ramp. The Deicke K-bentonite was deposited at a time of significantly increased water depths across the entire epicontinental sea that covered much of eastern North America in the Middle Ordovician (Leslie and Bergstrom, 1997). At this location, it was a time of very low sediment accumulation in the deepest water of the region (Leslie and Bergstrom, 1997). Burrowed and wavy laminated mudstones occur again above B13.

TR 3**,** the third sequence in the Trenton Group, begins at the base of the rhythmites in the lower Salona Formation (Figures 12 and 49). This contact represents an abrupt change to a deeper water environment: outer ramp mudstones are sharply overlain by distal rhythmites of the ramp slope and basin margin. This contact is another combined sequence boundary/ transgressive surface, and we interpret it as a drowning unconformity separating a highstand systems tract from a transgressive systems tract. This unconformity is what Schlager (1999) proposes to call a Type 3 sequence boundary. The Salona rhythmites continue to deepen upward for about 6 m (19.7 ft) to the Millbrig K-bentonite. Above this, the rhythmite beds thicken, coarsen, and become more fossiliferous indicating highstand deposition.

The shallowing upward trend of the TR 3 highstand systems tract extends to the base of the Roaring Springs member of the Salona Formation (just above 150m on our measured section on Figure 12). Patzkowsky et al. (1997) and Slupik (1999) place the M4/M5 sequence boundary of Holland and Patzkowsky (1996) here. Evidence for this sequence boundary includes the change from mudstones and argillaceous mudstones to laminated quartz- rich mudstones, an increase in terrigenous clay, and the evident changes in bedding thickness. This boundary also exhibits a remarkable shift in the δ13C value of carbonate and organic carbon indicating that sea level rise and changes in oceanographic conditions were associated with major perturbations to the carbon cycle (Patzkowsky et al., 1997, p. 912). We arbitrarily named this new sequence TR 4. The deepening transgressive systems tract extends upwards to the base of the Coburn Formation where the abrupt appearance of very fossiliferous, wave-agitated strata marks a turn around to progradational highstand deposition. This TR 4 highstand continues on up to about the 195 m (640 ft) mark of our measured section (Figure 12).

The two remaining third order sequences in the Trenton Group shown on Figure 12, TR 5 and TR 6, are interpreted from the detailed measured sections presented by Slupik (1999). These are tentative for the time being while our own work continues.

We warn that our ideas concerning the sequence architecture of this outcrop are conjectural at this time, and await further measurements, descriptions, and correlations before they can evolve into a useful concept of sequence stratigraphy in this part of the basin.

ARCH SPRING FARM

Group Meet, Lunch and Trip Coordination

Special thanks to Linda and George Pedlow for allowing us to meet and have lunch at this historic and geologically fascinating farm (Figure 21).

Arch Spring Farm: A Short History

By Linda Morrow

Dave and Linda Morrow bought Arch Spring Farm in 1983, virtually a life-long dream for Dave's, who had grown up on a farm two miles away. They restored the smaller Mill House in 1986 and the larger Manor House, the Jacob Isett house, ten years later. Linda and her family have continued to operate both as a B&B since Dave's passing.

This farm is the site of the once thriving small rural village of Arch Spring, still identified as such on PennDOT's standard roadmap. Both are named for the remarkable natural geologic wonder located on the farm property - Arch Spring - with its natural limestone arch and voluminous flow. It has been noted in publications, and visited continuously, as a site of natural beauty for well over 200 years. It can only be assumed that Native Americans knew of, and wondered at, this place long before that.

Jacob Isett came to Sinking Valley in 1785. He had been a shoemaker as well as a gristmill operator in the southeastern part of Pennsylvania. When he arrived in Sinking Valley he lived in an abandoned building at Ft. Roberdeau and earned his living making shoes which he traded for grain. He amassed a lot of wheat in a year before crop failure and so was able to sell his grain for enough money to buy the land at Arch Spring from William Penn's heirs in 1795, it having been part Lot 33 of the Penn's Manor of Sinking Valley.

Jacob Isett first built the small stone structure that is now behind the main house. The ground floor would have been used as kitchen/living room and the upstairs as sleeping quarters. The second floor is interesting as it has 4 slits for windows which are wider on the inside than the outside. This design permitted a rifle to be aimed at attacking Indians or other intruders. The British had enlisted Indians to help them in the Revolutionary War, so there may have still been unfriendly natives around when the "fort" was built. Between each set of windows are indentations of the same design that Dave and Linda had seen in Fort Michilimackinac, another Revolutionary War fort in upper Michigan. They were told there that the indentations were to hold ammunition.

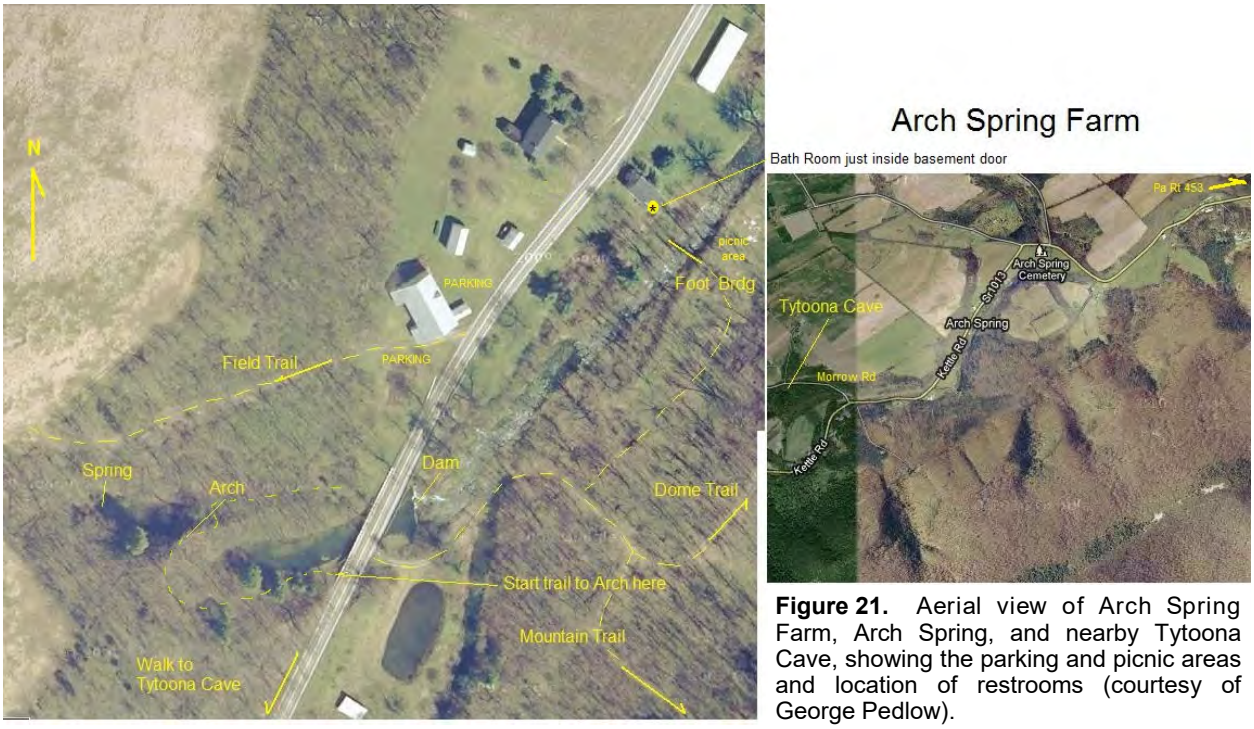

Figure 21. Aerial view of Arch Spring Farm, Arch Spring, and nearby Tytoona Cave, showing the parking and picnic areas and location of restrooms (courtesy of George Pedlow).

Jacob Isett built a saw mill and a very large wooden grist mill next to the stone building now called the Mill House. He diverted some of the stream from the spring into a mill race. The "upstream" end of that mill race can be seen near the road bridge crossing Arch Spring's outflow. The wooden mill was dismantled in 1942, but the covered bridge like structure, a scale house, still stands. Wagons were weighed empty and again with grain to determine the weight of the grain milled or sold. The "works" for the balance scale can still be seen. A blacksmith and wagon shop, a shoemaker's shop and a cider press were once part of the village in the 1850s. Remains of the foundations of small homes can be seen on the other side of the modern foot bridge.

The Mill House was historically a commercial building, having served variously as a general store, warehouse for the grist mill, and Arch Spring Post Office. There is no evidence of an original early chimney, indicating that it was not built for habitation.

It is intriguing to think that the Mill House might have been built in 1799 because of a threshold stone carved "ISETT 1799" in the building. However, the location of the stone, with lettering facing upward, on the threshold of the warehouse door 3 stories above the ground, may indicate that the stone was recycled from an earlier location. A Penn State historical geographer estimated the Mill House was built in the 1830's, but there is also an interesting architectural similarity to the 1817 version of Sinking Valley Church, of which a good photograph survives, taken in the 1870s before that church was rebuilt in its present form.

The plaque just under the gable at the north end of the "Manor House" indicates the building was completed in 1805 for Jacob and Eleanor Isett. Other stone houses of very similar design and trim exist in the Olny Valley of SE PA, so it may be the builder came from there and might have brought mill work and other building materials with him. Both houses at Arch Spring, viewed together, share architectural features with the Lemon House that served primarily as a restaurant and bar to patrons of the Allegheny Portage Railroad.

Originally the Manor house had no insulation, just plaster and wall paper and chair rail over the inside of the stone walls. It was probably the early 1900's, when electricity was put in, that the perimeter walls were studded and plaster was applied over lathe. In the 1920's there was a major fire in the living room which apparently destroyed the original woodwork there. Very ugly 1920's woodwork was taken out in the 1996 restoration. The built-in cabinets in the dining room are believed to be original to the house. When indoor plumbing was installed, maybe during fire damage repairs, a bathroom was added at the front of the upstairs hall. There were originally 5 bedrooms on the second floor with the 5th bedroom accessible only by the former back stairwell or through another bedroom. In 1996 the 5th bedroom was converted into two more bathrooms and an upstairs laundry. The Manor House now has two geothermal furnaces and hot water heaters. The pipes run under the field to the north of the house.

At the start of Mill House restoration in 1986, there were no studded or plastered walls, and of course no insulation. Although these features were added, heating is electric, so the building is winterized every year from January at least into April.

Figure 22. Arch Spring. View is from the top of the limestone arch (see Figure 26).

Arch Spring and Related Karst Features

by Christopher D. Laughrey

Arch Spring (Figure 22), with an average discharge of 8000 gallons per minute, is the eighth largest spring in

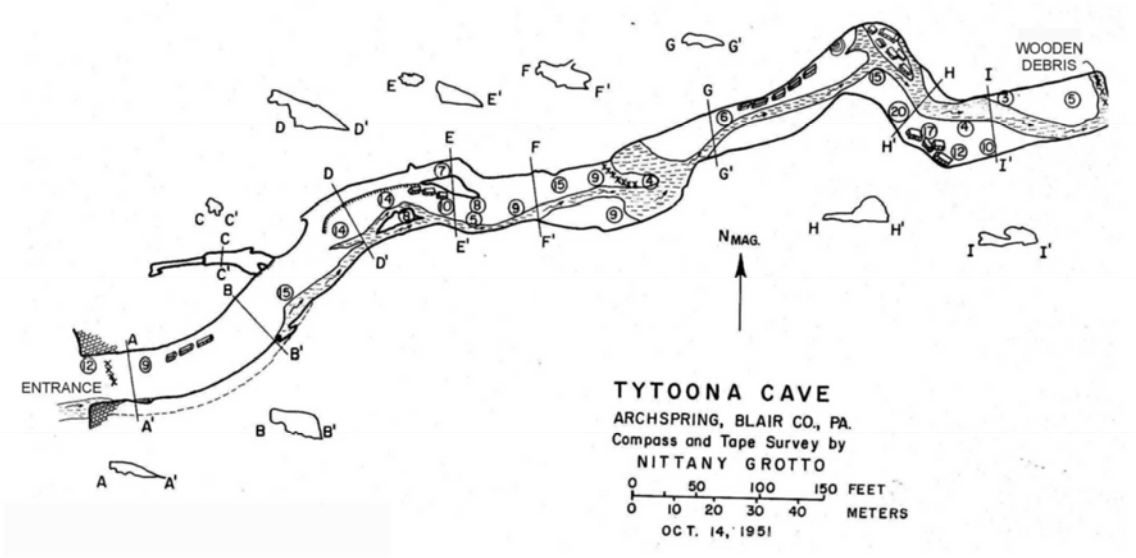

Figure 23. Map of Tytoona Cave as far as Sump 1(courtesy of W. B. White). This sump is only 2.4 m (8 ft) deep and 12 m (40 ft) long. It leads to a beautiful air-filled chamber with spectacular cave formations. Additional sumps and chambers lie beyond.

Figure 24. Stalagmites and stalactites in the first chamber beyond Sump 1 in Tytoona Cave. Photo courtesy of William Berkepile, leader of the current cave diving survey in Tytoona Cave.

Figure 25. Spectacular soda straw stalactites, up to 2.6 m (25 ft) in length, in the first chamber beyond Sump 1 in Tytoona Cave. Photo courtesy of William

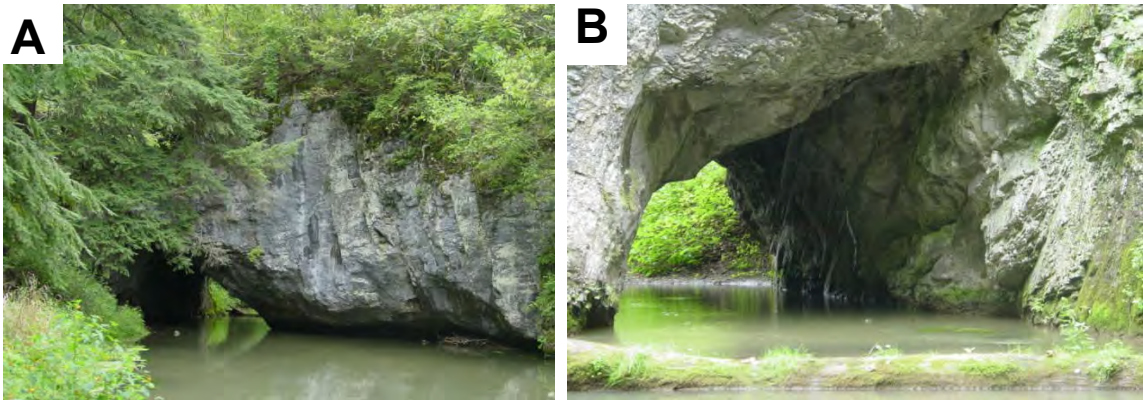

Figure 26. Two views of Pennsylvania's only natural limestone arch at Arch Spring. A) View from the road looking southwest. B) View from the spring basin looking northeast. The arch and spring are in the Loysburg Formation.

Pennsylvania. The discharge ranges from 2000 to 30,000 gallons per minute. This is the resurgence of Sinking Run, which disappears into a sump in Tytoona Cave (Figure 23), about 1.6 km (1 mi) southwest of Arch Spring. The entrance to Tytoona Cave is in a large collapsed sinkhole in the Hatter Formation. About 305 m (1,000 ft) of easily navigable passage extends from the entrance to the sump (Figure 23). Cave diving beyond the sump reveals additional dry passage, and some of the most beautiful flowstones, stalagmites, and stalactites in the state (Figure 24). The latter include spectacular soda straw stalactites (Figure 25), which are the second longest known in the world. Preservation and conservation of this resource are assured by the current ownership and stewardship of the National Speleological Society (NSS). The sump blocks the casual visitor, and cave diving operations, permitted for research only, are strictly managed by the NSS.

Dye tracing and surveying by cave divers have linked Tytoona Cave with Arch Spring. Several additional sumps and dry passages in Tytoona Cave lead northeast to a terminal sump with depths of about 24 m (79 ft). Breakdown there has prevented further underwater penetration to date. Diving operations at Arch Spring have revealed an additional dry passage and more sumps that lead to a large submerged room. This last underwater room descends to a tight, narrow passage at a depth of 32 m (105 ft) and then ascends to about 21 m (70 ft) where further penetration is impeded by breakdown. This is about 0.4 km (0.25 mi) from Arch Spring. Some explorers suspect this is the sa m e breakdown encountered when swimming northeast from Tytoona Cave. This is very speculative, however, and surveying has not yet physically linked the passages. Surveying efforts in the 1980s ended in tragedy with the death of Roberta Swicegood, an accomplished and capable cave diver, at Arch Spring. Underwater surveying has only recently resumed here. Dye tracing, chemistry, and analyses of suspended sediment load suggest that Tytoona Cave is the master conduit for the water resurging at Arch Spring (William B. White and Ellen K. Herman, per. Comm., 2003).

The arch here at Arch Spring (Figure 26) resembles the renowned Natural Bridge in Virginia, but is much smaller. The arch is approximately 15 m (49 ft) high, and its opening is about 6 m (19.7 ft) in diameter. Sinking Run flows through it. Upstream from the arch is a small spring basin in a large, steep-sided sinkhole. The latter is 30.5 m (100 ft) long, 15 m (49.2 ft) wide, and about 10 m (33 ft) deep. The actual spring opening is only about 1.2 m (4 ft) in diameter. The basin and sinkhole are the remnant of a large cave room that collapsed thousands of years ago.

The karst geology and hydrogeology of Sinking Valley are fascinating subjects. Interested readers should refer to White (1976) and White and White (1999) for further information.

As an interesting aside for field trip participants, there is a very small and obscure cave entrance in the Snyder Formation at the outcrop we will visit after lunch at Stop 3 (Figure 27). Dr. William B. White, Pennsylvania State University, kindly shared his copy of the cave survey done there (Figure 28).

Figure 27. Entrance to Field Trip Cave along PA Route 453 near Union Furnace. The exposed rocks are in the Snyder Formation.

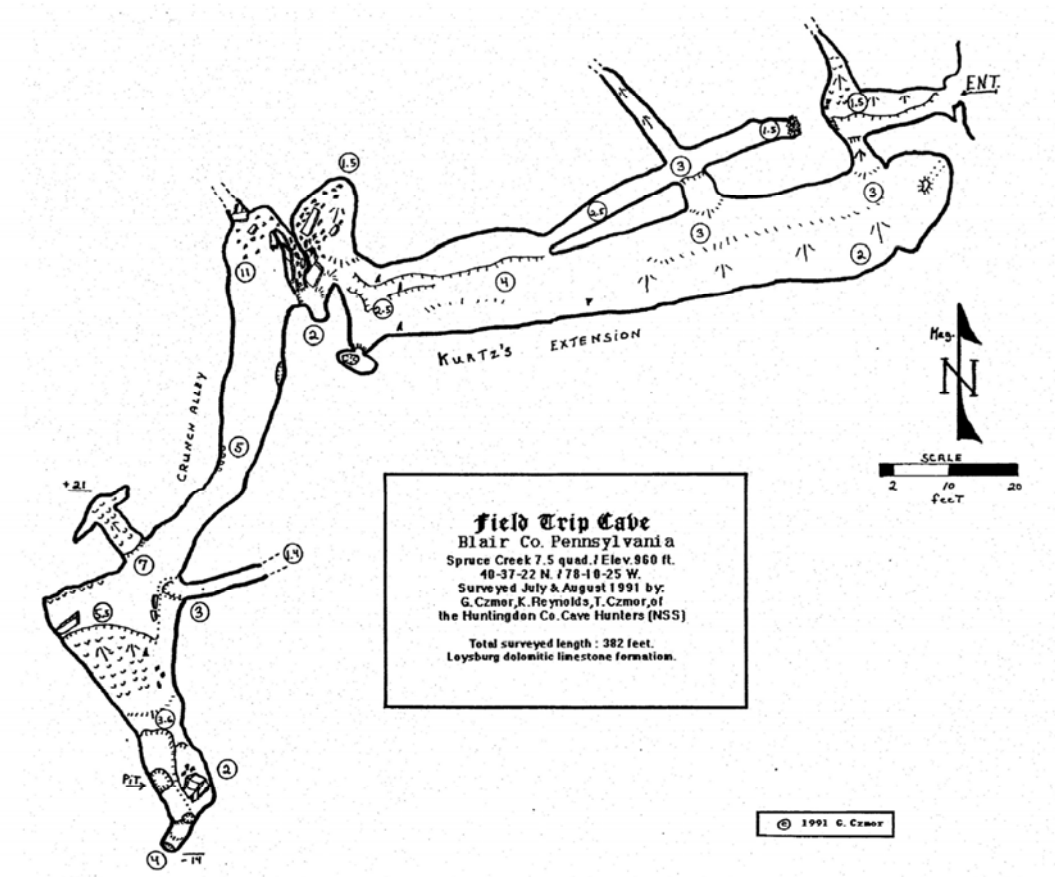

Figure 28. Map of Field Trip Cave (courtesy of W. B. White).

FIELD STOP: UNION FURNACE ROADCUT

Christopher D. Laughrey and Jaime Kostelnik

Introduction

The best exposed section of the Ordovician carbonates in central Pennsylvania is in the roadcuts along PA 453 between Tyrone and Water Street. From Shoenberger Road 2,107 m (6,912 ft) to the southeast (Figure 29), the stratigraphic succession of Nittany, Bellefonte, Loysburg, Hatter, Snyder, Linden Hall, Nealmont, Salona, and Coburn formations is exposed in almost continuous road-cuts. To the left (west) of Shoenberger Road is an abandoned quarry in the Mines Member of the Gatesburg Formation, and Stonehenge/Larke limestones and dolostones are exposed in the road-uts 183 m (200 yd) north of the intersection.

Although the emphasis of this field trip is on the formations in the Trenton and Black River Groups, we will examine the lithologies from the Coburn Formation to the Loysburg Formation that are exposed in the Union Furnace roadcut. We measured 240 m (787 ft) of Trenton and Black River Group rocks at the Union Furnace outcrop along PA 453 (Figure 12). A few more meters of partially to poorly exposed Trenton Group rocks extend above the top of our measured section on the southeast side of the road cut. We also measured 10 m (33 ft) of the Middle Ordovician Loysburg Formation below the Black River Formation in order to demonstrate the continuity of peritidal, low-energy shallowing-upward successions from the Loysburg up into the lower Black River Group.

Figure 29. Aerial photograph of Route 453, Union Furnace Quarry, and surrounding areas (March 2000).

You will find an abundance of abbreviations, numbers, names, and symbols marked on this outcrop. Numerous workers placed these over the past 25+ years. Note the green numbers on the rocks that denote the "mining units" shown in Figures 35, 41, 46, and 49. Although they were defined on both lithologic and convenient sampling intervals (i.e., thick sections of uniform lithology have been subdivided for sampling purposes), these units do not have stratigraphic significance. These subdivisions, established by Berkheiser and Cullen-Lollis (1986) (Figure 8), originally went from Unit 04 (Loysburg) to Unit 30 (Nealmont/Salona), and their work portrays the major element chemistry of these units graphically. The units have been extended into the Antes Formation. However, only units up to 47 in the Coburn (Trenton Group) are exposed in the roadcut. They have been carried into the roadcut by D.P. Gold and A.G. Doden from adjacent drill holes (see Plate 1 at the end of the guidebook). The units are discrete packages of strata that are convenient for chemical analyses and physical surface mining (Figure 8). We use the numbered units as a location guide at this outcrop, nothing more. The formation names are abbreviated here too, although in a few instances we question the formation boundaries. Previous workers have also marked the bentonites exposed here. These are designated B0 through B19. These designations are not related to the bentonites in the Salona Formation formally numbered by Kolata et al. (1996).

A vertical section (based on nearby cores) indicates a thickness of 55 m (180 ft) for the Salona Formation and at least 122 m (400 ft) for the Coburn Formation. A total thickness for the Trenton Group would be on the order of 183 m (600 ft). The chemistry of this group is characterized by an increasing presence upwards of alumina (0.8 – 4.0%), silica (14-21%), and 1-2% organic (?) "carbon". The basal Reedsville beds (Antes Member), despite their appearance as a black shale, are remarkably calcareous (25-37 % CaO, 3.6-4.2% Al2O3, 1-2% K2O, 21-43% SiO2, and 9-11% total carbon).

Structural Geology

by Duff Gold and Arnold Doden

The beds in the road-cut strike 060°-070°. The general dip is 30° southeast, but ranges from 22° to 45°. A dominant joint set, striking 140°-150° with near vertical dips, has been accentuated by the road-cut excavation. Apart from some mesoscopic scale folds near the east end, most of the deformation is manifest as faults (mostly mesoscopic scale, steeply dipping transcurrent with a shallow movement direction). Both left and right lateral senses of movement were recorded from jogged slickenlines (see red symbols on Plate 1). Movement sense also was determined from the accompanying *en echelon* tension cracks. Other faults include east-verging normal faults and west-verging oblique and dip-slip reverse faults. The regional faults are inferred from juxtaposed mapping units in the fields to the west. Except for the regional faults, no significant displacements were noted. These strata represent the northwestern limb of the Scotch Valley Syncline (Malik, 1999).

Stratigraphy, Depositional Environments, and Carbonate Petrology

Loysburg Formation

We will spend only a little time looking at the Loysburg Formation rocks exposed beneath the Black River Group. We want trip participants to see the peritidal low-energy, shallowing-upward successions that make up this formation (Chafetz, 1969), and note that these same cycles continue up into the lowermost Black River rocks.

Field (1919) named the Loysburg Formation for exposures of interbedded limestone and dolomite conformably overlying the Bellefonte Formation (upper Beekmantown Group – see Figure 5) in Bedford County, Pennsylvania. The Loysburg extends throughout the Valley and Ridge province in central Pennsylvania. Its thickness there is highly variable (Kay, 1944a; Faill and others, 1989). Faill and others (1989) report that the upper contact with the Hatter Formation of the Black River Group contact is sharp and conformable, but it is gradational here at Union Furnace along PA 453. The Loysburg is further subdivided into the Milroy ("Tiger Stripe" of Kay, 1944a) and Clover Members (Berg et al., 1983).

The Milroy Member consists of interbedded dolostone and limestone, i.e., ribbon rocks. The characteristic weathered banding of this unit provided Kay (1944a) with the name "Tiger Stripe" (Figure 30). The Clover Member constitutes the upper part of the Loysburg, and it consists of thick to very thick-bedded mudstones with minor amounts of wackestone, packstone, and grainstone.

Lithofacies and Depositional Environments – We concur with the interpretations of Chafetz (1969), Berkheiser and Cullen-Lollis (1986), and Gardiner-Kuserk (1988) that the Loysburg Formation is comprised of peritidal carbonate cycles. Chafetz (1969, p. 16) suggested that the Milroy Member was deposited in semi-isolated depositional basins, which were separated from one another by submergent or emergent ridges. The meter scale (or less) cycles exhibit vertical profiles indicative of low-energy peritidal shallowing-upward successions (Hardie and Shinn, 1986; Pratt et al., 1992).

Cycles begin with lags of intraclastic and/or bioclastic grainstone overlain by wave rippled, burrowed, skeletal wackestones (Figures 31A and 31B). Selective dolomitization occurred along some laminations, and around some burrows (Figure 31C). These rocks are subtidal deposits. The bioclastic and most intraclastic lags are transgressive, and sit on top of an underlying cycle. Some large, blocky intraclastic lags, however, probably are from the collapse

Figure 30. Alternating millimeter- to centimeter-thick layers of dolostone and limestone (mudstone) comprise the ribbon rocks in the Milroy Member ("Tiger Stripe") of the Loysburg Formation. The dolostone is light olive gray. The lime mudstone is light gray. See Demicco (1983) for an excellent explanation of the upper subtidal to intertidal origin of these rocks.

of tidal channel margins, and represent the base of a tidal channel fill (Figure 31A).

The rippled, burrowed skeletal wackestones are lagoonal sediments. These are overlain by thin, wavy, flaser, and lenticular bedded, variably bioturbated mudstones, with minor lenses and very thin beds of bioclastic and pelletal grainstone; these beds show evidence of periodic exposure such as mudcracks (Figure 32). These are intertidal facies. The ribbon rocks of the Milroy Member (Figure 30) were also deposited in subtidal to intertidal environments (Demicco, 1983).

The low energy shallowing-upward cycles are capped by microbially laminated mudstones, or stromatolites, which are partially to completely dolomitized (Figure 33). The stromatolites sometimes have a fenestral fabric, and may contain very thin interbeds of intraclastic or

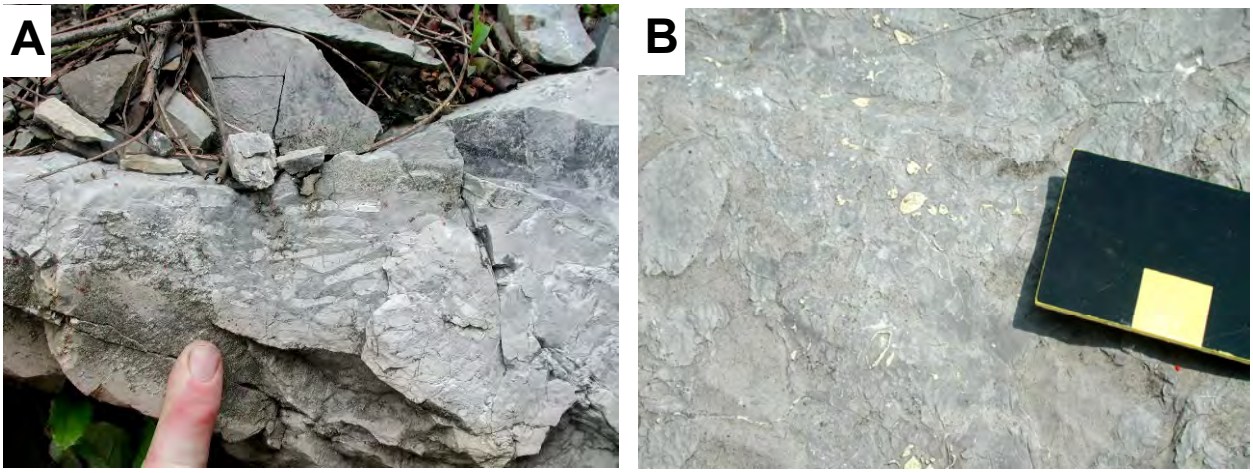

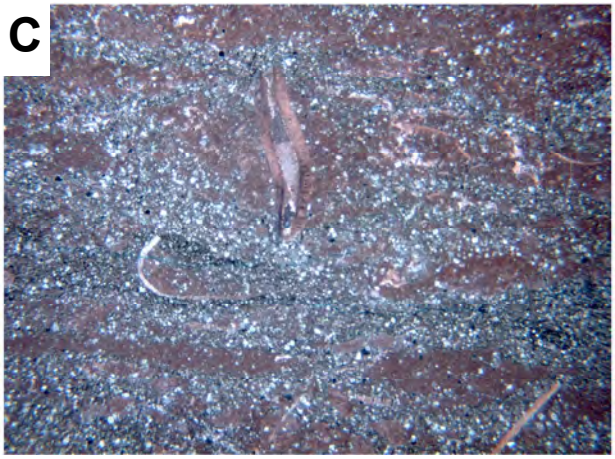

Figure 31. Subtidal peritidal facies in the Loysburg Formation. A - Intraclastic and bioclastic grainstone in the Loysburg Formation. Bioclastic and intraclastic lags at the base of shallowing-upward cycles typically are composed of sand-size grains. These large, blocky intraclasts, however, might be derived from collapse of a tidal channel margin within a cycle. B - Plan view of wave rippled and bioturbated skeletal wackestone in the Loysburg Formation. Skeletal material consists of brachiopods, bryozoans, echinoid fragments, and trilobite fragments. Note the isolated pockets of skeletal grainstone within the dominant muddier carbonate. C - Thin section of skeletal wackestone, like that shown in B. The scattered fossil fragments include brachiopods, bivalve mollusk debris, and trilobite fragments. The limestone is highly bioturbated. Dark, wispy compactional seams of organic matter and argillaceous material are pervasive throughout the matrix. Abundant idiotopic dolomite, and silt-sized quartz and feldspar are scattered throughout the sample. We believe the quartz and feldspar are authigenic.

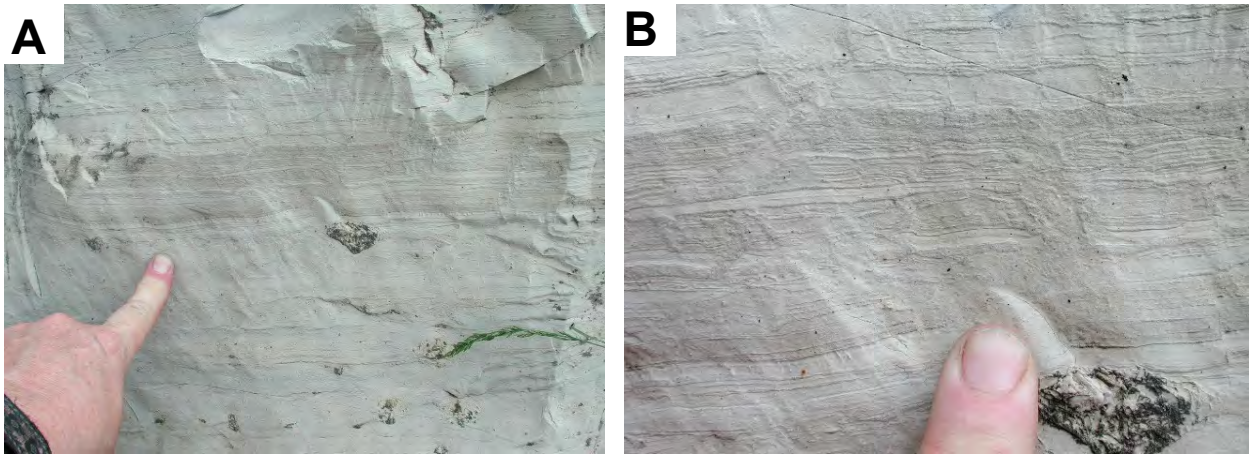

Figure 32. Two views of wavy, flaser, and lenticular bedding, and mudcracks in the Loysburg Formation.

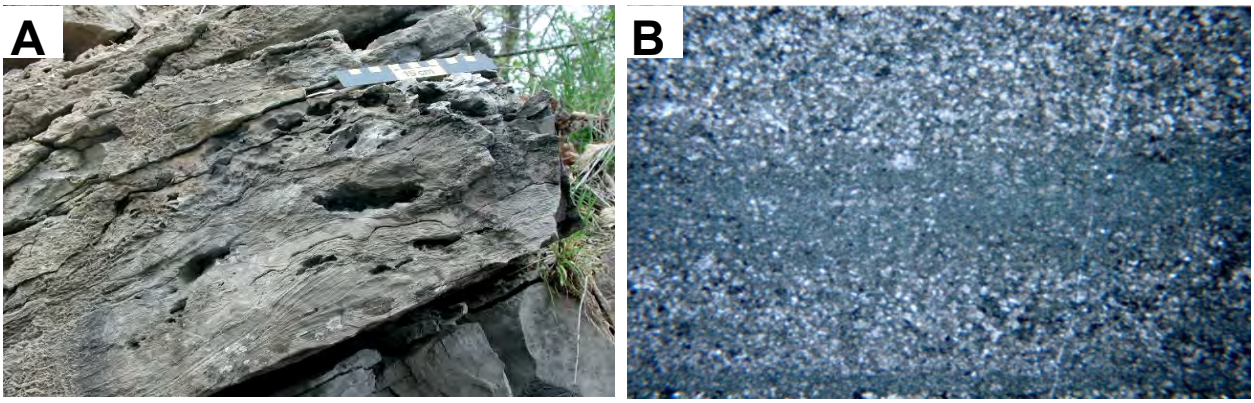

Figure 33. Microbially laminated mudstones in the Loysburg Formation. A - Outcrop view of stromatolites. Are the large vugs former evaporite nodules? B - Thin section photomicrograph of microbially laminated, dolomitic mudstone in the Loysburg Formation. Some lamina consists of rhombic-shaped euhedral to subhedral dolomite crystals (idiotopic dolomite) and micrite. Other lamina consists of clotted micrite. These internal fabrics, and the association of these cryptmicrobial laminites with flaser, wavy, and lenticular-bedded mudstones, indicate peritidal stromatolites, and possibly hypersaline conditions (Demicco and Hardie, 1994).

Figure 34. Chert at the top of a shallowing-upward peritidal cycle in the Loysburg Formation. Folk and Pittman (1971) suggested that chert such as this might be a replacement of former anhydrite.

bioclastic limestone. The microbially laminated mudstones may or may not show desiccation features. Some stromatolites exhibit large vugs, which might have originated as anhydrite nodules (Figure 33A). Chert nodules, lenses, and layers also might represent former anhydrite (Folk and Pittman, 1971) (Figure 34). These rocks were deposited in upper intertidal to supratidal environments (see Hardie and Shinn, 1986; Pratt et al., 1992).

Hatter Formation (Units 1 to 7) and Lowermost Snyder Formation (Unit 8)

Kay (1944a) named the Hatter Formation for exposures along Hatter Creek north of Roaring Spring in Blair County, Pennsylvania. He designated the exposure along the Conrail Tracks here at Union Furnace as the type section. Most exposures of the Hatter Formation in central Pennsylvania are very poor. The outcrop here along PA 453 offers the best exposure of the formation in the region; almost all of the formation is exposed here. Faill et al. (1989) report that the basal contact with the underlying Loysburg Formation is sharp and conformable, but it is gradational and conformable as marked at the PA 453 outcrop. Faill et al. (1989) place the upper contact with the overlying Snyder Formation at the oolite beds at the base of the latter.

We also discuss Unit 8, which is misplaced in the Snyder Formation here along PA 453, in this section of the guidebook. We suggest that Unit 8 as marked on the outcrop belongs to the Hatter Formation.

Figure 35 shows the details of our measured section through the Hatter Formation, and our interpretation of its sedimentary features.

Lithofacies and Depositional Environments – Berkheiser and Cullen-Lollis (1986) and Gardiner -Kuserk (1988) interpreted the Hatter Formation as tidal flat and lagoonal carbonates that developed on the updip region of a homoclinal ramp. We agree with this interpretation. The lower 6 m (20 ft) of the Hatter Formation consist of peritidal, low-energy shallowing upward successions similar to those found in the subjacent Loysburg Formation. These consist of meter -scale or smaller cycles composed of 1) bioclastic/intraclastic packstone or grainstone (subtidal, transgressive lags), 2) burrowed and bioturbated wackestone and mudstone, with minor wavy lamination (subtidal), 3) lenticular, flaser, and wavy laminated mudstone (intertidal), and 4) microbially laminated mudstone (supratidal). The first bentonite (B0) appears within this lower peritidal section of the Hatter Formation. The cycles of low-energy shallowing upwards successions end with a very thin bed of black, organic-rich, argillaceous mudstone.

The next 20 m (66 ft) of section above the peritidal cycles, the bulk of the Hatter Formation, consists of dark gray, burrowed and bioturbated, skeletal and peloidal wackestone and mudstone (Figure 36). These rocks have a number of characteristics typical of middle shelf lagoonal carbonate sediments described by Wilson and Jordan (1983). These characteristics are 1) a normal marine (stenohaline) biota (Figure 37), 2) muddy carbonate rock textures, 3) variable bedding thickness, and 4) extensive burrowing and bioturbation, with minor nodular, wavy, and flaser bedding. Very thin (centimeter-scale) layers of intraclasts and shell lags occur randomly throughout this lithofacies; these are storm layers (Types A and B1 of Gardiner-Kuserk, 1988) superimposed on a remarkably thick, homogeneous succession of lagoonal carbonate rocks. These sediments were likely deposited in a broad, largely protected lagoon behind the barrier banks of the middle ramp, as shown in Figure 9. Instructive partial modern analogues include the flat embayment plain of Hamelin Basin in Shark Bay, Western Australia (Logan et al., 1970; Harris and Kowalik, 1994), muddy carbonates of the semi-restricted Florida Bay (Enos and Perkins, 1977), Yalahau Lagoon on the northern Yucatan Peninsula (Logan et al., 1969; Harris and Kowalik, 1994), and Khor al Bazm lagoon along the Abu Dhabi 1973) (See Figure 38).

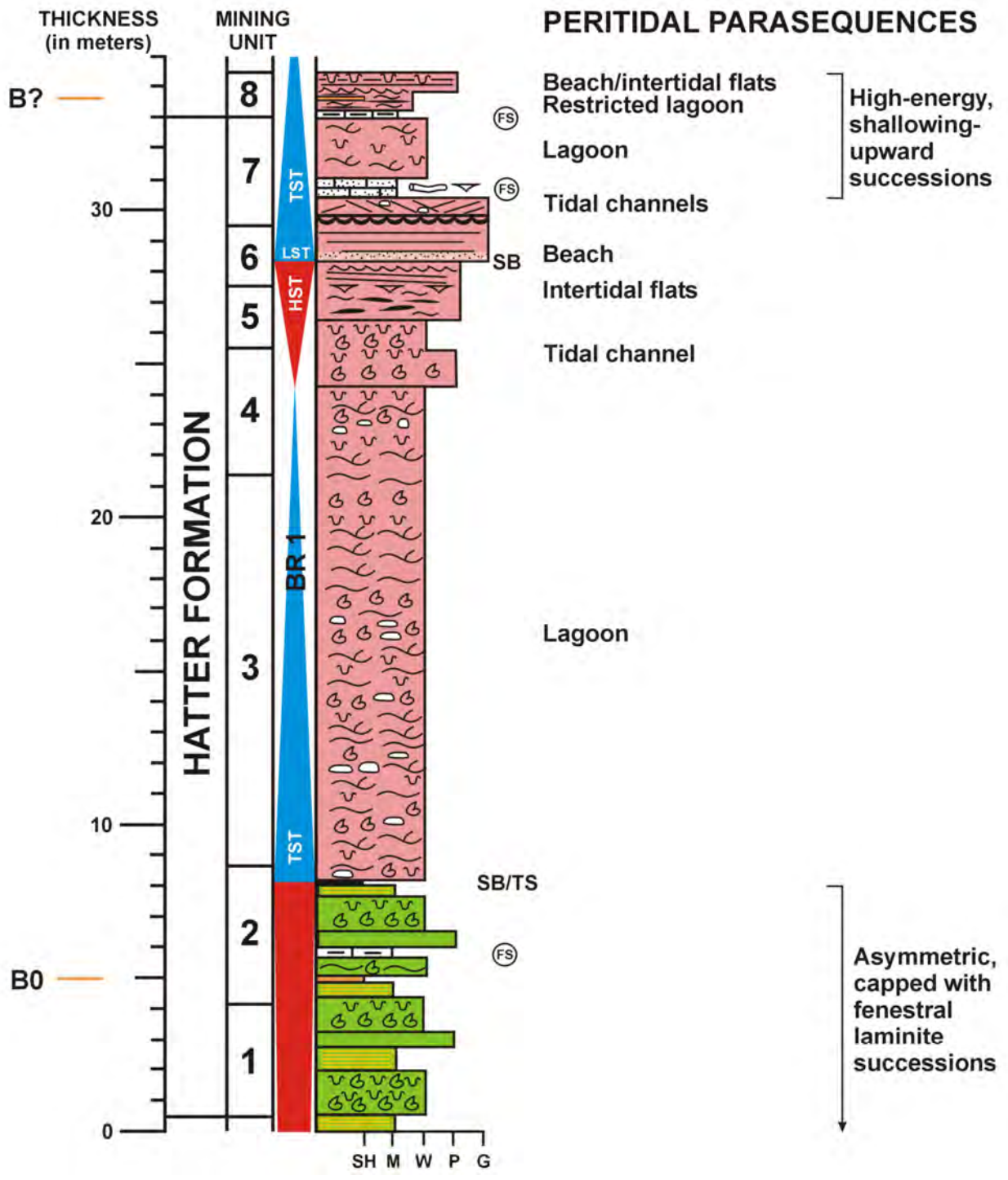

Figure 35. Vertical facies successions in the Hatter Formation exposed along Route 453 near Union Furnace, Pennsylvania. The lower 6 m (20 ft) of the formation consists of peritidal low-energy, shallowing-upward successions similar to those found in the Loysburg Formation. Most of the Hatter Formation contains lagoonal carbonates. The upper 7 m (23 ft) consist of peritidal high-energy shallowing-upward successions. See Figure 13 for symbol legend.

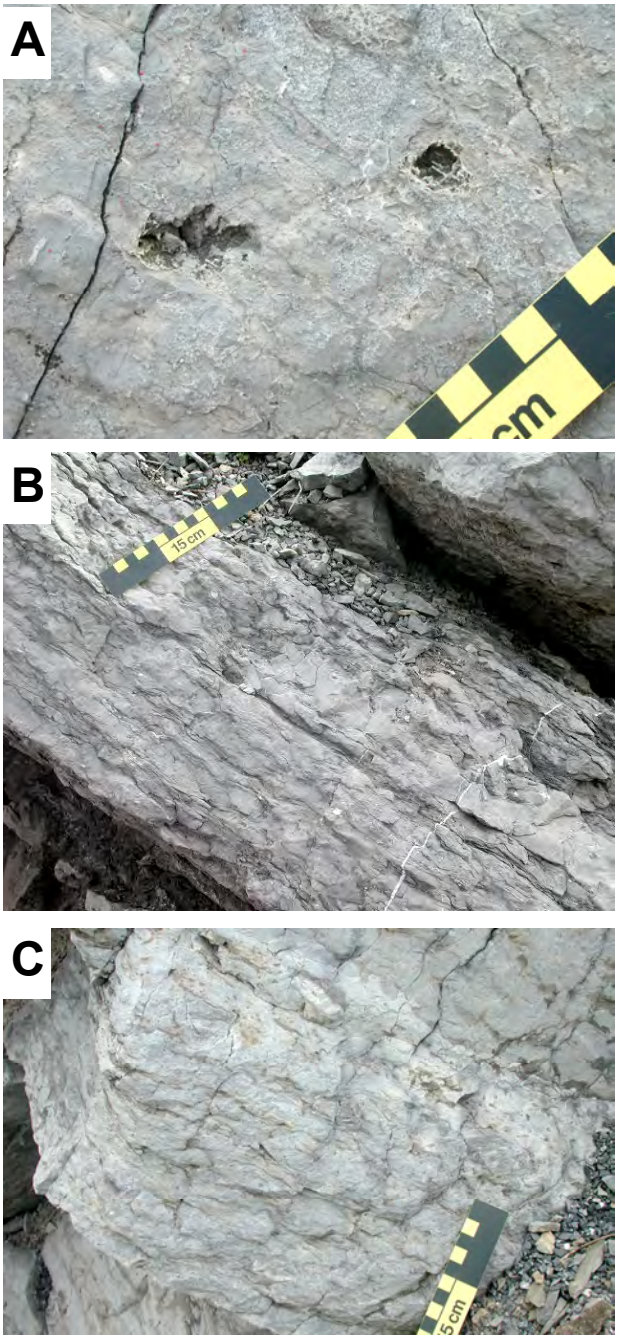

Figure 36. Lagoonal carbonate facies in the Hatter Formation. A - Dark gray, burrowed and bioturbated, skeletal and peloidal wackestone and mudstone. The rocks weather to the lighter gray seen here. B - Close up view of the typical Hatter Formation bioturbated fabric. Vugs in this facies are moldic pores after fossil material. C - Burrowed and bioturbated wackestone and mudstone similar to that shown if A, but some wavy, lenticular, and minor nodular bedding also are apparent.

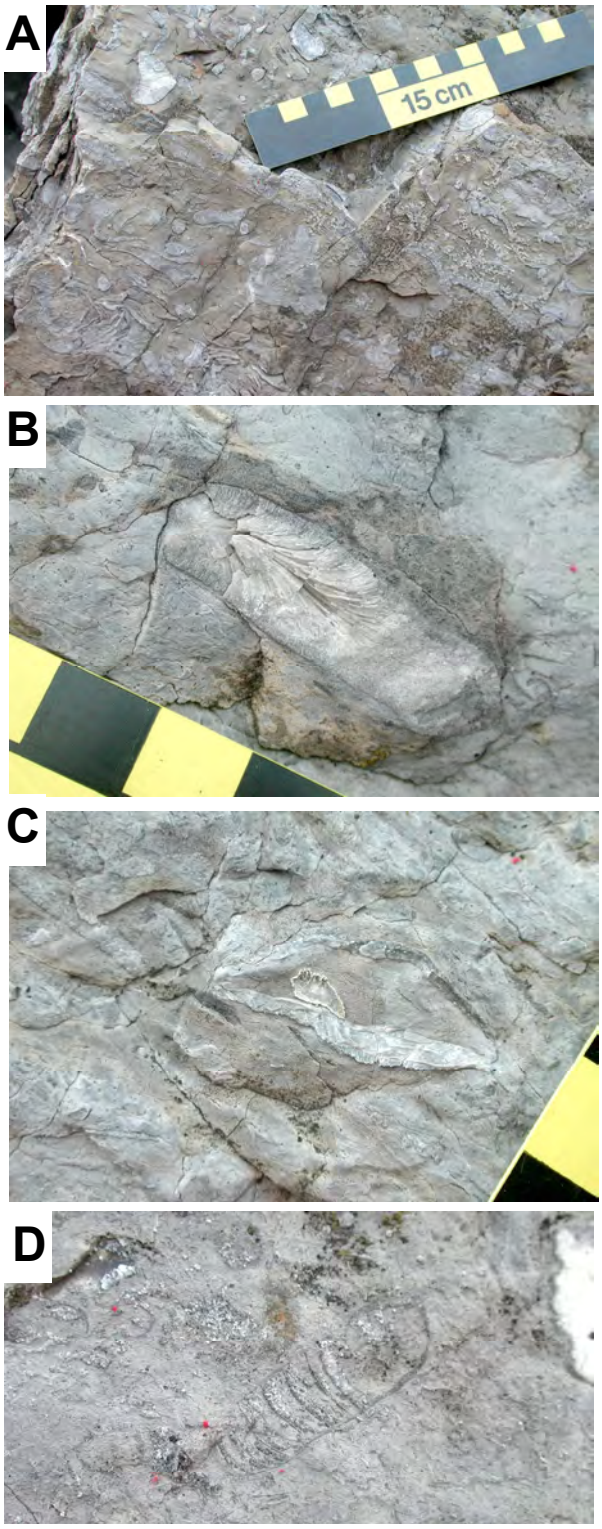

Figure 37. Fossils in the lagoonal facies of the Hatter Formation. A - Bryozoans in burrowed skeletal wackestone. B and C - Close-ups of bryozoans. D - Orthocone (straight-shelled) nautiloid and brachiopod shell hash in skeletal wackestone, Hatter Formation.

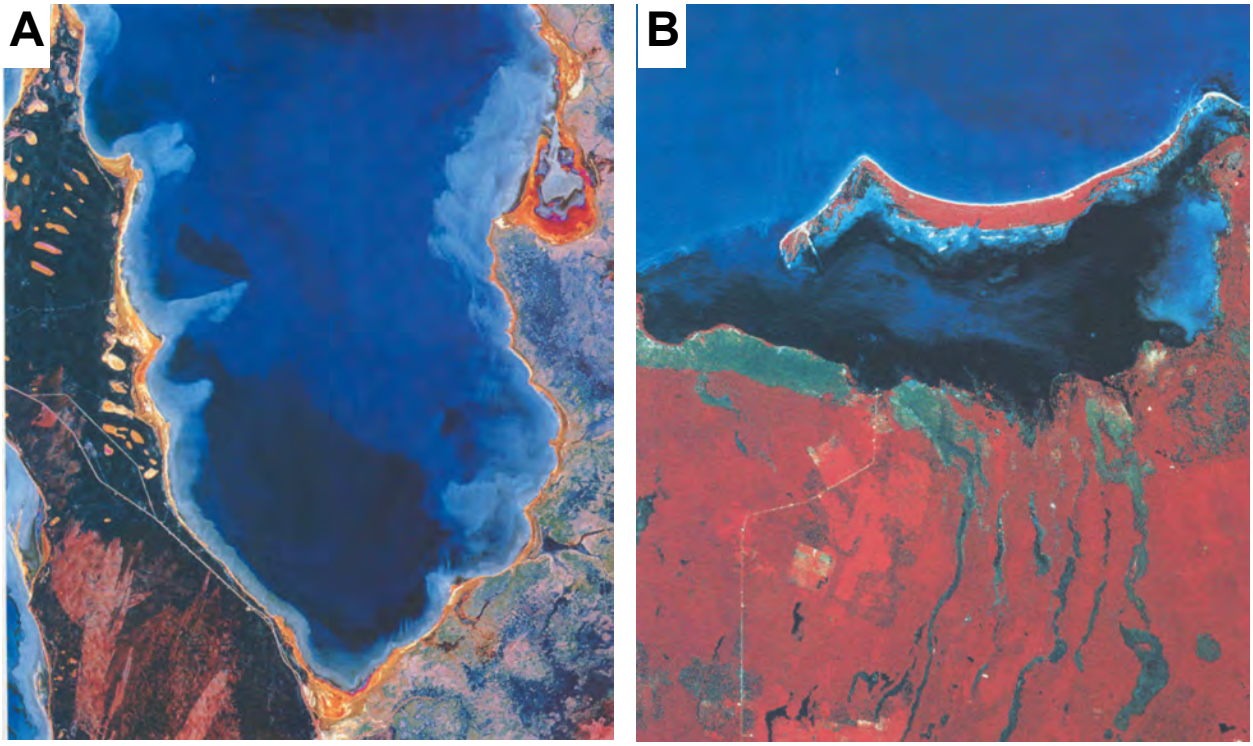

Figure 38. Landsat images. A - Hamelin Basin, Shark Bay, Australia. The embayment plain in the center of Hamelin Basin slopes from about 6 m depth in the south to 9 m in the north. B - Yalahau Lagoon, Yucatan, Mexico. Both lagoons are characterized by bioturbated muddy carbonate sediment.

The top 7 m (23 ft) of the Hatter Formation, and bottommost 1.5 m (5 ft) of the Snyder Formation (as marked on the outcrop) consist of peritidal, high-energy shallowing-upward successions (Figure 35). We recognize three of these successions; they comprise stacked peritidal parasequences separated by thin, dark, faunally- restricted argillaceous mudstones. These mudstones define transgressive flooding surfaces that separate individual parasequences. Lithofacies in these high-energy shallowing- upward successions include 1) wavy, flaser, and lenticular-bedded mudstone/wackestones/packstones (intertidal), 2) low-angle to horizontally bedded, and wave-rippled grainstones (upper intertidal to beach), and 3) coarse skeletal, intraclastic, cross-bedded grainstones (tidal channels) (Figure 39).

The first hardground to occur in the Black River and Trenton Groups at this outcrop is within one of these peritidal high-energy shallowing-upwards cycles near the top of the Hatter Formation, at the base of Unit 7 (Figure 17).

Unit 8 contains the uppermost high-energy peritidal cycle. The entire cycle is 1.5 m (5 ft) thick, and it differs from those beneath it by its apparently high organic content and more restricted biota (Figure 40). This represents more restricted depositional conditions.

Snyder Formation (Units 9 – 16)

Kay (1944a) named the Snyder Formation for outcrop exposures in southeastern Snyder Township, Blair County, Pennsylvania. These exposures are 2 km (1.2 mi.) south-southeast of Tyrone. The type section is along the Conrail tracks here at Union Furnace. Faill et al. (1989) described the Snyder Formation as an assemblage of conglomeratic to fine grained limestones containing oolites and numerous fossil fragments. They recognized four types of specific limestone units that were mappable in the field:

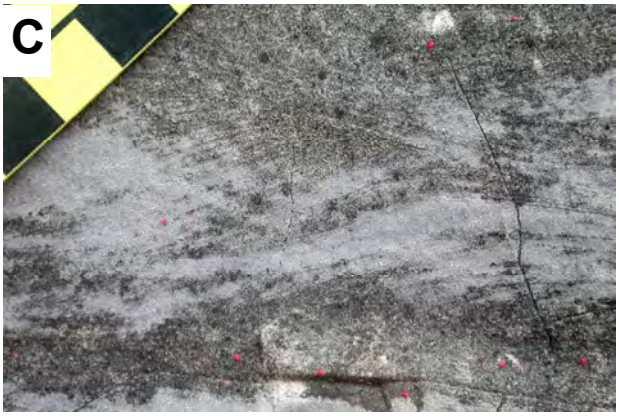

Figure 39. Grainstones in the high-energy, shallowing upward successions at the top of the Hatter Formation. A - Plan view of wave rippled, bioclastic grainstone. B - Low-angle cross bedding. C - Wave ripples with a form-discordant internal structure in

Figure 40. Bioturbated, dark, organic-rich mudstone in Unit 8, Snyder Formation. The clay zone is a probable bentonite.

1. Medium to thick bedded conglomeratic calcarenites
2. Thin to thick bedded, parallel laminated calcisiltites and calcilutites, with irregular argillaceous partings
3. Fucoidal (burrowed) calcisiltites
4. Oolite beds

Faill et al. (1989) state that the basal contact of the Snyder Formation with the subjacent Hatter Formation is sharp and conformable, and they place it at the base of the oolitic sequence. This differs from what other workers have marked here at the Union Furnace road cut (Figure 41). Faill et al. (1989) consider the top of the conglomeratic beds as the upper contact with the overlying Linden Hall Formation. The upper contact is conformable.

Lithofacies, Depositional Environments, and Diagenetic Features – Figure 41 shows our interpretation of the sedimentary successions in the Snyder Formation. We interpret most of the Snyder Formation at Union Furnace (Units 9–16) as oolitic to skeletal sands and carbonate muds of the barrier bank complex depicted in Figure 9. These barrier bank lithofacies occur within subtidal parasequences that we interpret as stacked shoal complexes (Figure 41). Two types of meter-scale cycles - depositional and diagenetic cycles - occur in the Snyder Formation parasequences; both cycles are common in carbonate strata deposited on subtidal ramps (Jones and Desrochers, 1992). In the lower portion of the formation, the subtidal parasequences consist of oolitic and mixed grainstone-capped, high-energy shoal successions (Lehrmann and Goldhammer, 1999). In the upper portion of the Snyder Formation, the parasequences consist of

hardground-bounded, amalgamated grainstone successions (Lehrmann and Goldhammer, 1999). Low-relief (≤ 1 m [3.3 ft]) bryozoan bioherms and biostromes are common throughout both types of successions.

Grainstone-capped, high-energy shoaling successions: These successions dominate the Snyder Formation at the Union Furnace outcrop from near the base of Unit 9 to the B1 bentonite, near the base of Unit 11 (Figure 41). The parasequences consist of shallowing upward successions comprised of deep marine offshore carbonates (thin bedded, argillaceous, sparsely fossiliferous, burrowed mudstone), lower shoreface carbonates (burrowed, wave rippled, skeletal wackestones and skeletal/peloidal packstones), and upper shoreface carbonates (cross bedded, oolitic grainstones or mixed grainstones).

The oolitic grainstones (Figure 42) are composed of fine- to medium-grained ooids (0.3 to 0.5 mm, mean = 0.2 mm) that exhibit a radial fabric. The concentric patterns of original growth lamellae are still visible in most of the ooids. Ooids make up 90 percent of the allochems. Many ooids are partially to completely micritized, and some are partially replaced by chert. Other allochems in this lithofacies include brachiopod (3 percent) and crinoid (1 percent) fragments, trilobite fragments (1 percent), peloids (1 percent), mollusk (gastropod and pelecypod) fragments (0.5 percent), and mudstone intraclasts (0.5 percent). All of these grains exhibit

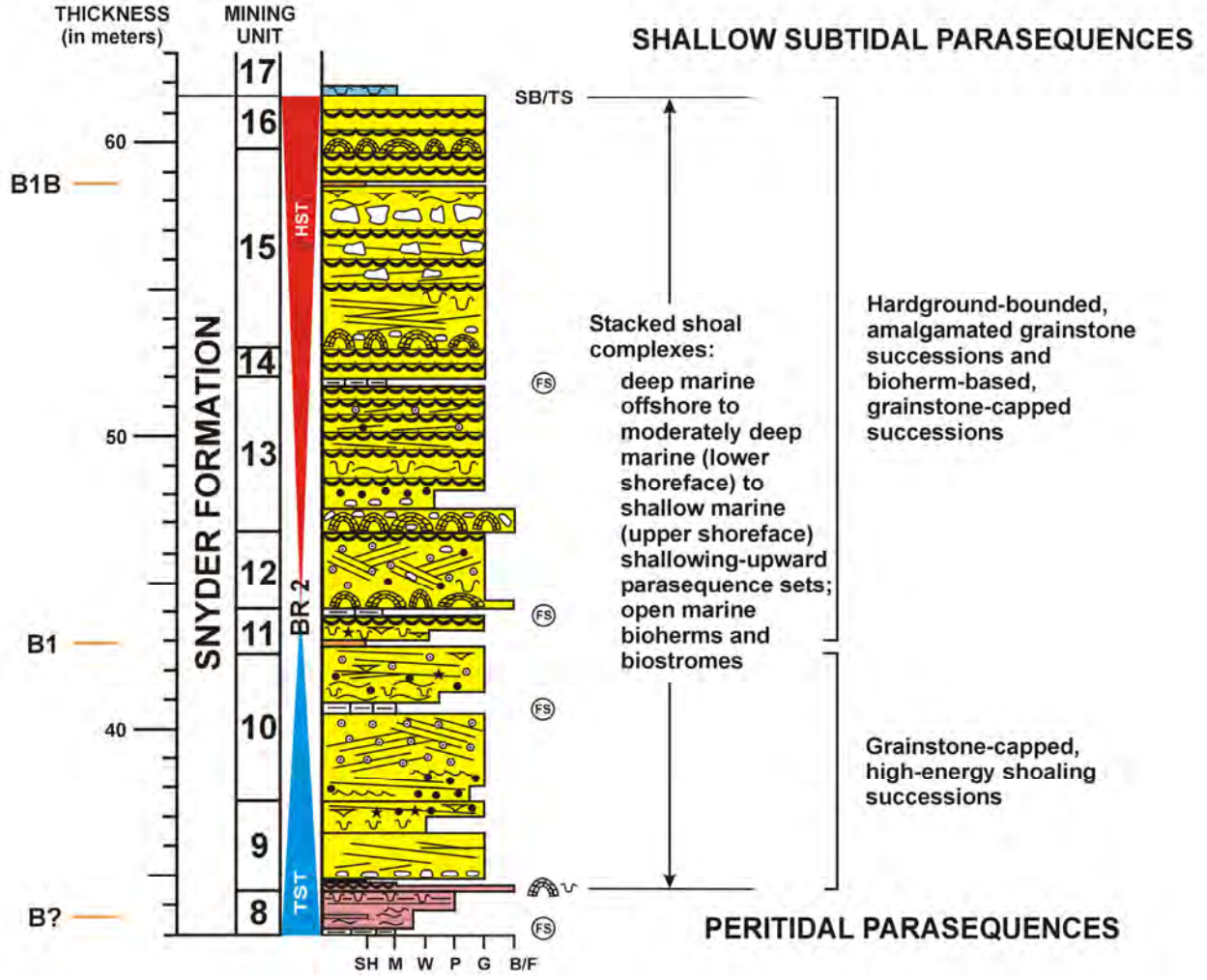

Figure 41. Vertical facies successions in the Snyder Formation exposed along Route 453 near Union Furnace, Pennsylvania. See Figure 13 for symbol legend.

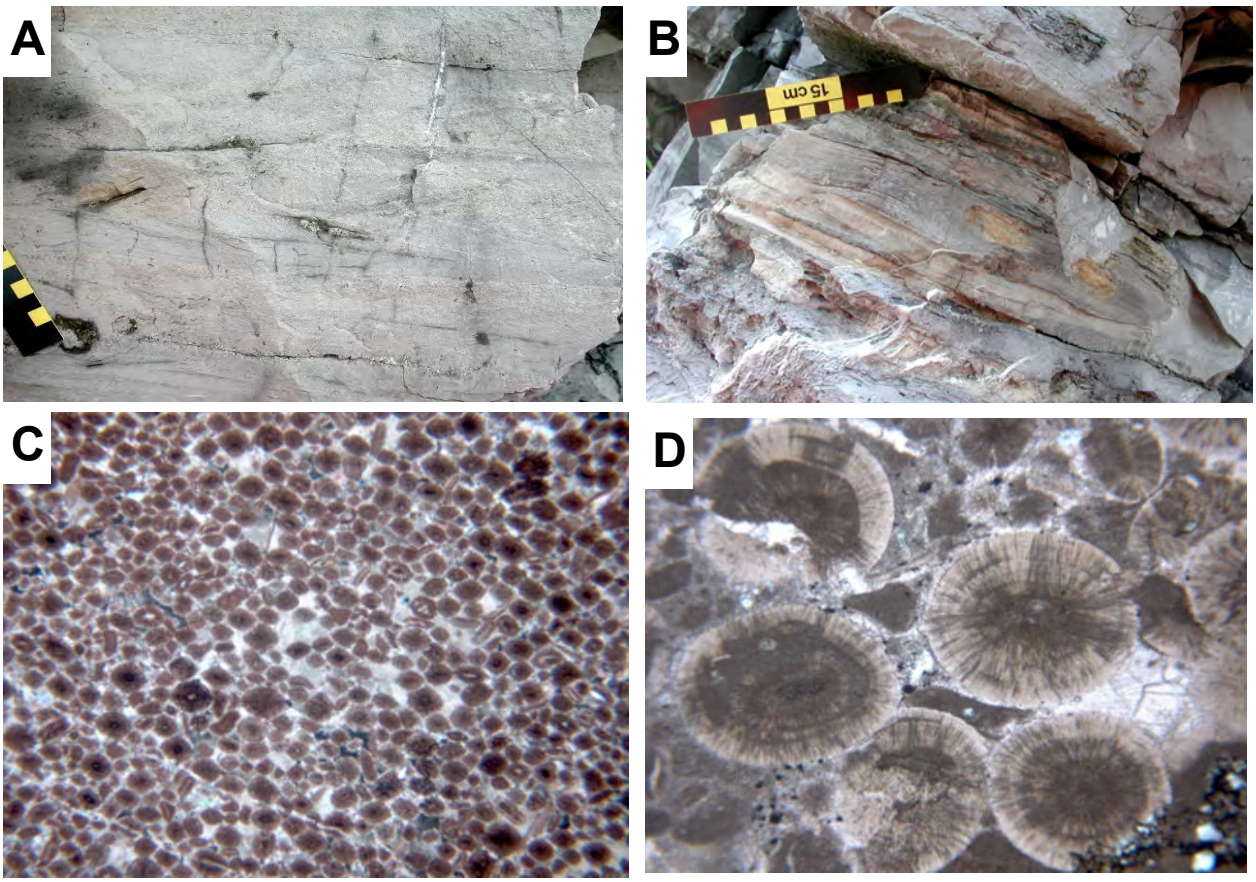

Figure 42. Oolitic grainstones in the Snyder Formation. A - Cross-bedded oolitic grainstone in Unit 10. B - Horizontal to wavy bedding and hummocky cross-stratification in oolitic grainstones in the Snyder Formation. C - Thin section photomicrograph of oolitic grainstone shown in A. Samples is stained with Alizarin Red-S. D - Higher magnification view of C showing smaller micritic intraclasts among the ooids, isopachous rims of radial-fibrous calcite, meniscus-type calcite cement, and compactional/pressure solution fabrics. Hillgartner and others (2001) recently distinguished *meniscus-type cement* was from vadose meniscus cements. It forms in subtidal environments through microbial filament calcification, trapping of percolating micrite, and microbially induced carbonate formation. Meniscus-type cement is important in hardground development (Hillgartner and others, 2001).

varying degrees of micritization, and some minor replacement by chert. Other minerals include authigenic quartz (1 percent) and feldspar (1 percent). The quartz has euhedral terminations, and replaces both allochems and cement. The feldspars include microcline and albite, and these minerals also replace allochems and cement. Cements in the oolitic grainstones include isopachous rims of radial-fibrous calcite, meniscus-type cement between some ooids, and pore-filling, non-ferroan equant calcite spar (Figure 42C and 42D). Compaction has deformed many ooids, and grain-to- grain pressure solution is common in these grainstones.

The mixed grainstones consist of intraclastic/oolitic/peloidal/skeletal grainstones (Figure 43). The intraclasts (up to 10 percent) occur as sporadic basal lags wherever storm beds are superimposed on the overall shoaling upwards successions. Intraclasts consist of mudstone, and oolitic, skeletal, or intraclastic wackestones. Other intraclasts are composed of unique aggregates of meniscus-cemented skeletal grains (small, impunctate brachiopods filled with peloidal sediment). All of these intraclasts resemble grain aggregates described from the Bahamas and Trucial coast (Bathurst, 1975; Tucker and Wright, 1990). They may be true carbonate lumps, or grapestones, formed through submarine cementation and alteration of microbially bound sediment grains (Gebelein, 1974; Winland and Matthews, 1974, and

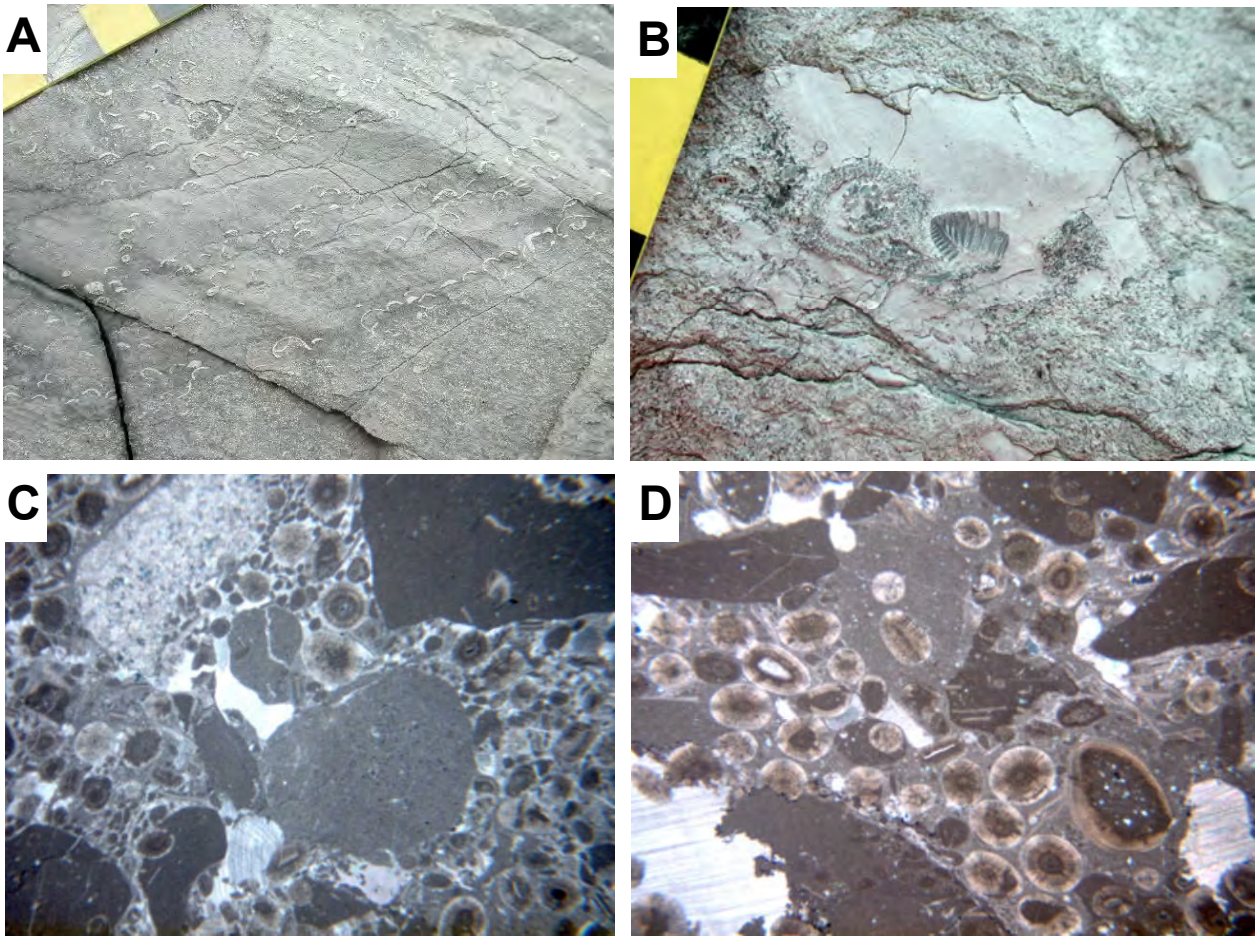

Figure 43. Mixed grainstones in the Snyder Formation. A - Outcrop view (Unit 10) of cross-bedded mixed grainstone facies. Note large brachiopod fossils with most shells convex-upwards. B - Trilobite fragment in mudstone intraclast. C - Thin section photomicrograph of mixed grainstone. Note large rounded and angular mudstone intraclasts, ooids, skeletal grains, and peloids. Also note that some ooids occur within micritic intraclasts. D - Another view of the thin section shown in C. Note stylolites, and pore-filling calcite spar.

Fabricius, 1977). Indeed, the presence of the meniscus-type cement in the intraclasts hints of nearby firmground and/or hardground development (Hillgartner et al., 2001).

Other allochems in the mixed grainstones include ooids, peloids, and various skeletal grains. Diagenetic fabrics are nearly identical to those in the oolitic grainstones, i.e., micritization of allochems, isopachous rims of radial-fibrous calcite, and non-ferroan equant calcite spar. Meniscus-type cements also lithify some ooids in mixed grainstones.

The oolitic and mixed grainstone-capped, high-energy shoal successions do occur higher in the Snyder Formation, but become subordinate to the hardground-bounded, amalgamated grainstone successions above Unit 10.

Hardground-bounded, amalgamated grainstone successions: These unique and spectacular diagenetic successions dominate the upper half of the Snyder Formation (above Unit 10). Some previous workers mistakenly identified the numerous hardgrounds in the Snyder Formation as mud-cracked beds (for example, see Rones, 1969). The cycles consist of closely spaced hardgrounds (sometimes spaced millimeters to centimeters apart), with interlayers of skeletal and peloidal grainstone, packstone, and/or wackstone (Figure 44). Some hardgrounds were initiated by "event deposition", i.e. the introduction of a storm-generated tempestite, followed

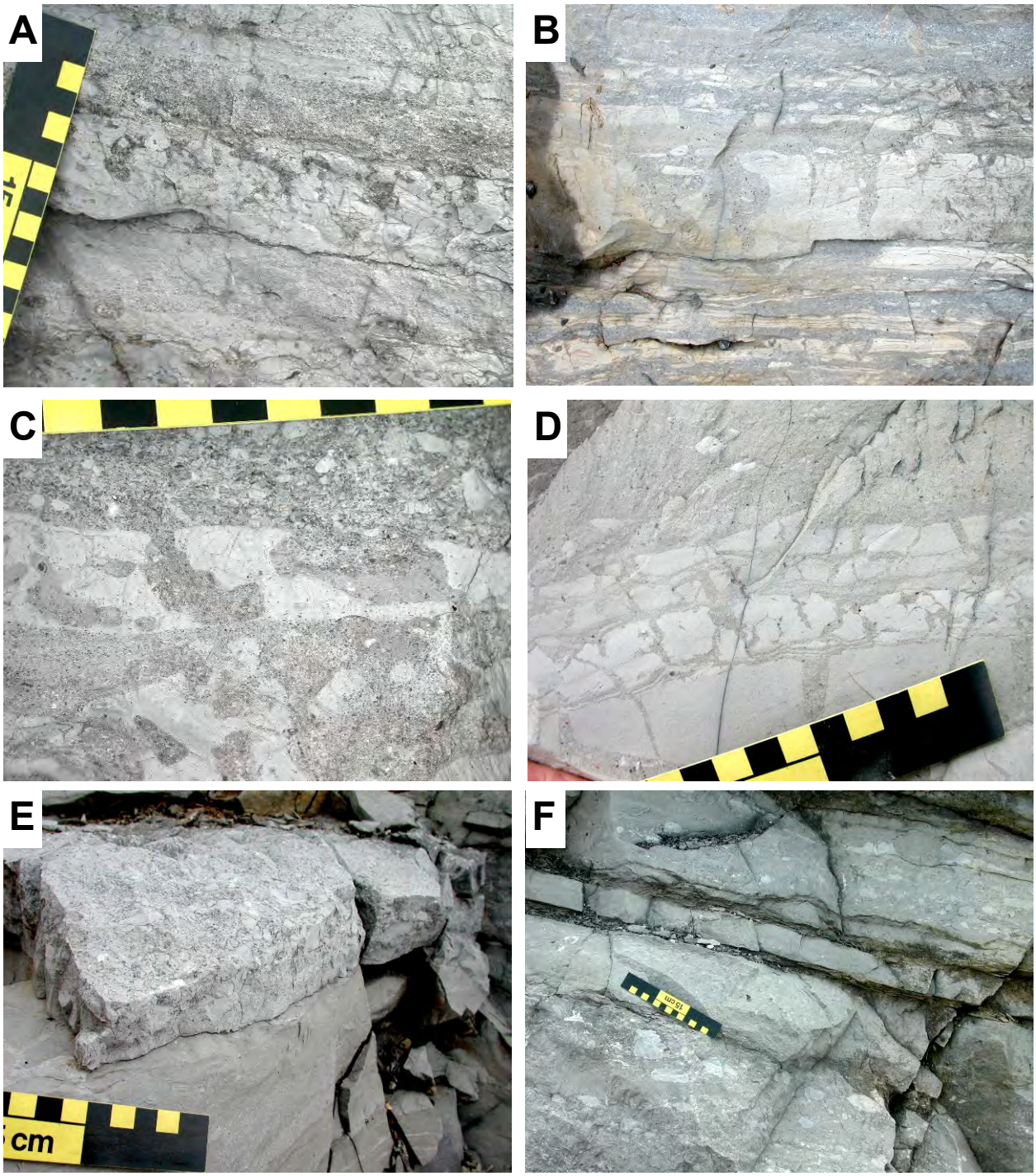

Figure 44. Hardgrounds in the Snyder Formation. A - Planar hardground in mixed grainstone. B - Composite hardgrounds. Note the large hardground in the center is undercut to pebbly and reworked. C - Undercut, pebbly, and reworked hardground. D - Composite hardground. E - Pebbly hardground. F - Reworked hardgrounds.

by a period of non-deposition and erosion. The storm generated character of these hardground beds is evident in their normally graded bedding: basal lags of skeletal and/or intraclastic grainstone are overlain by cross bedded or horizontally bedded peloidal grainstone and skeletal packstone, which is overlain in turn by burrowed and bioturbated wackestone and mudstone. The period of non-deposition is evident in the appearance of burrowing and bioturbation activity, and in the initiation of submarine cementation. Other hardgrounds consist of wackestone and mudstone, and may have been deposited as lower energy sediments between or behind shoal areas. The hardground-bounded, amalgamated grainstone successions in the Snyder Formation resemble subtidal diagenetic cycles in the Oligo-Miocene Abrakurrie Limestone of southern Australia described by James and Bone (1991). Hardground development occurred during times of relatively lower sea level when the ramp surface was above normal wave base and subject to active water pumping (Figure 15). This was a time of lithification and erosion. The interlayers of carbonate sediments between hardgrounds reflect sediment accumulation below the depth of wave abrasion during periods of relatively high sea level (Figure 15).

Hardgrounds in the Snyder Formation run the gamut from smooth and rolling types to undercut, pebbly, and reworked types (Figure 44). Brett and Brookfield (1984) suggested that different hardground types tend to be indicative of different sedimentary environments. If Brett and Brookfield's (1984) interpretations of Ordovician hardgrounds in equivalent strata in southern Ontario are correct, then we may be able to recognize the distal, middle, and proximal segments of carbonate cycles in these rocks, and refine our ability to recognize and interpret these subtidal parasequences.

Bryozoan buildups: Bryozoan-dominated bioherms and biostromes occur throughout the Snyder Formation (Figure 41). The largest buildup here at Union Furnace (at the base of Unit 13) is up to a meter high and extends across the width of the highway cut. The bioherms are centimeter- to meter-scale trepostome and fistuliporid (order Cystoporata) bryozoan bindstones, bafflestones, cruststones, biocementstones, and globstones (see Cuffey, 1985 for his extension of Dunham's carbonate rock classification to include bryozoan buildups). These bryozoan reef rocks are subtle. They consist of small, erect globular and branching colonies, encrusting sheets, and soft strands that cement carbonate sediment (Figure 45). Interframe sediments are skeletal and intraclastic wackestones and burrowed mudstones; much of this carbonate mud was most likely produced *in situ* by fragile, poorly calcified algae (Turmel and Swanson, 1976; Read, 1982). Baffling and cementation inhibited sediment movement and enhanced carbonate sedimentation. These reef rocks developed as open marine bioherms in a lower shoreface environment, possibly on lower shoal flanks, intershoal areas, and/or within the broad tidal exchange channels that crossed the banks. Bryozoan buildups also occur on hardgrounds.

Linden Hall Formation (Units 17 – 23)

Rones (1969) established the Linden Hall Formation to include the Stover and Oak Hall Limestones of Kay (1944a, 1944b). Faill et al. (1989) mapped the Linden Hall and Rodman Formation of Butts (1918) together, undivided. They described the Linden Hall as inter-bedded, homogeneous, fossiliferous, and "wormy" limestones (Faill et al., 1989, p. 18). The latter refers to the fucoidal, or burrowed, mudstones and wackestones that dominate the formation. The lower contact of the Linden Hall with the Snyder Formation is conformable. Rones (1969) and Ryder et al. (1992) placed an unconformity at the top of the Linden Hall at the approximate position of the B6 bentonite. This unconformity is difficult to see at Union Furnace, but we will argue that, although subtle, it is there.

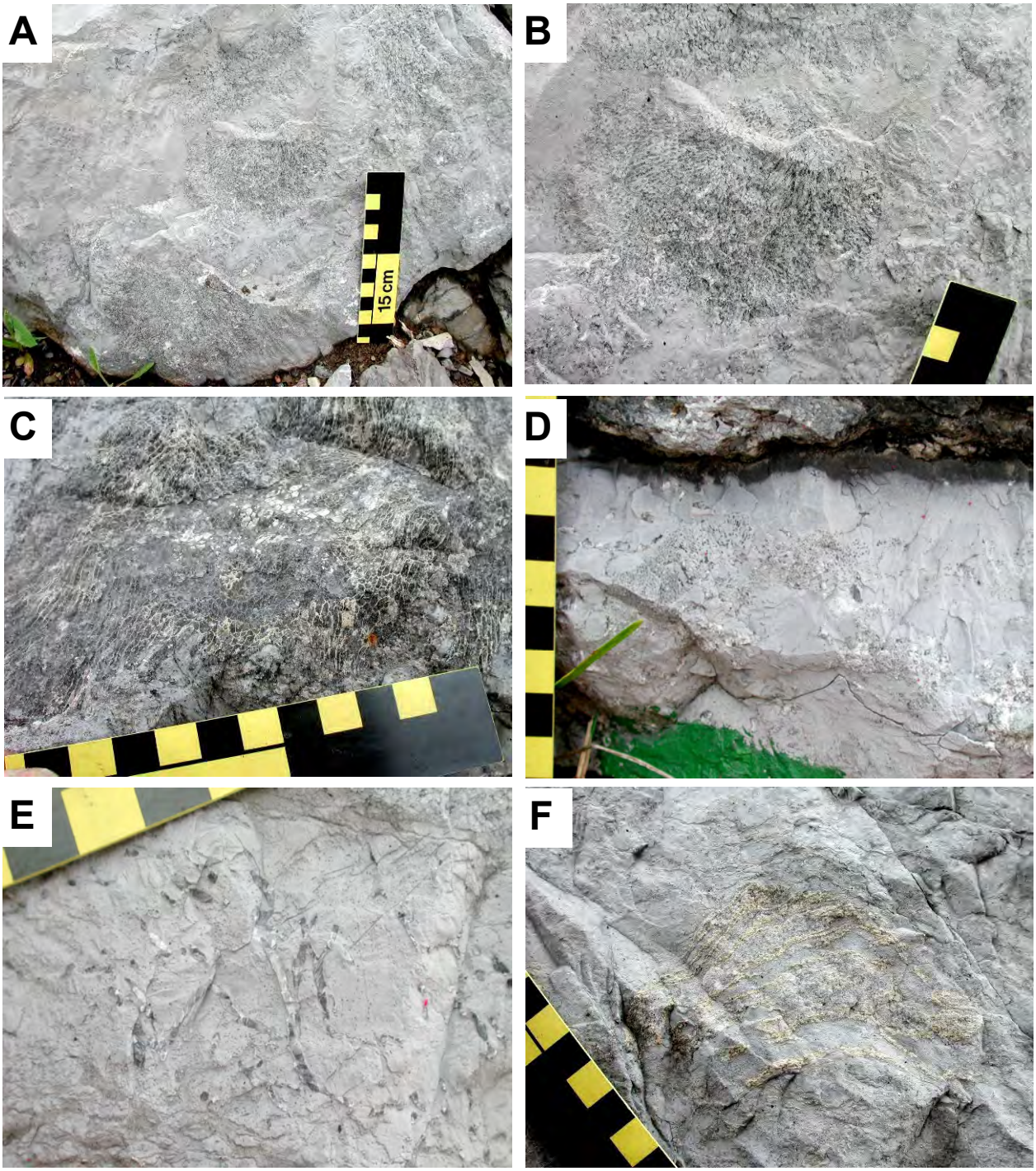

Figure 45. Bryozoans in the Snyder Formation. A, B and C - Bryozoan reef at base of Unit 13. D - Bryozoan buildup at base of Unit 9. E - Ramose bryozoans in Unit 11. F - Differential weathering exposes bryozoan colony.

Lithofacies, Depositional Environments, and Diagenetic Features – We interpret the Linden Hall Formation at Union Furnace mostly as packstones, wackestones, and mudstones deposited seaward of the barrier bank complex on a homoclinal ramp (Figure 9). There are subordinate amounts of skeletal and peloidal grainstones that we interpret as shoal flank or bank-fringe sediments, or storm beds. The rocks of the Linden Hall were deposited in deeper water than the underlying Snyder Formation with bottom conditions above storm wave base, but below normal wave base. Muddy carbonate textures, normal marine faunas, and extensive burrowing and bioturbation indicate deposition in a mid-ramp environment (Wilson and Jordan, 1983). Hardgrounds are very common throughout the Linden Hall Formation.

The Linden Hall Formation deepens upward and consists of meter scale diagenetic cycles of amalgamated packstone/wackestone-mudstone successions capped by hardgrounds (Figure 46). The hardground surfaces form during periods of low sea level when active seawater pumping facilitates submarine cementation. The successions of packstone/wackestone and mudstone are deposited during corresponding sea level highs (James and Bone, 1991).

Hardgrounds: Hardgrounds are the most outstanding feature of the Linden Hall Formation at Union Furnace (Figure 47). The hardgrounds are most abundant in the lower 5 m (16.4 ft) (Unit 17) and the upper 12.5 m (41 ft) (Units 22, 23, and 24) of the Linden Hall Formation. Hardgrounds are also observed in the central portion of the section, but they are not as common. The hardgrounds in the Linden Hall Formation are similar to those observed in the Snyder Formation, except that they occur in muddier carbonates. Hardground recognition criteria included sharp planar contacts with overlying bed, bored surfaces, and associated intraformational conglomerates. In thin section pyrite grains were concentrated along the hardground surface (Figure 47D).

Amalgamated packstone/wackestone-mudstone successions: Several relationships are observed between the packstones and wackestones/mudstones of the Linden Hall: 1) distinct storm/bank-fringe packstones and burrowed mudstones separated by dolomitized argillaceous laminae; 2) compactionally deformed packstone/grainstone lenses within a mudstone or most commonly; 3) burrow mottled packstone-wackestone beds with intergranular material ranging from micritic mud to sparry calcite.

The majority of the rocks of the Linden Hall Formation are mud-supported ranging from mudstones to floatstones to wackestones. Skeletal wackestones dominate and minor mudstones and floatstones occur most commonly in the upper third of the Linden Hall Formation.

Skeletal wackestones range in thickness from 0.5 to 4.5 m (1.6 to 14.8 ft) with the thickest successions occurring in Units 21 and 22. They are highly burrowed, contain wavy, argillaceous laminae and normal marine fossil assemblages dominated by brachiopods and bryozoans, but also including mollusks, trilobites, echinoderms, and corals. Skeletal grains as large as 3 mm are observed, but these are rare and most of the grains range from 0.1 to 0.3 mm. Large gastropods are present in Unit 23. Peloids comprise less than 5% of the wackestone, but there are also isolated pockets containing greater than 50% peloids forming peloidal grainstones or packstones.

Mudstones and floatstones are also burrowed and contain argillaceous laminae, but are more compositionally homogenous than the wackestones. Floatstones are composed of primarily brachiopod and bryozoan fragments that are less than or equal to 1 cm. Partial pyritization and chertification of these large skeletal grains are common. Dolomitic nodules are the only substantial feature of the mudstones. These nodules range in size from 3 mm to 1.2 cm. The smaller nodules are spherical or elliptical in shape. Larger nodules are very irregular and often associated with argillaceous laminae and fractures or stylolites.

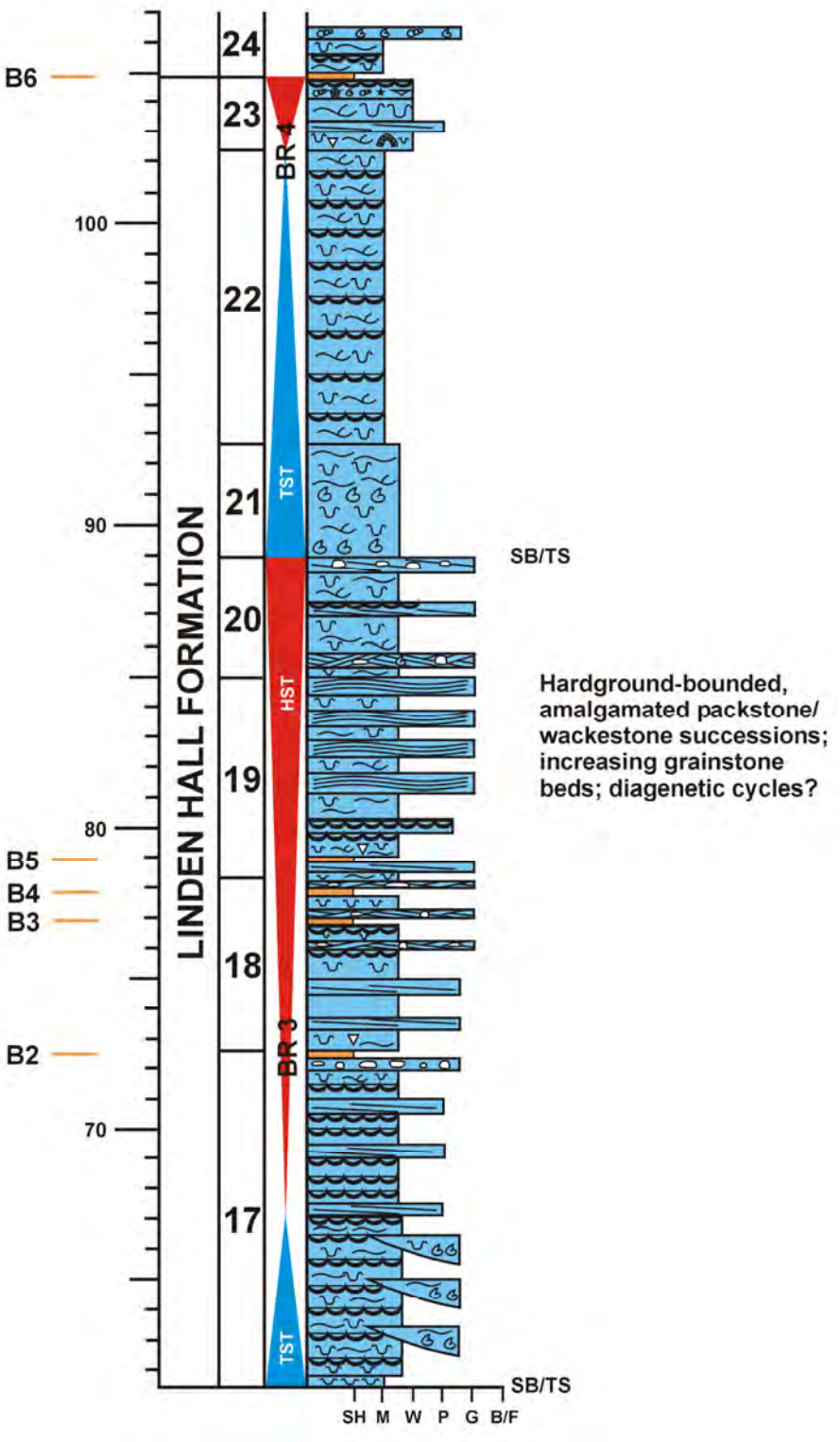

Figure 46. Vertical succession of sedimentary features in the Linden Hall Formation at Union Furnace. See Figure 13 for symbol legend.

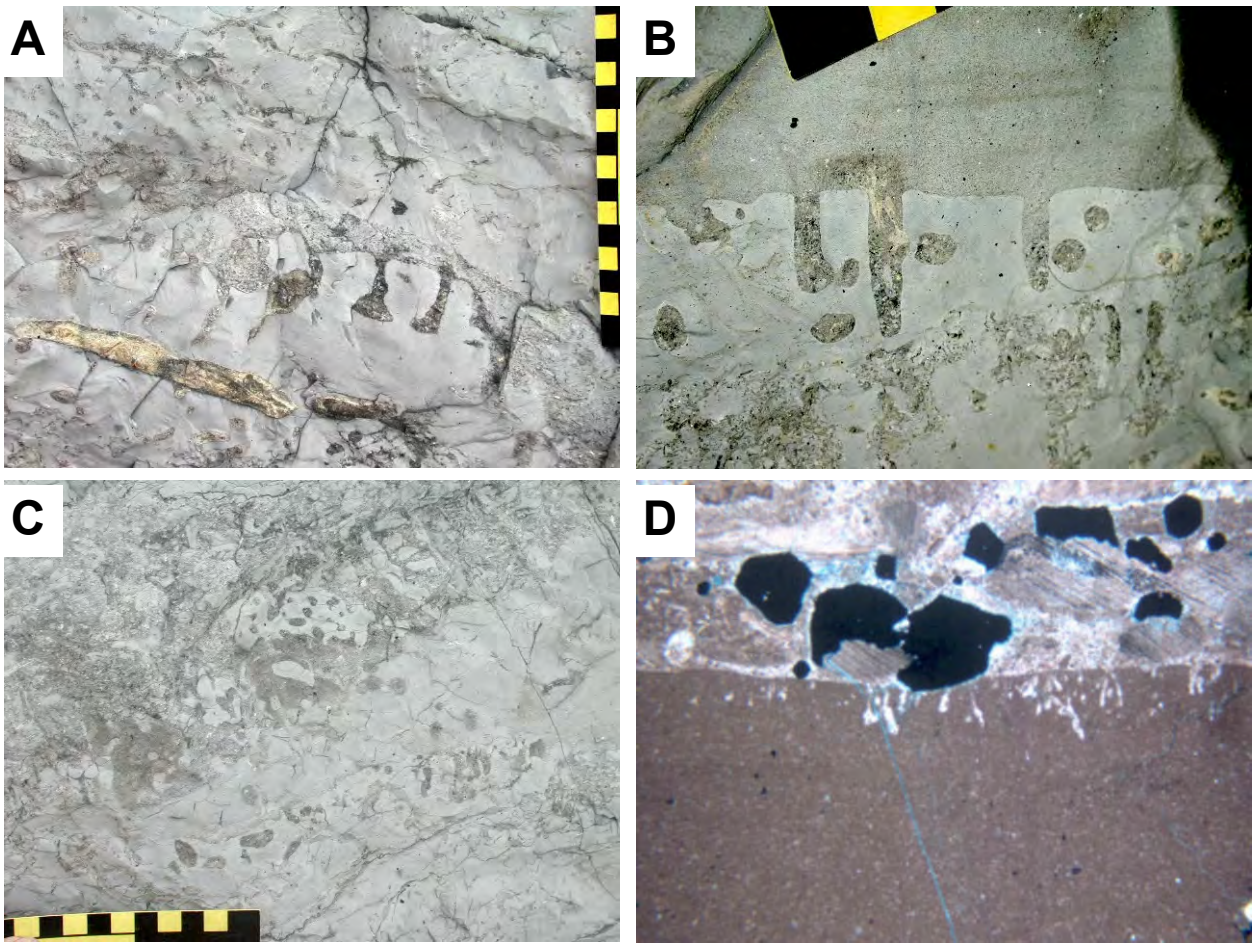

Figure 47. Hardgrounds in the Linden Hall Formation. A - Undercut and pebbly hardground. Note the brown chert layers. B - Complex rolling to hummocky and undercut hardground in mudstone. C - Composite hardgrounds. Compaction also complicates hardground classification. D - Thin section view of rolling hardground. The hardground formed in bioturbated mudstone, which is too fine-grained to discern marine cements with the petrographic microscope. Several other criteria allow identification of this bed as a hardground: 1) sharp upper contact with a rolling surface; 2) *Trypanites* borings; and 3) broken and reworked authigenic pyrite crystals in the sediment above the omission surface.

Dolomitization is common along most argillaceous laminae and appears to be associated with stylolites and fractures, and within burrows that have been filled with coarser material. Stylolitization is more obvious in the muddy units and is often associated with the argillaceous layers.

Packstones and grainstones, interpreted as storm beds or shoal flank or bank fringe sediments, occur as discontinuous lenses in the first 4 m (13 ft) of the Linden Hall Formation, within Unit 17, but occur as discrete, continuous beds up through the top of Unit 20. Significant packstone and grainstone units are absent between Units 21 and 22 and are present again in Unit 23 at the top of the Linden Hall. These are hummocky, planar and cross-stratified intraclastic, skeletal and peloidal packstones. Burrows are also observed in these coarser units. There is a thick peloidal grainstone/packstone near the base of Unit 23 composed of approximately 40% peloids and 15% skeletal grains. The peloids range in size from 0.04 mm to 0.3 mm. The larger peloids are less rounded than the smaller ones and may actually be muddy intraclasts. The smallest peloids resemble micritic mud, filling intergranular and intragranular spaces in the packstone. The skeletal grains range from 0.2 mm to 0.8 mm. Brachiopods are the

largest and most common grains, but bryozoans, mollusks, echinoderm, and trilobite fragments are also present. The skeletal grains are partially micritized and common grain molds (mostly bilvalves—Figure 48A) are filled with sparry calcite cement. The intraclastic packstones and grainstones in the Linden Hall are not as spectacular as those observed in the Snyder Formation, but they also form when hardgrounds are ripped up following lithification.

Dolomitization is not common in these coarser units and when present it does not penetrate the entire rock, but is confined to burrows and along fracture or stylolites. Figure 48 shows selected petrographic features of some of the Linden Hall carbonates.

As mentioned earlier, Rones (1969) placed a regional unconformity at the top of the Linden Hall Formation. He stated that the formation is, "…progressively arched and truncated southeast and southwestward from Oak Hall" (Oak Hall is approximately 32 km (20 mi) northeast of Union Furnace). Rones (1969) adds that this truncation is accompanied by onlap thinning. This unconformity is not readily apparent at the outcrop, but we think the sudden appearance of a thin, cross-bedded grainstone and thin beds of remarkably fossiliferous grainstones and floatstones in Units 23 and 24 might represent a subtle transgressive lag that is part of a combined sequence boundary/transgressive surface as described by Holland and Patzkowsky (1996) for Ordovician carbonate sequences in the eastern United States.

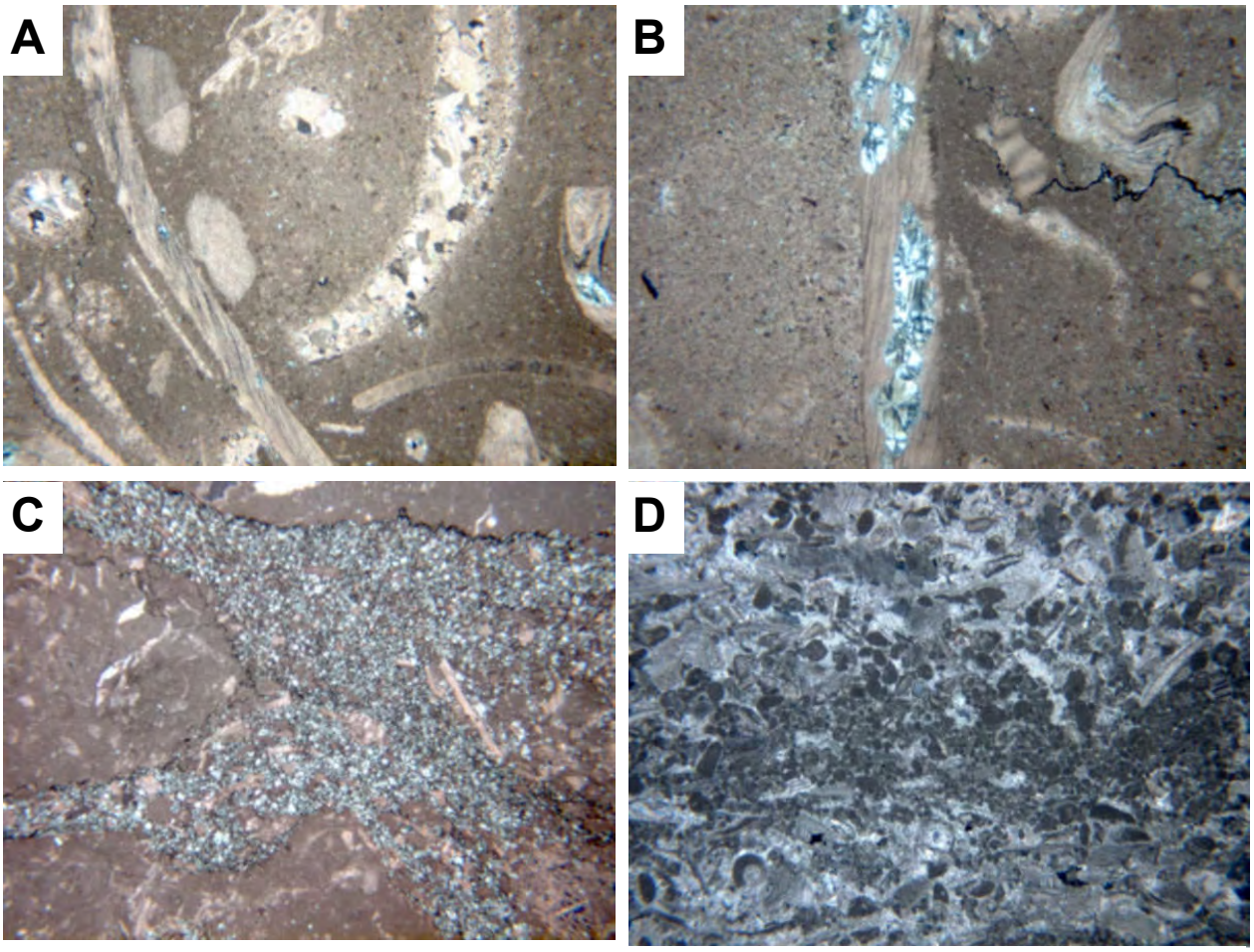

Figure 48. Linden Hall Formation photographs. A - Photomicrograph of wackestone from the Linden Hall Formation. B - Chert replacing a brachiopod fragment along a mudstone/wackestone contact in the Linden Hall Formation. C - Subhedral to euhedral idiotopic dolomite concentrated near microstylolites in a Linden Hall wackestone. D - Peloidal and skeletal grainstone from the Linden Hall formation. Most skeletal grains have undergone neomorphic replacement by sparry calcite.

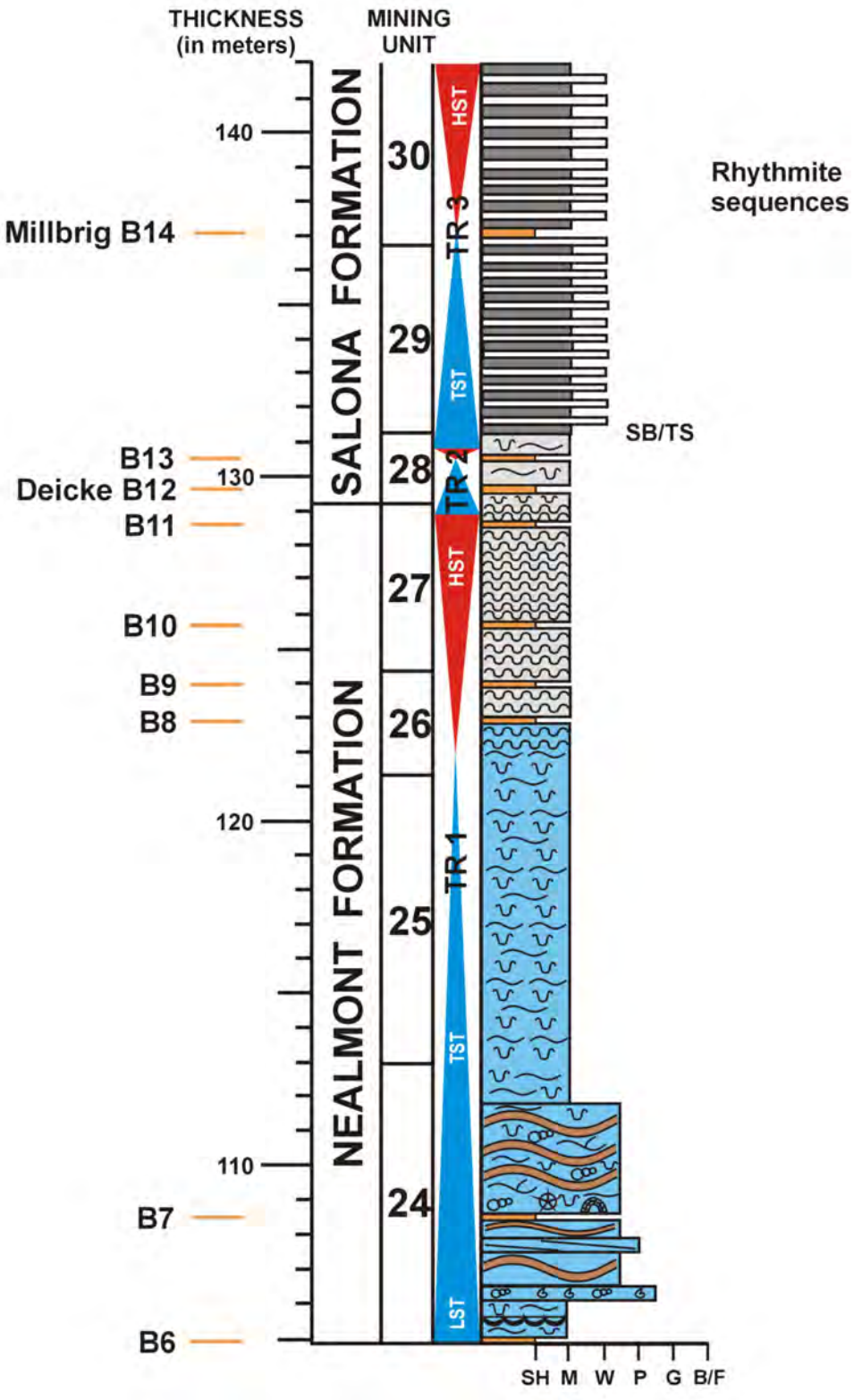

Figure 49. Vertical succession of sedimentary features in the Nealmont Formation and lowermost Salona Formation at Union Furnace. See Figure 13 for symbol legend.

Nealmont Formation (Units 24 To 27)

Kay (1944b) named the Nealmont Formation for 40 m (131 ft) of gray limestone at Union Furnace conformably underlying the Salona Formation, and unconformably overlying the Linden Hall Formation. The Nealmont Formation has two members, a lower Centre Hall Member and an Upper Rodman Member (Rones, 1969).

Lithofacies, Depositional Environments, and Diagenetic Features – The Nealmont Formation (Figure 49) consists of thick bedded, bioturbated wackestones and mudstones, with subordinate packstone lags and discontinuous skeletal floatstone and peloidal/skeletal grainstone lenses. Wavy and undulatory, argillaceous and dolomitic laminae and bands grade up to nodular bedding in the upper part of the formation (Figure 50). The nodular bedding defines the Rodman Formation (Faill et al., 1989). The nodular beds are coarser grained and more fossiliferous than the underlying wavy bedded Centre Hall Member. The nodular bedding may be the result of discontinuous sea floor cementation, compaction, and/or pressure solution.

We interpret the Nealmont Formation as relatively deeper water (lower shoreface to outer platform) carbonate sediments deposited on the middle to outer portions of a distally steepened ramp, seaward of the inner ramp shoals (Figure 9B). The change from wavy bedded to nodular bedded limestone reflects the deepening water across the outer ramp. Although below fair weather wave base, the lower Nealmont wackestones and mudstones, along with subordinate lithologies, were affected by storm events. Lenses of skeletal floatstone and packstone, and minor grainstones, attest to brief periods of higher energy. The nodular-bedded limestone of the upper Nealmont Formation reflects deeper water on the outer ramp. Organic matter preservation was higher, as reflected in the darker mudstones and the organic rich micrite matrix (Figure 52C). We have not yet examined the organic petrography and geochemistry of these rocks, but work by Obermajer et al. (1999) in Canada suggests that planktonic algal debris was a principal organic substrate for blooming microbes in these seas.

Some of the macrofossils are spectacular in the Nealmont Formation. Note the large macluritids in Unit 25 (Figure 51B). These big gastropods (or paragastropods – untorted, helically-coiled mollusks, if you accept the work of Linsley and Kier, 1984) have hyperstrophic shells with depressed spires and flat bottoms, and are thought to have been sedentary filter feeders in the Middle and Late Ordovician seas (Stearn and Carroll, 1989).

Marine cements lithify the grain-rich/matrix-poor Nealmont rocks (Figure 52). These cements include isopachous rims of radial-fibrous calcite, and pore-filling non-ferroan calcite spar. Some allochems are micritized. Many allochems show eviden ce of neomorphism and strain recrystalization. In some cases, micrite has recrystallized to microspar and pseudospar. Idiotopic dolomite occurs along stylolites and in more argillaceous limestones.

Salona Formation (Units 28 To 40)

Field (1919) named the Salona Formation for exposures at Salona in the Nittany Valley of Clinton County, Pennsylvania. The lower contact with the Nealmont Formation, as marked at this outcrop by previous workers, is conformable and gradational. The upper contact with the Coburn Formation is sharp and conformable. Faill et al. (1989) place it at the base of the first notably fossiliferous bed that is typical of the Coburn.

Two members are recognized in the Salona Formation by field mappers, the lower New Enterprise Member and the upper Roaring Spring Member. Faill et al. (1989) state that the New Enterprise Member consists of interbedded dark gray to grayish black calcisiltite and calcareous shale. They report the beds as nearly nonfossiliferous. Faill et al. (1989) distinguish the Roaring Spring Member from the New Enterprise by the appearance of calcarenites exhibiting ripples

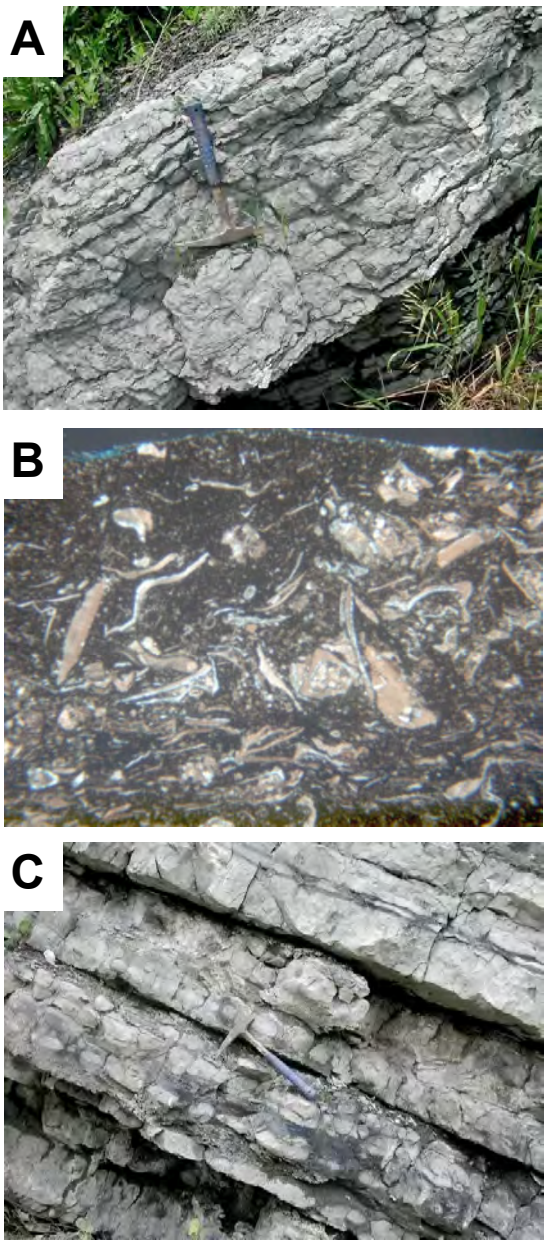

Figure 50. Nealmont Formation photographs. A and B - Two views of nodular bedding in the upper Nealmont Formation (Rodman Member). C - Thin section of wackestone from the nodular-bedded Nealmont Formation. Note the argillaceous, organic-rich micrite matrix.

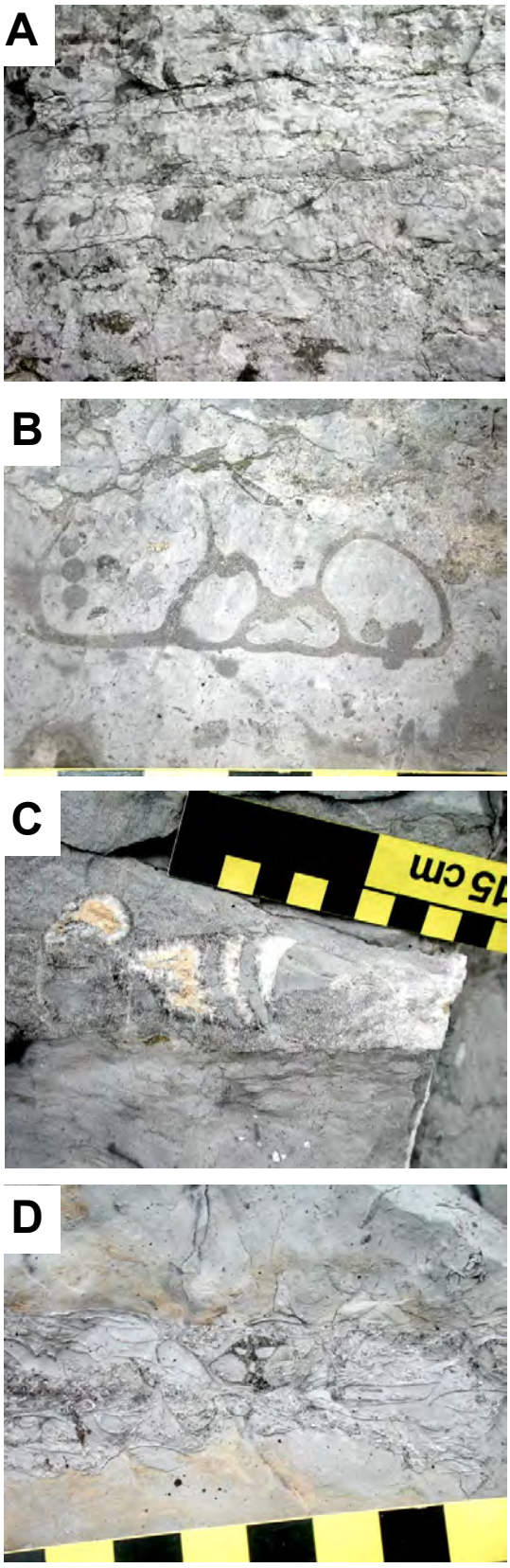

Figure 51. Nealmont Formation photographs. A - Thick bedded floatstones, wackestones and mudstones in the lower Nealmont Formation. B - *Maclurites*, a gastropod (paragastropod) with a large hyperstrophic shell, in wackestone/floatstone of the lower Nealmont Formation. C - Cephalopod fragment in lower Nealmont wackestone. D - Brachiopod floatstone with a gastropod in the lower Nealmont Formation.

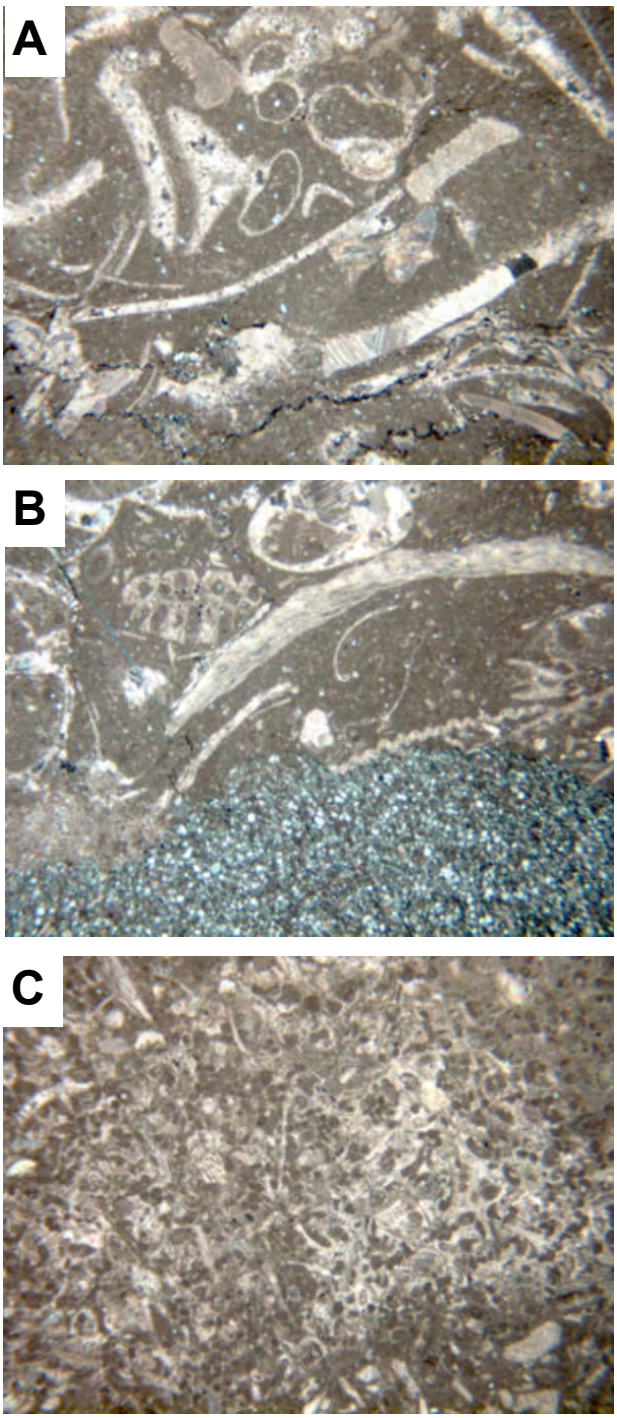

Figure 52. Lower Nealmont Formation thin sections. A - Skeletal wackestone/floatstone. B - Skeletal wackestone/floatstone, and idiotopic dolomite. C - Peloidal/skeletal grainstone lens.

and crossbedding. Slupik (1999, p. 23.) provided a more tangible description of the transition between these two members. She states that in the upper New Enterprise Member, most beds are medium to very thickly bedded, weathered light gray, and composed of micritic lime mudstone with thin skeletal lags, and argillaceous mudstone interbeds. The Roaring Spring Member is marked by a significant decrease in bed thickness, a notable increase in argillaceous material, and a change to laminated, quartz-rich lime mudstones as the dominant lithology.

Lithofacies, Depositional Environments, and Diagenetic Features – The Salona Formation here at Union Furnace consists of about 60 m (197 ft) of mostly carbonate rock rhythmites (Figure 12). The rhythmites are comprised of repetitive beds of skeletal wackestone/ mudstone and fissile, organic-rich mudstone (Figure 53). Both types of lithologies are variably argillaceous. Variable, but significant amounts of quartz silt appear in the upper parts of the formation.

The repetitive successions are 10 to 50 cm thick (Figure 54) and consist of a planar to scoured base overlain by a very sparse bioclastic lag. The fossils are primarily brachiopod, trilobite, crinoid, and ostracod fragments, but some coral, gastropod, pelecypod, bryozoan, and cephalopod fragments also occur in the rocks. Pyrite replaces some fossils. Skeletal wackestone/ mudstone displaying diffuse to distinctly horizontal to low-angle bedding, or hummocky bedding overlies this basal lag. Possible wave ripples may be present; these are very low amplitude, apparently symmetrical ripples with long, short crests (<0.16 cm heights) and long wavelengths (1.6 to 2.5 cm) with multiple periods. These ripples might be antidunes, however, or longitudinal combined current/ wave ripples (Reineck and Singh, 1980). Some burrowing is evident in the outcrop exposures; acetate peels reveal extensive bioturbation. The trace fossils *Chondrites* and *Phycodes* are common. Each succession is capped with fissile, organic-rich mudstone, argillaceous mudstone, or highly calcareous shale. The beds contain some dolomitic layers.

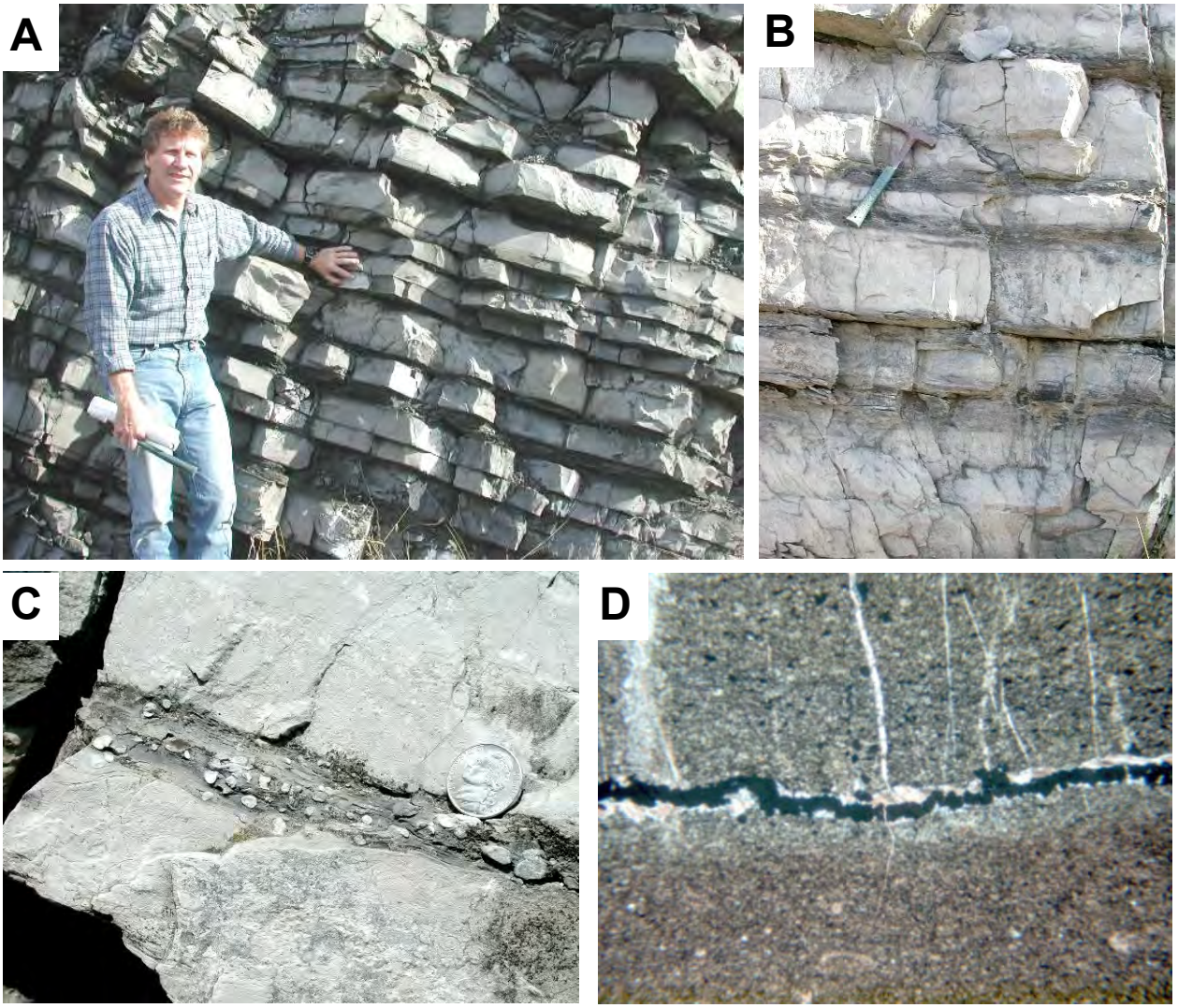

Figure 53. Salona Formation photographs. A - Thin-bedded to medium-bedded cycles. B - Thick-bedded cycles. C - *Chondrites* and possible *Planolites* trace fossils in the Salona Formation. D and E - Thin section photomicrographs of typical Salona Formation limestone. The mudstone is sparsely fossiliferous. Pyrite, minor neomorphic shell material, and phosphatic material are concentrated along a horizontal compaction seam. Kerogen is abundant. Numerous horizontal fractures are filled with epigenetic calcite.

We interpret the Salona Formation as relatively deep water, slope and basin margin sediments deposited on the far reaches of a distally steepened ramp. The Salona Formation has several features cited by Cook and Mullins (1983) as evidence for deeper water carbonate slope sediments:

- Dark gray to black mudstones, silty mudstones, and wackestones

- Insoluble residues composed of organic carbon, pyrite, quartz silt, and clay minerals
- Planar, parallel, and somewhat continuous bed contacts
- Preservation of thin bedding and laminations.

Some scoured bases, sparse fossil lags, sedimentary structures, and burrowing suggest tempestite deposition below fair weather wave base, and conceivably below storm wave base, in waters with normal marine circulation.

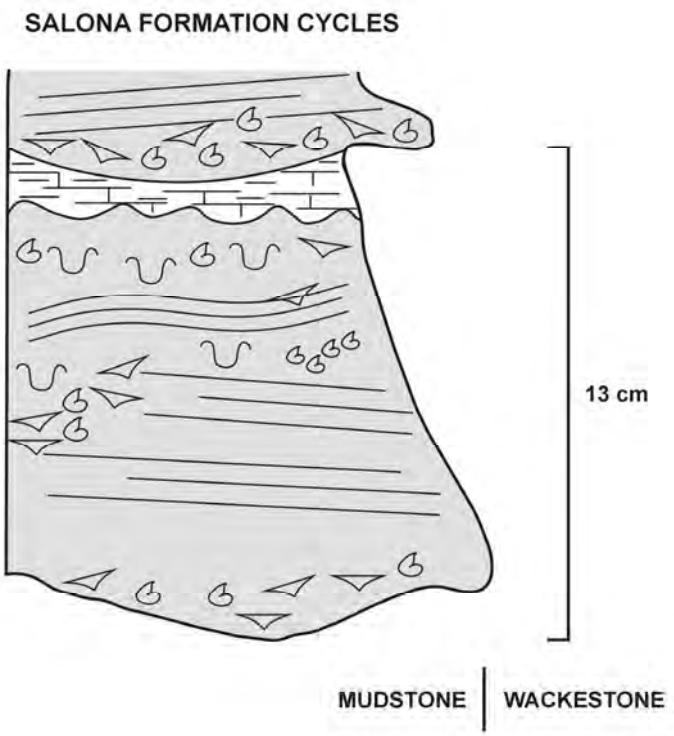

Figure 54. Diagram of ideal Salona Formation cycles. See Figure 13 for symbol legend.

Coburn Formation

Field (1919) named the Coburn Formation for exposures at Coburn, in Penns Valley, Centre County, Pennsylvania. He noted that the lower and middle portions of the Coburn Formation consist of interbedded crystalline, highly fossiliferous limestones and black shaly limestones, and the upper Coburn becomes increasingly argillaceous as it grades into the Antes Shale. In contrast to the Coburn Formation, the underlying Salona Formation lacks abundantly fossiliferous limestones. The Coburn Formation begins with the *Prasopora* zone (a hemispherical trepostome bryozoan), which is dramatically exposed here at the Route 454 outcrop (Figure 55A). This contact is sharp and conformable. The upper contact with the Antes Shale is gradational and conformable (Faill et al., 1989).

Lithofacies, Depositional Environments, and Diagenetic Features – The Coburn Formation here at Union Furnace consists of about 55 m 180.5 ft) of mostly carbonate rock rhythmites (Figure 12). The rhythmites are comprised of repetitive beds of skeletal grainstone and packstone, skeletal floatstone and wackestone, and fissile, organic-rich mudstone or argillaceous shale (Figure 12). Repetitive successions are 10 to 30 cm thick. They typically begin with scour surfaces overlain by a skeletal lag which fines upwards into laminated or cross laminated limestone, then into quartz-rich, mudstone, and finally into argillaceous mudstone and/or calcareous shale. The skeletal lags usually contain abundant brachiopod, crinoid, trilobite, and bryozoan fragments (Figure 55C and 55D). Sedimentary structures include horizontal planar and wavy laminations, low-angle cross bedding, hummocky cross tratification, and flame structures. Bioturbation and *Chondrites* trace fossils are common towards the tops of beds. An intern working with the Geological Survey in mid-2000s documented dramatic pebbly hardgrounds and convolute bedding/ slump structures in cores of the Coburn Formation recovered on the Wallace Farm just south of the outcrop (Figure 55E and 55F).

The dramatic increase in fossil content of the Coburn Formation, and the increase of wave- and current-induced sedimentary structures indicate that the Coburn Formation reflects a shallowing upwards from the underlying Salona Formation. The hardgrounds attest to periods of lower sea level, marine cementation, and erosion on the sea floor. The slump structures of the

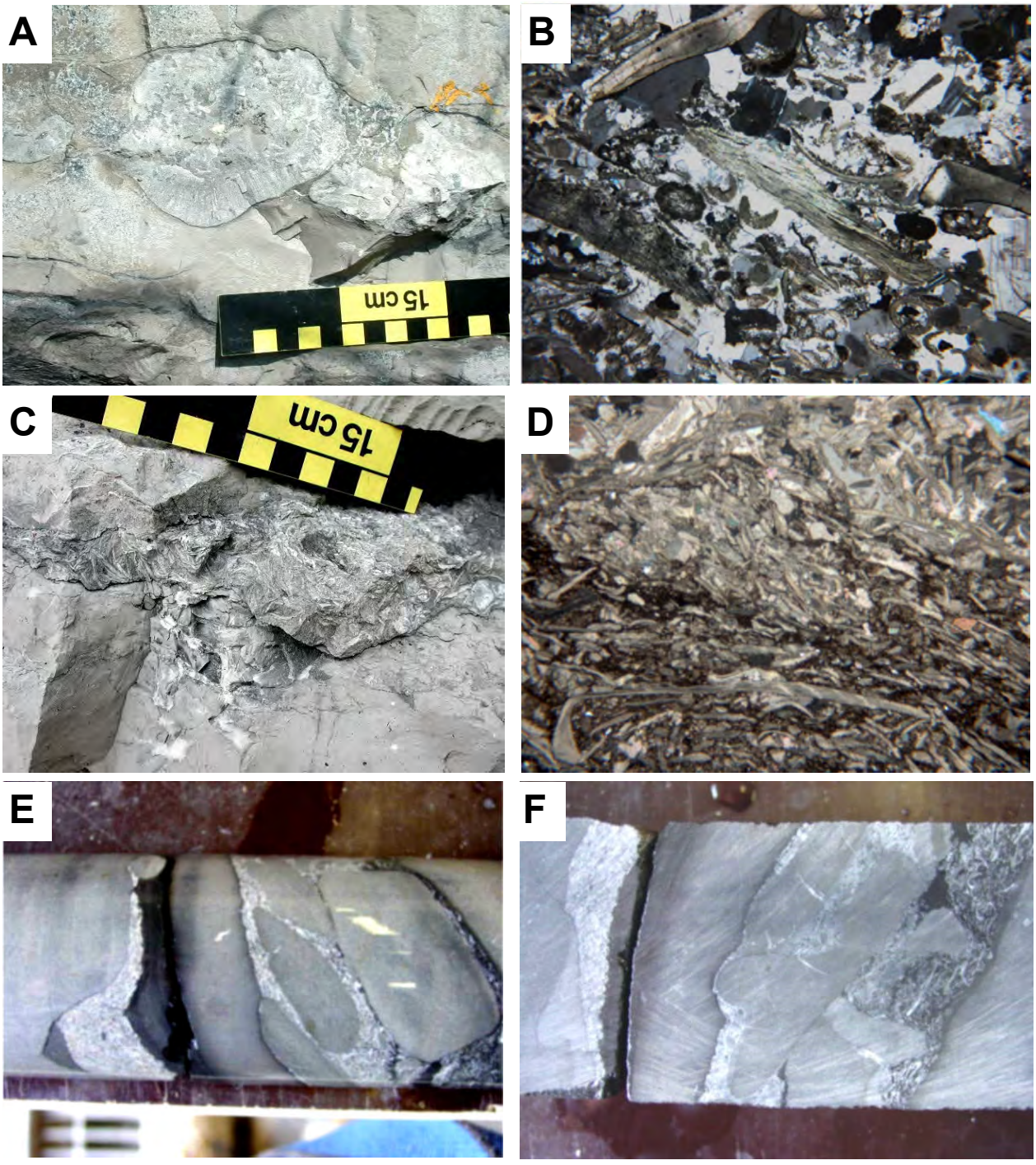

Figure 55. Selected features of the Coburn Formation. A - *Prasopora* zone that marks the base of the Coburn Formation. B - Thin section photomicrograph of Skeletal grainstone in the Coburn Formation. Note abundant brachiopod, trilobite, crinoid, bryozoan, and algal allochems. Micritization is evident around the trilobite fragments. Cements include isopachous rims of radial-fibrous calcite and equant calcite spar. C - Brachiopod coquina in the Coburn Formation. D - Thin section photomicrograph of C. E and F - Two views of a core sample of the Coburn Formation from the Wallace Farm south of the PA Route 453 outcrop showing gutters filled with mudstone and skeletal grainstone, and imbricate, reworked hardground supported in a skeletal matrix.

suggest some higher slope and sediment instability on the more proximal region of the distally steepened ramp. Another interpretation is the slump structures represent ancient seismites (Pope et al., 1997; Ettensohn et al., 2002). Slupik (1999) interpreted the Coburn repetitive successions as more proximal (as compared to the distal Salona successions) storm tempestites deposited below fair weather wave base, but above storm wave base. She suggested that the Coburn represents a gradual shallowing from the deep carbonate ramp or slope environment of the the Salona to a middle ramp environment. We tentatively concur for now, but wish to map the regional facies distributions of the Salona and Coburn Formations before advancing a more comprehensive interpretation. A paradox of the Salona and Coburn Formations is the fact that total organic carbon increases upwards from the Salona through the Coburn, and organic matter preservation was significantly higher in the greater energy environment of the Coburn. Our next step is a more detailed investigation of the sedimentology, petrology, and organic geochemistry of the Salona and Coburn Formations here in central Pennsylvania and in the subsurface to the west.

Carbonate cements in the Coburn include isopachous rims of radial-fibrous calcite, and pore-filling non-ferroan calcite spar. Some allochems are micritized.

ACKNOWLEDGEMENTS

This guidebook is only one of many results of several years of research on the Trenton and Black River carbonates in Pennsylvania and surrounding states in cooperation with geologists at our sister agencies in Kentucky, New York, Ohio, and West Virginia. Although most of the research was related to subsurface oil and gas activity, we spent a lot of time at the Union Furnace outcrop trying to tie what we saw into subsurface cores, drilling samples, and log suites. The original guidebook was prepared for an AAPG Eastern Section meeting in Pittsburgh in 2003, and revised for a Pittsburgh Association of Petroleum Geologists spring field trip in 2004. This guidebook is updated and corrected. Hopefully we fixed all of the previous mistakes.

We thank Duff Gold and Arnold Doden for doing a mountain of work on the Ordovician carbonates in the Union Furnace Quarry and the surrounding area, and for providing us with many insights, as well as several figures used in this guidebook. William Berkepile freely donated his wonderful photographs of cave formations in Tytoona Cave. William B. White, Pennsylvania State University, shared his maps of Tytoona Cave and Field Trip Cave. George Pedlow arranged for us to use the facilities at Arch Spring Farm, which is owned by his wife, Linda Morrow. We thank Linda and George for graciously providing access to the property and facilities for our lunch and fieldtrip coordination.

.

REFERENCES

Arens, N. C. and Cuffey, R. J., 1989, Shallow and stormy: late Middle Ordovician paleoenvironments in central Pennsylvania. Northeastern Geology, v. 11, p. 218 – 224.

Avary, K.L., 2002, Recent drilling activity in the Upper Ordovician Trenton-Black River Limestone, West Virginia and New York. Eastern Section American Association of Petroleum Geologists Annual Meeting Abstracts, p. 11.

Baird, G. C., Brett, C. E., and Cornell, S. R., 2000, Sequence stratigraphy of the Trenton Group (Upper Middle Ordovician) in central New York State and Southern Ontario. Geological Society of America Abstracts with Programs, Northeastern Section, p. A-3.

Bathurst, R. G. C., 1975, Carbonate Sediments And Their Diagenesis. New York, Elsevier, 658 p.

Berkheiser, S. W., and Cullen-Lollis, J., 1986, Stop 1. Union Furnace section: Stratigraphy and sedimentology, *in* Sevon, W. D., ed., Selected geology of Bedford and Huntingdon

Counties. Guidebook, 51st Annual Field Conference of Pennsylvania Geologists, Huntingdon, PA, p. 111-119.
Berg, T. M., McInerney, M. K., Way, J. H., and MacLachlan, D. B., 1983, Stratigraphic correlation chart of Pennsylvania. Pennsylvania Geological Survey, 4th ser., General Geology Report 75.
Brett, C. E., 1988, Paleoecology and evolution of marine hard substrate communities: an overview. Palaios, v. 3, p. 374 – 378.
Brett, C. E. and Brookfield, M. E., 1984, Morphology, faunas, and genesis of Ordovician hardgrounds from southern Ontario, Canada. Palaeogeography, Palaeoclimatology, and Palaeoecology, v. 46, p. 233 – 290.
Butts, C., 1918, Geologic section of Blair and Huntington Counties, central counties, central Pennsylvania. American Journal of Science, 4th ser., v. 46, p. 523-537.
Canich, M. R., and Gold, D. P., 1985, Structural features in the Tyrone-Mounty Union lineament, across the Nittany anticlinorium in central Pennsylvania, p. 120-137 *in* Gold, D. P., ed., Central Pennsylvania geology revisited. Guidebook, 50th Annual Field Conference of Pennsylvania Geologists, State College, PA, 290 p.
Chavetz, H.S., 1969, Carbonates of the Lower and Middle Ordovician in central Pennsylvania. Pennsylvania Geological Survey, 4th ser., General Geology Report 58, 39 p.
Colquhoun, I. M. and Trevail, R. A., 2000, Carbonate cores of the Middle Ordovician Trenton and Black River Groups of southwestern Ontario. Core Workshop, 2000 Eastern Section American Association of Petroleum Geologists 29th Annual Meeting, London, Ontario, September 23 – 27, 54 p.
Cook, H. E. and Mullins, H. T., 1983, Basin margin environment, *in* Scholle, P. A., Bebout, D. G., and Moore, C. H., eds., Carbonate depositional environments. American Association of Petroleum Geologists Memoir 33, p. 539 – 617.
Cornell, S. R., Brett, C. E., and McLaughlin, P. I., 2001, Sequence stratigraphy and spectral gamma ray analysis of Upper Ordovician carbonates of the northern Appalachian basin: linking surface and subsurface stratigraphy (abst.). Geological Society of America 2001 Annual Meeting and Exposition, Program and Abstracts, November 5 – 8, Boston MA.
Cuffey, R. J., 1985, Expanded reef-rock textural classification and the geologic history of bryozoan reefs. Geology, v. 13, p. 307 – 310.
Cuffey, R. K., 1985, Expanded reef-rock textural classification and the geologic history of bryozoan reefs. Geology, v. 13, p. 307-310.
Cullen-Lollis, J. and Huff, W. D., 1986, Correlation of Champlainian (Middle Ordovician) K-bentonite beds in central Pennsylvania based on chemical fingerprinting. Journal of Geology, v. 94, p. 865 – 874.
Demicco, R. V., 1983, Wavy and lenticular-bedded carbonate ribbon rocks of the Upper Cambrian Conococheague Limestone, central Appalachians. Journal of Sedimentary Geology, v. 53, p. 1121 – 1132.
Demicco, R. V. and Hardie, L. A., 1994, Sedimentary structures and early diagenetic features of shallow marine carbonate deposits. SEPM Atlas Series Number 1, 265 p.
Dravis, J. J., 1979, Rapid and widespread generation of Recent oolitic hardgrounds on a high-energy Bahamian Platform, Eleuthera Bank, Bahamas. Journal of Sedimentary Petrology, v. 49, p. 195 – 208.
Enos, P. and Perkins, R. D., 1977, Evolution of Florida Bay from island stratigraphy. Geological Society of America Bulletin, v. 90, p. 59 – 83.
Ettensohn, F. R., Kulp, M. A., and Rast, N., 2002, Interpreting ancient marine seismites and apparent epicentral areas for paleoearthquakes, Middle Ordovician Lexington Limestone, central Kentucky, *in* Ettensohn, F. R., Rast, N., and Brett, C. E., eds., Ancient seismites. Geological Society of America Special Paper 359, p. 177 - 190.

Fabricus, F. H., 1977, Origin of marine ooids and grapestones. Contributions to Sedimentology, v. 7, 113.
Faill, R. T., 1999, Chapter 33, Paleozoic, p. 418-433 *in* Shultz, C. H., ed., The Geology of Pennsylvania, Part VI: Geologic History. Pennsylvania Geological Survey, 4th ser., Special Publication 1, 888 p.
Faill, R. T., Glover, A. D., and Way, J. H., 1989, Geology and mineral resources of the Blandburg, Tipton, Altoona, and Bellwood quadrangles, Blair, Cambria, Clearfield, and Centre Counties, Pennsylvania. Pennsylvania Geological Survey, 4th ser., Atlas 86, 209 p.
Field, R. M., 1919, The Middle Ordovician of central and south central Pennsylvania. American Journal of Science, 4th series, v. 48, p. 403 – 428.
Folk, R. L. and Pittman, J. S., 1971, Length-slow chalcedony: a new testament for vanished evaporites. Journal of Sedimentary Petrology, v. 41, p. 1045 – 1058.
Fursich, F. T., 1979, Genesis, environments, and ecology of Jurassic hardgrounds. Neues Jahrbuch fur Geologisches und Paläontologisches Abhandlung, v. 158, p. 1 – 63.
Gardiner-Kuserk, M. A., 1988, Cyclic sedimentation patterns in the Middle and Upper Ordovician Trenton Group of central Pennsylvania. American Association of Petroleum Geologists Studies in Geology 29, p. 55 – 76.
Gebelein, C. D., 1974, Guidebook for modern Bahamian platform environments, St. George, Bermuda. Geological Society of America Annual Meeting Fieldtrip Guidebook, 93 p.
Ginsberg, R. N., 1982, Actualistic depositional models for the Great American Bank (Cambro-Ordovician) [abs.]. International Congress on Sedimentology, 11th, Hamilton, Ontario, Canada, Abstracts, International Association of Sedimentologists, p. 114.
Goldhammer, R. K., Dunn, P. A., and Hardie, L. A., 1987, High-frequency glacio-eustatic sea level oscillations with Milankovitch characteristics recorded in Middle Triassic platform carbonates in northern Italy. American Journal of Science, v. 287, p. 853 – 892.
Hardie, L. A. and Shinn, E. A., 1986, Carbonate depositional environments modern and ancient, part 3: Tidal flats. Colorado School of Mines Quarterly, v. 81, p. 1 – 74.
Harris, P. M. and Kowalik, W. S., 1994, Satellite images of carbonate depositional settings. American Association of Petroleum Geologists Methods in Exploration Series, Number 11, 147 p.
Hillgartner, H., Dupraz, C., and Hug, W., 2001, Microbially induced cementation of carbonate sands: are micritic meniscus cements good indicators of vadose diagenesis? Sedimentology, v. 48, p. 117 – 131.
Holland, S. M. and Patzkowsky, M. E., 1996, Sequence stratigraphy and long-term paleoceanographic change in the Middle and Upper Ordovician of the eastern United States, *in* Witzke, B. J. Ludvigson, G. A., and Day, J., eds., Paleozoic sequence stratigraphy: views from the North American craton. Geological Society of America Special Paper 306, p. 117 - 129.
James, N. P. and Choquette, P. W., 1990, Limestones – the seafloor diagenetic environment, St. Johns, Newfoundland. Geological Association of Canada, Geosciences Canada Reprint Series 4, p. 13 – 34.
James, N. P. and Bone, Y., 1991, Origin of a deep cool water Oligo-Miocene limestone, Eucia Platform, Australia. Sedimentology, p. 323 – 341.
Jones, B. and Desrochers, A., 1992, Shallow platform carbonates, *in* Walker, R. G. and James, N. P., eds., Facies Models, Response to Sea Level Change. Geological Association of Canada, GeoText 1, p. 277 – 301.
Kay, G. M., 1944a, Middle Ordovician of central Pennsylvania. Journal of Geology, v. 52, p. 1-23.
Kay, G. M., 1944b, Middle Ordovician of central Pennsylvania: Part II. Later Mohawkian (Trenton) formations. Journal of Geology, v. 52, p. 97-116.

Kolata, D. R., Huff, W. D., and Bergstrom, S. M., 1996, Ordovician K-bentonites of eastern North America, Boulder, Colorado, Geological Society of America Special Paper 313, 84 p.

Lehrmann, D. J. and Goldhammer, R. K., 1999, Secular variation in parasequences and facies stacking patterns of platform carbonates: a guide to application of stacking-patterns analysis in strata of diverse age and settings, *in* Harris, P. M. and Simo, J. A., eds., Advances in carbonate sequence stratigraphy: application to reservoirs, outcrops, and models. SEPM Special Publication Number 63, p. 187 – 225.

Leslie, S. A. and Bergstrom, S. M., 1997, Use of K-bentonite beds as time-planes for high-resolution lithofacies analysis and assessment of net rock accumulation rate: an example from the upper Middle Ordovician of eastern North America, *in* Klapper, G., Murphy, M. A., and Talent, J. A., eds., Paleozoic sequence stratigraphy, biostratigraphy, and biogeography: studies in honor of J. Granville ("Jess") Johnson, Boulder, Colorado. Geological Society of America Special Paper 321, p.11- 21.

Linsley, R. M., and Kier, W. M., 1984, The Paragastropoda: A proposal for a new class of Paleozoic Mollusca. Malacologia 25: 241-254.

Logan, B. W., Davies, G. R., Read, J. F., and Cebulski, D. E., 1970, Carbonate sedimentation and environments, Shark Bay, Western Australia. American Association of Petroleum Geologists Memoir 13, 223 p.

Malik, P.A., 1999, Geology of the Union Furnace area, Huntingdon and Blair Counties, Pennsylvania. Unpublished BS thesis, Pennsylvania State University, 58 p.

Mullins, H. T., Neumann, A. C., Wilber, R. J., and Boardman, M. R., 1980, Nodular carbonate sediment on Bahamian slopes: possible precursors to nodular limestones. Journal of Sedimentary Petrology, v. 50, p. 171 – 131.

Obermajer, M., Fowler, M. G., and Snowdon, L. R., 1999, Depositional environment and oil generation in Ordovician source rocks from southwestern Ontario, Canada: organic geochemical and petrological approach, American Association of Petroleum Geologists Bulletin, v. 83, p. 1426–1453.

Patakowsky, M. E., L. M. Slupik, M. A. Arthur, R. D. Pancost, and K. H. Freeman, 1997, Late Middle Ordovician environmental change and extinction: Harbinger of the Late Ordovician or continuation of Cambrian patterns? Geology, v. 25, p. 911 – 914.

Pope, M. and Read, F. J., 1997, High-resolution surface and subsurface sequence stratigraphy of Late Middle to Late Ordovician (Late Mohawkian – Cincinnatian) foreland basin rocks, Kentucky and Virginia. American Association of Petroleum Geologists Bulletin, v. 81, p. 1866 – 1893.

Pope, M. C., Read, F. J., Bambach, R. and Hofmann, H. J., 1997, Late Middle to Late Ordovician seismites of Kentucky, southwest Ohio, and Virginia: sedimentary recorders of earthquakes in the Appalachian basin. Geological Society of America Bulletin, v. 109, p. 489 – 503.

Pope, M. and Steffen, J. B., 2003, Widespread, prolonged late Middle to Late Ordovician upwelling in North America: a proxy record of glaciation? Geology, v. 31, p. 63 – 66.

Pratt, B. R., James, N. P., and Cowan, C. A., 1992, Peritidal carbonates, *in* Walker, R. G. and James, N. P., eds., Facies Models, Response to Sea Level Change. Geological Association of Canada, GeoText 1, p.302 – 322.

Railsback, L. B., Holland, S. M., Hunter, D. M., Jordan, E. M., Diaz, J. R., and Crowe, D. E., 2003, Controls on geochemical expression of subaerial exposure in Ordovician limestones from the Nashville Dome, Tennessee, USA. Journal of Sedimentary Research, v. 73, p.790 – 805.

Read, J. F., 1980, Carbonate ramp-to-basin transitions and foreland basin evolution, Middle Ordovician, Virginia Appalachians. American Association of Petroleum Geologists Bulletin, v. 64, p. 1575 – 1612.

Read, J. F., 1982, Geometry, facies, and development of Middle Ordovician carbonate buildups, Virginia, Appalachians. American Association of Petroleum Geologists Bulletin, v. 66, p. 189 – 209.
Read, J. F., 1985, Carbonate platform facies models. American Association of Petroleum Geologists Bulletin, v. 66, p. 860 – 878.
Reineck, H.E. and Singh, J. B., 1980, Sedimentary Depositional Environments. Springer-Verlag, New York, 439 p.
Rones, M., 1969, A lithostratigraphic, petrographic and chemical investigation of the lower Middle Ordovician carbonate rocks in central Pennsylvania. Pennsylvania Geological Survey, 4th ser., General Geology Reporet 53, 224 p.
Ryder, R. T., Harris, A. G., and Repetski, J. E., 1992, Stratigraphic framework of Cambrian and Ordovician rocks in the central Appalachian basin from Medina County, Ohio though southwestern and south-central Pennsylvania to Hampshire County, West Virginia. U.S. Geological Survey Bulletin 1839, 31 p.
Ryder, R. T., Burruss, R. C., and Hatch, J. R., 1998, Black shale source rocks and oil generation in the Cambrian and Ordovician of the central Appalachian basin, USA. American Association of Petroleum Geologists Bulletin, v. 82, p. 412 – 441.
Schlager, W., 1999, Type 3 Sequence Boundaries, *in* Harris, P. M. and Simo, J. A., eds., Advances in carbonate sequence stratigraphy: application to reservoirs, outcrops, and models. SEPM Special Publication Number 63, p. 35 – 45.
Scotese, C.R., and McKerrow, W.S., 1991, Ordovician plate tectonic reconstructions, in Barnes, C.R.,and Williams, S.H., eds., Advances in Ordovician Geology. Geological Survey of Canada, Paper 90-9, p. 271-282.
Shinn, E. A., 1969, Submarine lithification of Holocene carbonate sediments in the Persian Gulf. Sedimentology, v. 12, p. 109 – 144.
Shinn, E.A., 1978, Atlantis: Bimini Hoax. Sea Frontiers, v. 24, p. 13 – 16.
Slupik, L. M., 1999, Sedimentology and stable isotope chemostratigraphy of Late Middle Ordovician carbonates in central Pennsylvania. Unpublished MS thesis, Pennsylvania State University, 135 p.
Smith, T. and Nyahay, R., 2002, Update on New York Trenton Black River play and introduction to Matejka #1 core, *in* Harris, D., Drahovzal, J., and White T., (workshop coordinators), Outcrop analogues for Trenton/Black River fractured dolomite reservoirs: a field trip and core workshop in central Kentucky, June 4, 2002. Kentucky Geological Survey Core and Sample Library, Lexington, KY, variously paginated.
Stearn, C. W. and Carroll, R. L., 1989, Paleontology: The Record Of Life. John Wiley and Sons, New York, 453 p.
Thompson, A. M., 1999, Chapter 5: Ordovician, p. 74 – 89 *in* Shultz, C. H., ed., The Geology of Pennsylvania, Part II, Stratigraphy. Pennsylvania Geological Survey, 4th ser., Special Publication 1, 888 p.
Thompson, R.R., 1963, Lithostratigraphy of the Middle Ordovician Salona and Coburn formations in central Pennsylvania. Pennsylvania Geological Survey, 4th ser., General Geology Report 38, 154 p.
Tucker, M. E. and Wright, V. P., 1990, Carbonate Sedimentology. Blaxkwell Science Ltd., Oxford, 482 p.
Turmel, R. J. and Swanson, R. G., 1976, The development of Rodriguez Bank, a Holocene mudbank in the Florida reef tract. Journal of Sedimentary Petrology, v. 46, p. 497 – 518.
Wagner, W.R., 1966, Stratigraphy of the Cambrian to Middle Ordovician rocks of central and western Pennsylvania. Pennsylvania Geological Survey, 4th ser., General Geology Report 49, 156 p.
White, W. B., ed., 1976, Geology and biology of Pennsylvania caves. Pennsylvania Geological Survey, 4th ser., General Geology Report 66, 103 p.

White, W. B., and White, E. L., 1999, Chapter 56: Caves, p. 804 – 809 *in* Shultz, C. H., ed., The Geology of Pennsylvania, Part X, The Geologic Tourist. Pennsylvania Geological Survey, 4th ser., Special Publication 1, 888 p.
Wilde, P., 1991, Oceanography in the Ordovician, *in* Barnes, C. R., and Williams, S.H., eds., Advances in Ordovician geology. Geological Survey of Canada, Paper 90-9, p. 283-298.
Wilson, J. L. and Jordan, C., 1983, Middle shelf environment, *in* Scholle, P. A., Bebout, D. G., and Moore, C. H., eds), Carbonate depositional environments, American Association of Petroleum Geologists Memoir 33, p. 297 – 343.
Wilson, M. A. and Palmer, T. J., 1992, Hardgrounds and hardground faunas. University of Wales, Aberystwyth, Institute of Earth Studies Publications No. 9, 131 p.
Winland, H. D. and Matthews, R. K., 1974, Origin and significance of grapestone. Journal of Sedimentary Petrology, v. 44, p. 921 – 927.

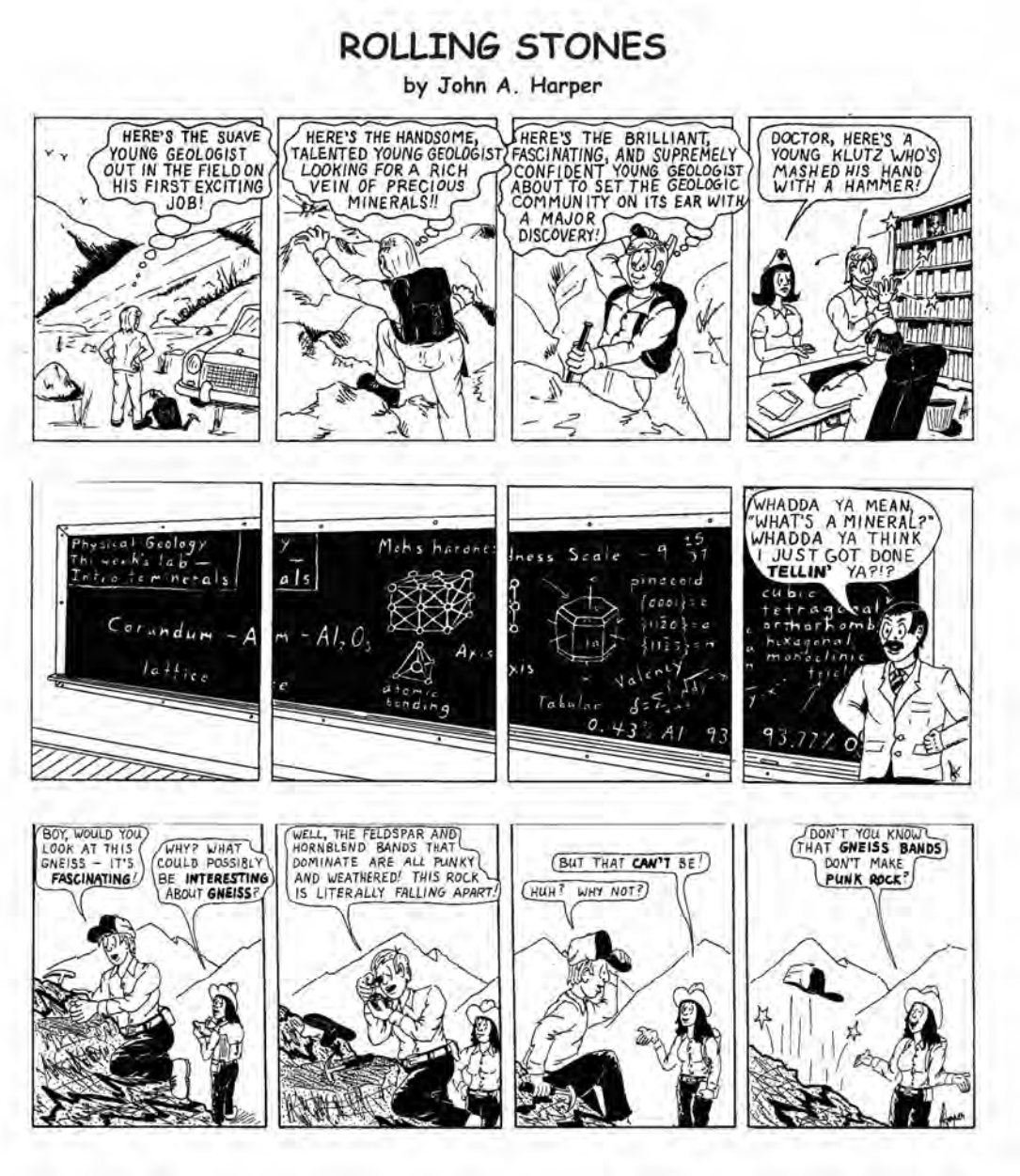

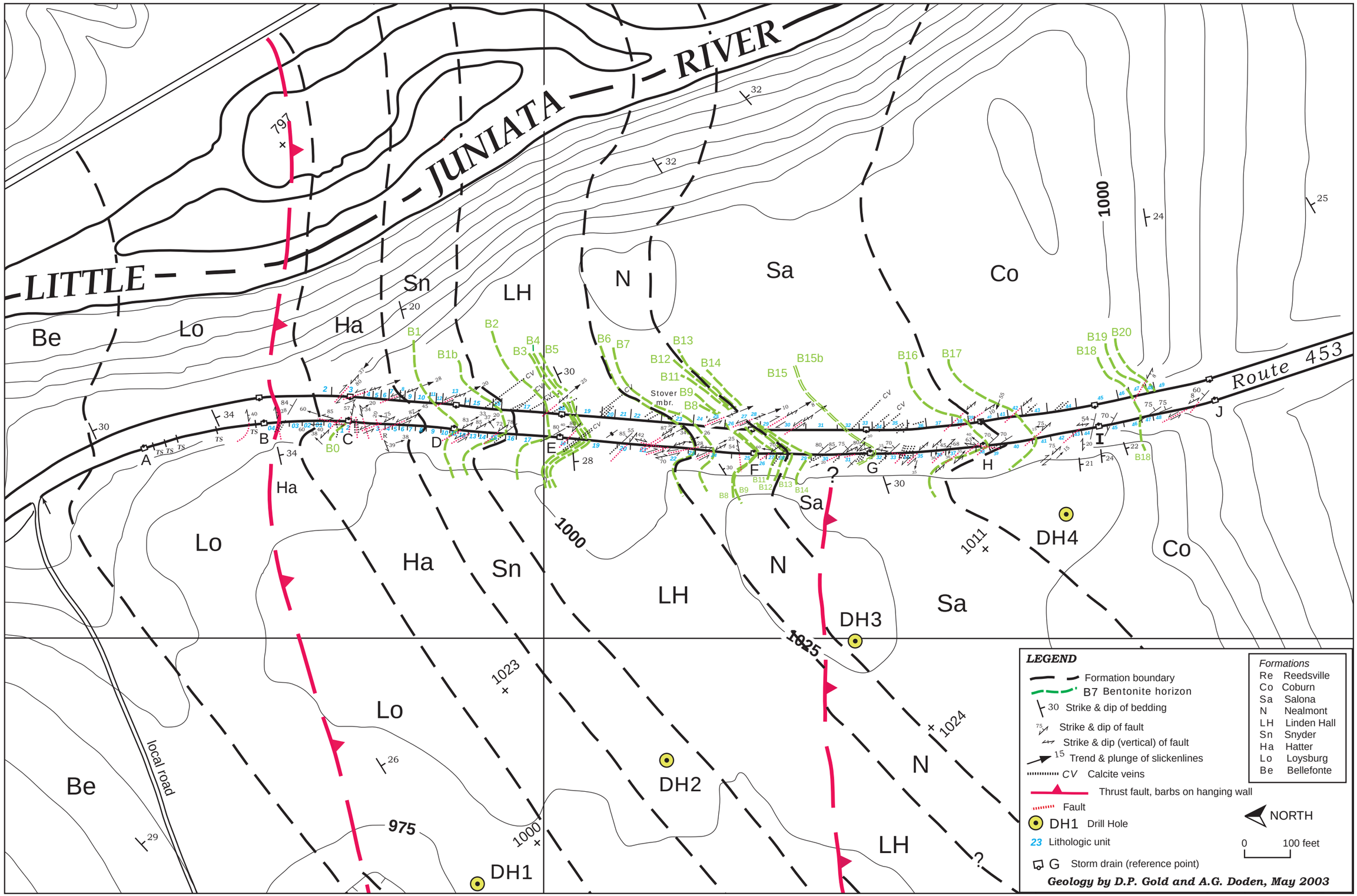

Plate 1. Geologic map of the Union Furnace roadcut.